Adaptation of *Mycobacterium tuberculosis* to Biofilm Growth is Genetically Linked to Drug Tolerance

by

Jacob Patrick Richards

BS, University of Pittsburgh, 2010

MS, University of Pittsburgh, 2013

Submitted to the Graduate Faculty of

The Department of Infectious Diseases and Microbiology

Graduate School of Public Health in partial fulfillment

of the requirements for the degree of

Doctor of Philosophy

University of Pittsburgh

2019

UNIVERSITY OF PITTSBURGH

GRADUATE SCHOOL OF PUBLIC HEALTH

This dissertation was presented

by

Jacob Patrick Richards

It was defended on

July 26, 2019

and approved by

Phalguni Gupta, PhD, Professor and Vice Chairman, Infectious Diseases and Microbiology, Graduate School of Public Health, University of Pittsburgh

Graham Hatfull, PhD, Eberly Family Professor of Biotechnology and HHMI Professor, Department of Biological Sciences, School of Arts and Sciences, University of Pittsburgh

Jeremy J. Martinson, DPhil, Assistant Professor, Infectious Diseases and Microbiology, Graduate School of Public Health, University of Pittsburgh

Dissertation Advisor: Anil K. Ojha, PhD, Associate Professor, Wadsworth Center-New York State Department of Health, Department of Infectious Diseases and Microbiology Graduate School of Public Health, University of Pittsburgh

iii

Anil K. Ojha, PhD

Adaptation of *Mycobacterium tuberculosis* to Biofilm Growth Is Genetically Linked to Drug Tolerance

Jacob Patrick Richards, PhD

University of Pittsburgh, 2019

Abstract

Infections of *Mycobacterium tuberculosis* (MTB) require at least 6 months of multiple antibiotics for sterilization. This lengthy antibiotic regimen is widely attributed to a subpopulation of cells that acquire phenotypic tolerance to antibiotics. MTB readily forms pellicle biofilms at the air-media interface *in vitro*. These MTB biofilms contain more phenotypically antibiotic tolerant persister cells than cultures grown suspended in liquid medium (planktonic). Molecular mechanisms for the increase in persister frequency in MTB biofilms remain largely unknown. We utilized a high-throughput genomic approach (Tn-seq) to identify genes required by MTB to adapt to biofilm growth, but not planktonic growth, and to analyze their relationship with biofilm-associated stress and antibiotic tolerance. We identified multiple classes of mutants for formation of MTB pellicle biofilms. We hypothesized that the heterogeneous microenvironments of MTB biofilms create endogenous stressors that allow for self-selection of a population enriched for stress and antibiotic tolerant cells. Through use of a rifampicin (RIF)-hypersensitive mutant Δ*pstC2-A1* strain that forms pellicle biofilms morphologically indistinguishable from wild-type (WT), we observed that intrinsic drug tolerance in constituent cells of biofilms determines the frequency of persisters: after 7 days of exposure to 50 μg/mL RIF, WT biofilms harbored approximately 20-fold more persisters than the mutant. These findings suggest that self-selection of tolerant cells during biofilm growth significantly promotes persister frequency. Using a transcriptomic analysis

iv

to characterize how constituent bacteria within MTB biofilms respond to environmental cues, we demonstrate biofilm-specific induction of the synthesis of isonitrile lipopeptides (INLP), which seem to be required for the development of MTB biofilm architecture based on mutant analysis. This work provides further insight into the antibiotic tolerant persistence of MTB biofilms, and identifies a biofilm-specific biomarker in INLPS for use in further investigation of this phenomenon. These findings provide molecular tools and potential antibiotic targets for investigation of MTB persisters, a significant public health obstacle to shortening the antibiotic treatment of TB.

Table of Contents

List of Tables

List of Figures

Preface

The completion of the scientific work detailed below, and my doctor of philosophy degree in general, would not have been possible without the assistance and support of so many other individuals. First and foremost, I would like to thank my dissertation advisor Dr. Anil K. Ojha. Dr. Ojha has been a patient and understanding mentor since I started in his laboratory as a master's student, and has invested many hours developing my scientific acumen. For volunteering their time and effort and attending meetings, providing valuable feedback, and reviewing this manuscript, I would next like to thank my committee members Dr. Phalguni Gupta, Dr. Graham Hatfull, and Dr. Jeremy J. Martinson. Science is a collaborative effort, and I would like to thank our collaborators at the University of California-Berkeley, Dr. Wenjun Zhang, Dr. Wenlong Cai, and Nicholas A. Zill for their insightful contributions in biochemistry to this project. I would like to acknowledge the helpful input in methodology and data analysis from Christopher Sassetti and Richard Baker. Additionally, I would like to thank several faculty and staff at the Wadsworth Center: Richard Cole for training me in microscopy and image analysis, providing guidance and feedback, hiking tips for upstate New York, and his amazing sense of humor; Keith Derbyshire, Todd Gray, Pallavi Ghosh, Joe Wade, and the members of their labs past and present for providing thoughtful feedback and the occasional borrowed reagent; Pascal Lapierre and Matt Schudt for their assistance in bioinformatics and genomics, respectively. For all of their support and friendship, I would like to greatly thank my colleagues in the Ojha laboratory: Yunlong Li, Patricia Lederman, Jamie Corro, Kathy Kulka, Joe Thomas, and special thanks to Yong Yang for all of his training and technical assistance in mutant construction, and Jennifer Gundrum for her technical assistance in performing PCRs and gel extractions for the mutant strain construction, as well as

Permission for figures used in this paper:

Portions of figures used in this document have also been used in a manuscript titled "Adaptation of *Mycobacterium tuberculosis* to Biofilm Growth is Genetically Linked to Drug Tolerance" that is currently under revision at the American Society for Microbiology journal *Antimicrobial Agents and Chemotherapy*, and are used here in accordance with ASM's Author Rights policy.

1.0 Introduction

Mycobacterium tuberculosis (MTB), the pathogenic agent that causes tuberculosis (TB), has maintained a constant presence throughout recorded human history. Writings concerning TB occur in the Old Testament of the Bible (1), have been dated back to 3300 and 2300 years ago in India and China (2, 3), respectively, and while written records are less clear, skeletal deformities consistent with MTB spinal infection (Pott's disease) were regularly depicted in Ancient Egyptian art that is dated over 5000 years old (4). TB has gone by many names (consumption, pthisis, White Plague, King's Evil, etc.) (5, 6), shaped society and policy (6, 7), perpetually served as a subject of art and literature (8, 9), and caused the sickness and death of innumerable people (7, 8, 10). It has been estimated that a quarter to a third of Earth's 7.4 billion human population carries an MTB infection, most of which are clinically asymptomatic. The World Health Organization (WHO) estimates that there were ten million new cases of TB and 1.6 million TB-related deaths in 2017 (11). Despite a global reduction in disease burden, MTB remains one of the world's deadliest and most successful pathogens and a significant public health challenge, especially in overburdened healthcare systems where TB is endemic. These difficulties are further exacerbated by MTB's recalcitrance to antibiotics. Treatment of TB requires the administration of multiple antibiotics for at least 6 months to clear the infection (12). It is hypothesized that a subpopulation of MTB cells are able to tolerate the presence of antibiotics necessitating the prolonged the treatment (13, 14). Elucidating how some MTB cells phenotypically tolerate antibiotic exposure on the molecular level is crucial to novel treatment options that could substantially reduce the time and cost required to treat TB in the clinic, providing a new advantage against one of humanity's most persistent pathogens.

1.1 Infection and Pathogenesis

TB infection exists in the human host along a spectrum across two states: active disease with the typical TB symptoms of coughing, chills, fever, fatigue, shortness of breath, weight loss, and malaise; and an asymptomatic, latent state. MTB can remain at the latent end of the spectrum in the lungs of infected individuals for years to decades. Latent TB can reactivate, progressing to active disease when the immune system is compromised by conditions including HIV co-infection, smoking, malnutrition, stress, and age. Approximately 90% of individuals infected with MTB will carry the pathogen in the asymptomatic state, which provides a large reservoir for the pathogen (13, 15). MTB primarily spreads from coughing or sneezing of individuals with active disease, generating aerosolized bacilli, which are then inhaled by nearby healthy individuals (16).

Pathogenesis of MTB is primary understood through mouse, guinea pig, rabbit and non-human primate models (17-20). In the respiratory system, MTB encounters alveolar macrophages (AM), which constitute the central weapon of innate immunity in the lung. These AM phagocytose MTB and attempt to destroy the invading pathogen. Some MTB cells survive phagocytosis via various mechanisms. For example, MTB can prevent apoptosis intended to limit pathogen replication (21), arrest phagosome maturation and acidification by responding to changes in pH through modulation of its gene expression profile (22), and prevent fusion of the late endosome with lysosomes containing antimicrobial hydrolases (23). While subverting the host's immune system, MTB replicates intracellularly, either within the phagosome or after phagosomal escape, depending on host conditions (24). Eventual lysis of infected AM releases MTB to perpetuate the infection cycle, ultimately spreading to various regions of the body, typically to the apex of the lung and the lymph nodes. The early stage of intracellular replication is followed by infiltration of T-cells at the site of infection.

MTB can form various lesion types in the human lung, the hallmark of which is the highly organized granuloma structure. Some TB granulomas eventually develop into necrotic caseous lesions at their cores (25). This region containing the majority of the MTB cells in the granuloma is typically hypoxic in several animal models (26). In the core of the caseating TB granuloma in a Guinea pig model, a region at the caseum's rim harbors acellular aggregates of MTB bacilli (27). Activated macrophages containing MTB bacilli may either combine into multi-nucleated giant cells, or differentiate into lipid-rich foamy cells (28). It is hypothesized that oxygenated mycolic acids produced by intracellular MTB play a role in driving macrophage differentiation into foamy macrophages. Multi-nucleated giant cells and foamy macrophages are typically located on the outer edge of the MTB-aggregate region and caseous center (25). Foamy macrophages may play a role in dysregulation of synthesis of host lipids, sustaining MTB persistence, and cavitation that leads to bacterial release (29).

Infected macrophages are surrounded by various other immune cells, mostly CD4+ and CD8+ positive T lymphocytes, but also B lymphocytes, neutrophils, dendritic cells, Natural Killer (NK) cells, fibroblasts, and cells that secrete extracellular matrix (ECM) material. The cytokine tumor necrosis factor alpha (TNF-α) produced by macrophages and T lymphocytes is a principal signaling molecule in formation and maintenance of the granuloma with probable involvement of interferon gamma (IFN-γ) and interleukin-12 (IL-12) (25). TB granulomas are a dynamic interaction between host and microbe, where growth and pathogenesis of MTB is limited by the host, but also provide an environmental niche for the pathogen to survive and modulate the host immune response.

1.2 TB Treatment

The current standard antibiotic regimen for treating active TB entails the administration of isoniazid (INH), RIF, pyrazinamide (PZA), and ethambutol (EMB) for the first 2 months of treatment, followed by 4 months of INH and RIF. Latent TB is commonly treated with either INH or RIF alone for 6 to 9 months (7, 12), possibly due to non-replicating, drug-tolerant bacilli (30). If antibiotic treatment ceases before sterilization, the infection can reactivate to the disease state (31, 32). Continuous antibiotic administration is necessary for up to 6 months to clear MTB infections completely. TB antibiotics come with their own complications and side effects, potentially causing nausea, hepatotoxicity and nerve damage, which increases non-compliance among patients and complicates treatment. Non-compliance increases the risk of emergence of multi-drug resistant TB (MDR-TB) (33). MDR-TB is defined as MTB strains that are resistant to at least both INH and RIF (7). Treating MDR-TB can require medicating for up to 2 years with less effective second-line antibiotics such as fluoroquinolones. MDR-TB treatment can carry an estimated cost between $10,000 and $435,000 USD per patient (34).

The frontline TB antibiotics were introduced with INH in 1951, followed by PZA in 1952, RIF in 1957, and EMB in 1962 (12). Strains carrying resistance mutations to each drug emerged soon after, and emergence of resistance forms the basis of the current multi-drug regimen (12, 25). In 2012, a new anti-TB drug the ATP synthase inhibitor bedaquiline was approved by the FDA for treating MDR-TB strains (35). There are also several new anti-TB drugs currently in development, but their efficacy in shortening the TB treatment regimen is unclear (11, 36). Because of the length of time and resources required to treat TB, there is need for novel approaches targeting persistent TB infections that could be used in a combinatorial manner with conventional antibiotics to shorten

treatment time. This will require both a better understanding of the pathogenesis of MTB, and the manner in which it persists when challenged by antibiotics.

To test the sterilizing activity of various drug regimens, colony forming units (cfu) of MTB in sputum samples collected from human subjects undergoing antibiotic treatments for TB were determined and shown to decrease by 90% during the first 14 days of treatment with the most rapid killing within the first two days (37). This biphasic curve of killing indicates a heterogenic population of MTB with varying tolerance to antibiotics. When drug-susceptible clinical isolates were exposed to various anti-tuberculosis drugs *in vitro*, it was determined that the duration of persistence in infection could be predicted by the isolates' tolerance to INH and RIF, despite isolates' comparable minimum inhibitory concentrations (MIC) to less antibiotic tolerant strains (30). Caseum from MTB-infected rabbits also contained non-replicating bacilli with extreme phenotypic tolerance to multiple antibiotics (38). From these experiments, it is hypothesized that a subpopulation of MTB are able to tolerate the presence of antibiotics longer, and occurrence of these cells necessitates the extended administration of drugs (13, 38-40). This biphasic killing pattern leaves a small subpopulation of MTB cells that are genetically susceptible to killing, yet display a phenotypic tolerance to antibiotics. The mechanisms by which this phenotypic drug tolerance is established are the focus of much of the current TB research, including this study.

1.3 Drug-Tolerant Persisters of MTB

In 1944, in one of the earliest descriptions of phenotypically drug-tolerant bacteria in the scientific literature, Joseph Bigger described the survival of a small population of staphylococcal bacteria after *in vitro* treatment with penicillin that remained susceptible to killing by the antibiotic

5

when re-cultured in fresh medium (41). He dubbed these cells "persisters", and this difficult-to-kill subpopulation of cells has been observed in all species of bacteria studied thus far (14). The hypothesis of drug-tolerant persisters was extended to MTB in the 1950's when Bulgarian-French physician Georges Canetti described the pathology of human TB lesions and the differing number of bacilli found within various types of lesions, including acellular aggregates encapsulated in matrix in caseating lesions (42). Using a mouse model (which lacks the organized granuloma structure observed in human infections), Robert McCune contributed several key observations regarding the heterogeneic properties of MTB pathogenesis. McCune and colleagues observed that the bacterial burden in the lungs and spleen of mice stabilized after 2 weeks of treatment with antibiotics, regardless of the drugs administered. Further treatment for 3 to 6 months did not sterilize infections despite a low bacterial burden. These persistent bacteria, when isolated and cultured, were still susceptible to antibiotics (43). Further studies demonstrated that growth rates, bacterial burden, and antibiotic susceptibility of MTB isolated from different types of lesions varied (15, 43, 44). This heterogeneity of MTB has also been observed in other animal models, including non-human primates (13) and guinea pigs (45). Later work by Wallis and colleagues with clinical isolates of sputum from human TB subjects demonstrated the link between phenotypic drug tolerance and risk of relapse (30).

Investigation of MTB persisters *in vitro* suggests that their rate of formation increases sharply during late-exponential phase, continuing into early stationary phase, when persisters constitute approximately 1% of the total population. *In vitro* transcriptomic analysis into MTB persisters isolated after exposure to D-cycloserine identified downregulation of pathways involved in metabolic processes and biosynthetic pathways, and an induction of a small subset of genes associated with dormancy. A total of 1,408 genes were downregulated at least 2-fold, compared to

282 upregulated by at least 2-fold (46). This large number of downregulated genes concentrated in biosynthesis and growth-related pathways compared to a smaller set of upregulated genes indicates a tendency toward dormancy, but the genetic expression profile of *in vivo* MTB persisters remains unknown. The metabolic downshift was similar to that previously observed in *Escherichia coli* persisters (47, 48). Genes encoding ribosomal proteins were downregulated with the exception of a single 4-gene operon: *rpsR2-rpsN2-rpmG1-rpmB2*. Other pathways that were downregulated included cellular respiration, glycolysis, electron transport, and oxidative phosphorylation (46). Analysis of MTB isolated from heterogeneous lesions determined MTB exists in a variety of growth stages with different susceptibilities to antibiotics (15, 43, 44). There currently have not been any persister genes identified in MTB, but the genetic factors that control persister formation have been reported in other bacterial species, especially the laboratory workhorse *E. coli*. Most notably, the toxin-antitoxin (TA) module in *E. coli*, HipAB, has been implicated in determining the frequency of persisters (46, 47, 49, 50). *In vitro* MTB persisters were also found to overexpress ten toxin-antitoxin (TA) modules, but their role in persister formation is unknown (46).

1.4 Mechanisms of Persister Formation

When studying bacterial susceptibility to antibiotics, it is vital to differentiate phenotypic drug tolerance from genotypic resistance. Genotypic resistance refers to bacteria that have acquired a genetic mutation that renders a specified antibiotic ineffective. For example, MTB resistance to RIF in clinical isolates most often arises from mutations in a common region of the *rpoB* gene, which encodes RIF's target: the beta subunit of RNA polymerase (51). Resistance mutations are acquired randomly during DNA replication, and amplified under selective pressure of antibiotic

7

exposure, or through horizontal gene transfer (HGT). Although there is no evidence of HGT-conferred resistance in MTB, HGT has been observed experimentally in pathogenic *M. canetti* strains (52), and notably, in *M. smegmatis* biofilm formation facilitated conjugative HGT (53).

Conversely, antibiotic tolerance is described in phenotypic terms. Phenotypically drug tolerant bacteria transiently display less killing by antibiotics by responding to changes in their environment and remodeling their gene expression profiles, altering their growth rate, metabolism, and/or lifestyle. This includes growth arrest or a slow-growing state, induction of genes for enzymes that modify the antibiotic target, drug efflux pumps to remove concentrations of the antibiotic from the target cell, and formation of multicellular aggregates called biofilms. Phenotypic drug tolerance via each of these mechanisms is described in the following subsection

1.4.1 Growth Arrest and Metabolic Downshift

Downshift in metabolic processes leading to growth arrest is a common state for drug tolerant bacteria. Several classes of antibiotics, target only actively growing bacteria, rendering non-replicating bacteria unsusceptible to killing. Animal models have implicated a non-replicating population of dormant cells in persistent MTB infections (54, 55). In the case of MTB, this includes frontline antibiotic INH which targets a cell wall biosynthesis enzyme involved in MTB's fatty acid synthetase II (FAS-II) generation of long-chain fatty acid precursors of mycolic acids (56). There are multiple conditions in the host that may lead to growth arrest of MTB. Indeed, *in vitro* growth models of nutrient starvation, hypoxia, low pH, and stationary phase all affect growth rate of MTB and susceptibility to INH (46, 48, 57, 58). Increasing concentrations of ciprofloxacin, a DNA gyrase-targeting, fluoroquinolone class antibiotic, and an alternative treatment for MDR-TB, has no effect against non-replicating MTB as well (46). RIF, which targets the beta subunit of

RNA polymerase, and is therefore capable of killing all metabolically active cells, is also less effective against slow-growing cells. For comparison, in one study, a 64-fold increase in INH concentration and a 4-fold increase in RIF concentration was required to achieve equivalent killing activity in metabolically slow cultures compared to rapidly-growing cultures (59). Additionally, subjecting MTB to a combination of nutrient starvation, low pH, hypoxia and high carbon dioxide simultaneously produced cells more tolerant to RIF than previous studies using hypoxia alone (60). These data indicate that the stress and growth limitations that push MTB to growth arrest impact the nature of multidrug tolerance. It has therefore been hypothesized that MTB persisters arise from stochastic fluctuations in metabolism and gene expression, comparable to other species of pathogenic bacteria (14).

Bacterial commonly respond to environmental stress by altering their genes expression profile via the stringent response. Transcriptomic analyses of persisters of both *E. coli* and MTB show downregulation of various growth related and biosynthetic pathways (46, 47). The alarmone guanosine tetra- or pentaphosphate [(p)ppGpp] signals the stringent response in bacteria to multiple environmental stressors: amino acid starvation, heat shock, iron limitation, etc. Accumulation of (p)ppGpp in cells alters the transcriptional profile and decreases the synthesis of translational machinery like tRNA and rRNA (61, 62). During the stringent response, (p)ppGpp slows mRNA synthesis by binding stable RNA polymerase, facilitating the binding of alternate sigma factors to "stringent" promoters (63, 64). The stringent response has been linked to persister formation through the activation of toxins of TA systems (65, 66). In a "high persistence mutant" (*hip*) *hipA7* mutant background of *E. coli*, deletion of *relA* and *spoT,* which synthesize (p)ppGpp, results in the loss of persister formation, while ectopic, plasmid-borne expression of *relA* in *hipA7*/*relA* double mutants increased persister frequency by 100-fold or more (65). These findings

suggest that induction of *relA,* and subsequent accumulation of (p)ppGpp, increases persister frequency in *hipA7* mutants of *E. coli*. In MTB, (p)ppGpp is synthesized by bifunctional *Rel$_{MTB}$*. *Rel$_{MTB}$* is required for chronic infection in both mice and guinea pigs (67, 68) and also linked to drug tolerance and biofilm formation (69). *Rel$_{MTB}$*-deficient MTB fails to slow replication rate and was metabolically similar to exponentially growing WT MTB during nutrient starvation. The deficient strain was also more susceptible to killing by INH during both nutrient starvation and chronic infection in mouse lungs (70).

Protein synthesis is also interrupted to induce antibiotic tolerance of persisters (48). During stationary phase, bacteria become highly tolerant to the ribosome-targeting aminoglycoside class antibiotics. Ribosomes hibernate by dimerizing into translationally inactive states via hibernation promoting factor (HpF) and ribosome modulation factor (RMF). Deletion of *hpf* in *Listeria monocytogenes* and deletion of *rmf* in *E. coli* resulted in increased sensitivity to gentamycin during stationary phase (71). Zinc starvation acts as a trigger for ribosome remodeling that implicated in antibiotic tolerance of mycobacteria. During zinc starvation, zinc-free paralogs of ribosomal proteins replace the zinc-bindings ones active in zinc-rich conditions. Zinc-starved *M. smegmatis* remodels ribosomes into an inactive, aminoglycoside-resistant state via binding of mycobacterial Y protein (MPY) and MPY recruitment factor (MRF) to ribosomes. MPY structurally stabilizes the inactive, zinc-free ribosomes and also inhibits aminoglycoside binding. Induction of genes encoding the zinc-free ribosome paralogs during mouse infection with MTB implicates ribosome hibernation as another possible mechanism for MTB's recalcitrance to antibiotics *in vivo* (72).

1.4.2 Drug Efflux Pumps

It is common among bacteria to induce genes that encode drug reflux pumps to lower exposure to antibiotics (73). This mechanism of phenotypic drug tolerance renders bacteria intrinsically resistant to killing. In the opportunistic pathogen *Pseudomonas aeruginosa*, mutation of the component genes encoding efflux pump MexAB-OprA results in the creation of more drug sensitive strains (74). Multidrug efflux pumps and antibiotic tolerance have been described in multiple Gram-negative pathogens including *E. coli*, *Salmonella enterica*, and *Neisseria gonorrhoeae* (75). In methicillin-resistant *Staphylococcus aureus* (MRSA), a Gram-positive pathogen notorious for its recalcitrance to antibiotic treatment, overexpression of multidrug efflux pump NorA has been identified in clinical isolates (76).

Mycobacteria display drug tolerance through a combination of impermeability of their lipid-rich cell walls and activation of single component drug efflux pumps as well. Mutations in efflux pump genes of MTB have also been linked to emergence of antibiotic resistance (77). LfrA was the first efflux pump characterized in mycobacteria for its ability to induce resistance to fluoroquinolones in *M. smegmatis* when expressed on a plasmid (78). Induction of efflux pumps has been identified in clinical isolates of mycobacteria that are multidrug tolerant (79, 80). In at least two pathogenic mycobacterial species, MTB and *Mycobacterium avium*, macrophage infection can induce expression of efflux pump genes that make the bacteria more tolerant to treatment with RIF within 4 days post-infection (81). Induction and regulation of efflux pumps in mycobacteria appears linked to virulence and responding to hostile host environs (75), though the relationship between infection, persistence in the host, and efflux pumps is not understood. Recent research has identified efflux pump inhibitors can restore antibiotic susceptibility in mycobacteria, demonstrating a potential therapeutic counter to one mechanism of multidrug tolerance (81-83).

1.4.3 Toxin-Antitoxin Systems

One of the first genetic determinants of persister formation discovered was *hipA* in *E. coli*. Starting in the 1980's, *hip* mutants were isolated from *E. coli* cultures as being phenotypically more tolerant to multiple antibiotics (57, 84). It was later determined that an allele *hipA7* resulted in ~1000-fold increase in persister frequency after exposure to ampicillin and increased persister frequency following exposure to antibiotics of the fluoroquinolone and aminoglycoside classes as well (85, 86). Despite this increased tolerance, *hipA7* mutants display similar MIC to antibiotics as WT strains separating them from genetically resistant mutants. HipA has since been revealed to be a toxin in a TA module, a common component of intrinsic tolerance to antibiotics in bacteria (85).

TA modules typically consist of a two gene operon with the antitoxin situated directly upstream of its corresponding toxin gene. Generally, toxins bind to a specific target that alter the cell's growth rate, but during normal growth are inactivated by their corresponding antitoxins. Antitoxins tend to be quickly degraded by cellular proteases. In the case of *hipAB* TA, HipA phosphorylates elongation factor TU to stop protein synthesis. When antitoxin HipB is present, it binds HipA and the complex is degraded (49, 85). Studies investigating the regulation of TA-mediated persister formation have linked genes of the stringent response *spoT, relA,* and *dksA* in *P. aeruginosa* to antibiotic tolerance of quinolones (87) and *phoU* to tolerance of multiple antibiotics and stressors in *E. coli* (88). In *E. coli*, the TisB toxin acts as mechanism of persister formation in an ATP-dependent manner to trigger dormancy, and was induced by exposure to the DNA-damaging antibiotic ciprofloxacin. Deletion of the TisAB also resulted in reduced persister frequency (50). Drops in intracellular ATP levels as part of the stringent response has also been demonstrated as an inducible mechanism of persisters in *E. coli* (89).

As previously mentioned, TA modules are reported to be overexpressed in persister cells of multiple bacterial species. This could be due to stochastic induction of toxin genes that result in slow-growing and drug tolerant cells representing a substantial proportion of the surviving subpopulation. Another potential mechanism of TA-mediated drug tolerance is that expression of toxin genes could result in inactive targets for antibiotics to bind to in persister cells. MTB persisters that overexpress toxin genes, do not demonstrate the same multidrug tolerance as their *E. coli* counterparts. Ten TA modules were overexpressed in MTB persisters, yet each module significantly increased tolerance to only a single antibiotic (46). Some MTB TA modules, including MTB's three *relE* toxin homologs, are physiologically upregulated under specific stresses, but unlike *E. coli*, their effect on antibiotic tolerance is limited (90, 91). A potential explanation for this difference from *E. coli* is that toxin overexpression in MTB is more driven by specific environmental conditions rather than stochastically, and result in subpopulations of persisters specialized to survive across a variety of conditions.

1.4.4 Bacterial Biofilms Produce Persisters

Bacteria of a multitude of species form biofilms, and more than half of clinically associated bacterial infections are biofilm related (92). Chronic infections of *P. aeruginosa* in cystic fibrosis, polymicrobial infections in gingivitis, and colonization of medical devices and implants are well studied examples of biofilm-associated infections (93-97). Treatment of infectious biofilms is often challenging as the resident microbial population acquire extreme tolerance to antibiotics (98, 99). For these reasons, the process of biofilm formation, maturation, and the regulation of this process, warrant an in-depth examination.

1.5 Biofilms

Biofilms are sessile, multicellular communities of microbes that contain phenotypically heterogeneous populations of cells encapsulated within extracellular matrix (ECM) (Fig. 1) (99-103). Attachment of individual cells to a substratum, and to each other, is followed by growth of cellular aggregates into complex three-dimensional architecture (104). Growth and development of planktonic cells into biofilms is a multi-stage process that requires dedicated genetic programs in a temporal order, from substratum attachment to matured architecture (Fig. 1) (105-107). The term biofilm was first coined by JW Costerton to describe the slick, slimy community of microbes present on the surface of rocks in a stream bed. Using electron microscopy, Costerton and colleagues described adherent, multicellular communities of microbes growing on the surface of medical devices and surgical implants and encapsulated in exopolysaccharide (EPS). These communities developed into organized structures and were also highly tolerant to antibiotics. This work also importantly established that biofilms rather than a unicellular bacterium were the predominate lifestyle of bacteria in both environmental and clinical settings (108-111).
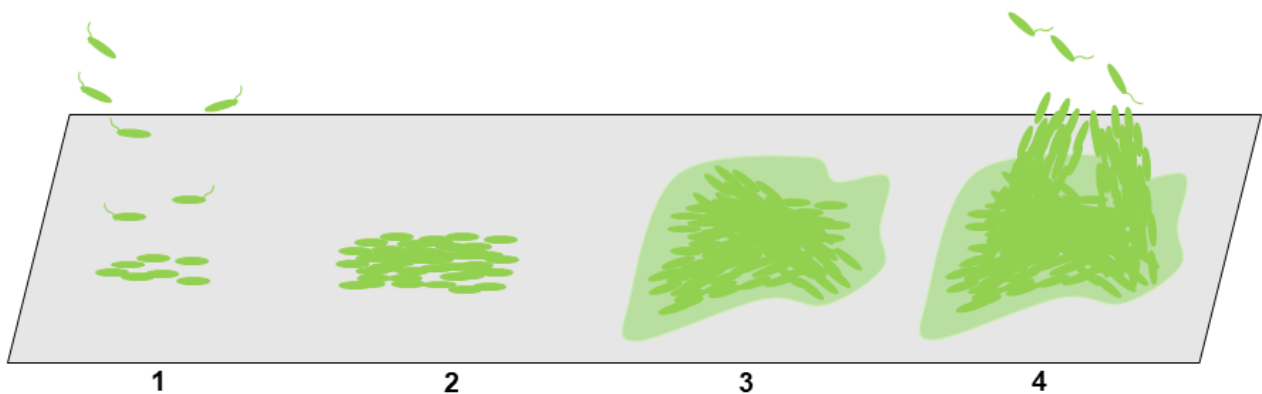
Figure 1: Schematic representation of the developmental stages of microbial biofilms

Attachment (1): Microbes attach to substratum; motility factors are suppressed while adhesion factors are upregulates. Sessile growth (2): Attached cells divide and begin to grow into three-dimensional structures; intracellular communication occurs. Maturation (3): ECM is produced; complex architecture forms. Dispersal (4): Quorum sensing and disassembly factors shed motile cells.

1.5.1 Architecture and ECM

Microscopic analysis of biofilms across many bacterial species reveals cells growing in sophisticated architecture encapsulated in ECM. CLSM investigation into biofilms of *Pseudomonas fluorescence* revealed mushroom shaped structures with thin stem-like portions and round bulb like portions raised toward the top of the biofilm (112). Biofilms also universally have water channels that it is hypothesized to facilitate oxygen and nutrient diffusion throughout the inner components of architecture (113). In the case of *P. aeruginosa*, it has been demonstrated that particles as great as 5 microns in size can flow through these channels unrestricted (114). ECM production comes at significant energy cost, yet is crucial to the maturation of biofilms and protection from exogenous stress (98, 109, 115, 116).

The components of ECM in bacterial biofilms varies from species to species and even from strain to strain within a species. There are, however, some common components observed to be present in biofilm ECM. EPS is commonly a principal component of ECM in Gram-positive and Gram-negative bacteria (108, 111, 117). Extracellular DNA (eDNA) serves a structural component in ECM of *P. aeruginosa* and *S. aureus* biofilms (118, 119). Adhesive proteins are also often present within the ECM. A group of adhesive proteins in *S. aureus* call biofilm-associated proteins (Bap) are sufficient to produce mature biofilms even without EPS suggesting multiple pathways to maintaining structural integrity during biofilm maturation (120). In *Vibrio cholerae*, the causative agent of cholera, Bap are required for rugose colony types and biofilm formation and the

production of *Vibrio* polysaccharides necessary for biofilm ECM (121, 122). Strains with mutation in the *vps* gene cluster also showed deficiency in colonizing the mouse intestine (122). In *Bacillus subtilis*, mutation of the *tasA* gene results in loss of production of extracellular matrix during biofilm growth, thereby disrupting the spatiotemporal organization of motile and sporulating cell types, implying that matrix production and architectural maturation are necessary for the phenotypic differentiation in biofilms (123, 124). Type IV pili in *P. aeruginosa* and type I fimbria and curli in *E. coli* are required for cell-to-cell and cell-to-surface adhesion (106, 125, 126). Structural proteins such as these may also create scaffolding for EPS and stabilize biofilm architecture (124, 126, 127). Physical contacts and chemical communication among cells, as well as physiological adaptation to self-generated heterogeneity in microenvironments during development of biofilm architecture, appear to play an important role in development of biofilm-specific traits (99, 123, 128).

1.5.2 Phenotypic Heterogeneity

Perhaps the most remarkable aspect of microbial biofilms is the rich phenotypic heterogeneity within a clonal population (129). The phenotypic diversity is presumably responsible for the establishment of many biofilm-specific traits including antibiotic tolerance. In *P. aeruginosa* biofilms, cellular growth only occurs at the outer edges of the community. This was demonstrated through fluorescent microscopy with an expression reporter, the promoter region of growth-rate dependent gene *rrnBP1* fused to a green fluorescent protein, in *P. aeruginosa* biofilms (130). Differential growth rates and cell-to-cell variations in gene expression are the result of cellular response to non-uniform environmental conditions across different strata of the biofilms, including limitations to nutrients and oxygen (123, 131, 132).

1.5.3 Genetic Control of Biofilm Development

Biofilm development is associated with gene regulation both in space and time that also partly define distinct developmental stages. Each developmental stage in biofilm growth has specific genetic requirements regulated through hierarchal processes (105-107). Motility genes like those producing flagellar proteins are downregulated in *E. coli* after substratum attachment, while genes involved in sessile growth and matrix synthesis are induced (106). Attachment of *P. aeruginosa* to a substratum is first reversible, followed by an irreversible attachment stage and two distinct phases of maturation that can be identified by the activity of several genetic factors. Activity of *bfiS* is required to transition from reversible to irreversible attachment stages. Maturation phases involve expression of two-component regulatory system genes *bfmR* for early maturation, and then *mifR* activity for late maturation. Inactivation of all three factors arrested biofilm formation at the reversible attachment stage but does not affect planktonic growth, motility or initial attachment (105). Similarly, genetic requirements in *V. cholerae* vary in the monolayer growth and biofilm maturation. Mutations in *cheY-3* resulted in deficient monolayer formation but normal biofilm maturation while deletions of *bap1* and *leuO* formed normal WT-like monolayers but displayed decreased accumulation of ECM (133). Transcriptomic and proteomic analysis of *B. subtilis* pellicle biofilms revealed extensive metabolic remodeling during biofilm development. Notable findings included intracellular changes in concentration of metabolites during biofilm development, increased activity of the tricarboxylic acid (TCA) cycle and *de novo* nucleotide synthesis during early biofilm growth, transient induction of *eps* and *tasA* genes despite stable accumulation of TasA protein, fatty acid degradation as compared to biosynthesis, induction of iron acquisition genes, and a change in fermentation of acetate to acetoin (134).

17

In some *Pseudomonas* and *Burkholderia*, signaling by second messenger cyclic diguanosine-5'-monophosphate (c-di-GMP), small RNAs (sRNA), and quorum sensing (QS) play a role in regulating production of ECM components like EPS and eDNA, or bacterial dispersal, though the molecular mechanisms for this are not identified (135). QS-mediated dispersal could be considered the final stage of biofilm development. Signaling molecules responding to biofilm population density via environmental cues (i.e. changes in nutrient concentration) alter the genetic expression of individual cell which disperse from the biofilm structure. Some of these cells may be genetic variants specialized for colonization of new surfaces (136).

1.5.4 Microbial Persistence Through Biofilms

Bacterial biofilms acquire extreme antibiotic tolerance both clinically and *in vitro* (98, 99). Tolerance is likely contributed by multiple factors including limited diffusion of antibiotics through the ECM, slow growth and metabolism of cells in the interior of biofilms, physiological adaptation to heterogeneous microenvironments, and increased activity of efflux pumps (137-144). Biofilms exhibit multidrug tolerance under antibiotic exposure when compared to single cell bacteria (115). These multicellular aggregates are encapsulated in ECM that create a less penetrable barrier to antibiotics and host immune factors (98, 145-147). The architecture and organization of biofilm superstructure also creates microenvironments via a gradient of conditions throughout the biofilm which leads to the generation of multiple subpopulations within the biofilm with varying growth rates and genetic expression profiles—two key inducers of phenotypic antibiotic tolerance (98). As might be expected, biofilms of some species have shown induction of efflux pump and TA modules and downregulation of metabolic genes. This results in communities

of cells remarkably tolerant to multiple antibiotics through a variety of mechanisms and harboring subpopulations of specialized persisters.

Biofilms of some pathogens also persist through evasion of the host immune system; cells in biofilms are resistant to phagocytosis by macrophages (148, 149). *P. aeruginosa* forms biofilms in the host during long term infections of cystic fibrosis patients. ECM components produced by *P. aeruginosa,* alginate and rhamnolipid subvert host immunity via protection from IFN-γ or macrophage phagocytosis and induction of necrosis of leukocytes, respectively (147, 150). *S. aureus* biofilms have been shown to subvert the T-cell mediated inflammation in a mouse model away from the effective regulation of the immune response for clearing the infection (151).

1.6 Mycobacterial Biofilms

Mycobacteria have a strong tendency to attach to substrata and clump together when cultured *in vitro*. The addition of surfactants such as Tween-80 and tyloxapol to culture media is necessary to obtain the single-cell planktonic suspensions required for much experimental work, but this method leads to fundamental changes in the physiology of the bacteria. Aggregated growth of mycobacteria is both commonly found in the environment as well as in certain clinical settings, and generates traits and challenges altogether unique from studying these microbes at the level of an individual cell. Mycobacterial biofilm development is also characterized by distinct genetic requirements for aggregation and maturation stages (107), and biofilms of this genus are detailed in-depth below.

1.6.1 Mycobacterial Biofilms in Environmental and Clinical Settings

Many mycobacterial species thrive in wet soil and on wet surfaces. A 2005 review reported that 33 of the approximately 100 different species of mycobacteria had been isolated from water distribution samples. Several investigations into water distribution systems, with a history of testing positive for mycobacterial contamination, identified members of the genus growing in polymicrobial biofilms attached to the surface of water pipes as the reservoirs for contamination (152). Multiple *Mycobacterium* ssp., some of them opportunistic pathogens, including *Mycobacterium kansasii*, *Mycobacterium flavscens*, *Mycobacterium chelonae*, *Mycobacterium gordonae*, *Mycobacterium tarrae*, *Mycobacterium xenopi*, *Mycobacterium fortuitum*, *Mycobacterium intracellulare,* and *M. avium* were identified in the biofilms (152-157). Commonly detected mycobacterial species grew in biofilms attached to the surface of water pipes and were more resistant to chlorine, ozone, and UV based disinfectant methods (152, 157). Mycobacteria was more likely to attach to organic substrates such as plastics and rubber than inorganic substrates like copper and glass (155).

Mycobacterial biofilms have also been detected on other aquatic environments of public health relevance. Growing biofilms of the opportunistic pathogen *M. avium* were identified attached to the side surfaces of hospital therapy pools (158). The livestock pathogen responsible for Johne's disease, *Mycobacterium. avium* subsp. *paratuberculosis*, survives in biofilms attached to steel surfaces in the drinking troughs of ruminants (159). Various species of non-tuberculosis mycobacteria (NTM) were found growing in biofilms in the waterlines of dental units leading to potential infection of patient oral wounds (160). Metagenomic DNA sequencing of biofilms collected from household showerheads in the United States identified NTM species enriched greater than 100-fold over the background levels detected in water distribution systems.

Particularly, *M. avium* complex subspecies were enriched in the showerheads, identifying a potential source of aerosolization and pathogen exposure (161).

In vitro studies demonstrate the propensity of mycobacterial species to grow in the multicellular biofilms that develop through dedicated genetic processes, and exhibit enhanced tolerance to disinfectants and antibiotics. PVC-attached biofilms of the rapidly-growing model organism *M. smegmatis* have a MIC twice that of planktonic cells (162). Under both low and high nutrient conditions, NTM species *M. fortuitum* and *M. chelonae* form *in vitro* biofilms, and *M. fortuitum* forms surface-attached biofilms as soon as 48 hours after inoculation (163, 164). *M. xenopi,* a cause of nosocomial infections, readily formed biofilms *in vitro* on PVC piping typically used for water distribution systems (165). Colonies of *M. chelonae* and an emerging NTM pathogen *Mycobacterium abscessus* were grown by inoculating PVC pipes with contaminated water. The NTM species survived exposure for seven days to several common disinfectants including ammonium, iodophor, chlorine, phenolic detergent, or glutaraldehyde based solutions, and were able to reestablish biofilms following disinfectant exposure (166). Clinical isolates of *M. avium* cultured as biofilms were more resistant to common biocides than high volume planktonic cultures. The presence of Zn^{2+}, Ca^{2+}, and Mg^{2+} ions correlated with increased biofilm formation, while subinhibitory concentrations of the antibiotics amikacin and clarithromycin present in the supernatant decreased surface attachment biofilm growth (167, 168). *M. avium* has also been shown to adhere to catheters and form biofilms which display tolerance to clarithromycin and RIF. Interestingly, when *M. avium* cells grown in the catheter biofilms were dispersed immediately prior to antibiotic exposure, they still remained more tolerant, indicating the bacteria had undergone physiological changes during biofilm development that induced tolerance to antibiotics (169). This could be due to adaptation to biofilm microenvironments, such as decreased access to

nutrients or oxygen, or an arrest in growth, suggesting that origins of increased antibiotic tolerance is not simply because physical protection by the architecture.

Scanning electron microscopy (SEM) of *in vitro* biofilms of NTM species *M. fortuitum* and *M. marinum* revealed a morphologically distinct architecture between the two species. *M. fortuitum* formed filamentous strands with EPS, while the slower growing *M. marinum* formed more typical microcolonies. Biofilms of both species contained water channels typical of all microbial biofilm architecture. *M. fortuitum* biofilms were more resistant to biocides than planktonic cells, but *M. marinum* biofilms were as or more susceptible to killing than planktonic cells (170). This potentially suggests the more sophisticated biofilm architecture and EPS of *M. fortuitum* contributes to its increased tolerance to biocides compared to planktonic suspension, which was not observed in *M. marinum*. In a later investigation of *M. marinum* biofilms by CLSM, *M. marinum* biofilms grew in a distinct cording morphology with EPS production contrasting with the previous report. This difference may be due to loss of architecture during the dehydration process for preparing samples for SEM. *M. marinum* prefers to form biofilms on hydrophobic surfaces, suggesting that the properties of the substratum surface could play a role in NTM biofilm development (171). *M. fortuitum* cultured from the blood of a patient with prosthetic valve endocarditis with acid-fast bacteria in EPS attached to the prosthetic further indicates a role of NTM biofilms in pathogenesis in the clinic (172).

Evidence of a relationship between mycobacterial biofilms and pathogenesis is demonstrated in the case of *Mycobacterium ulcerans,* the cause of Buruli's ulcers, an emerging pathogen in slow-moving water in Africa and Australia. *M. ulcerans* not only grows in environmental biofilms on aquatic plant species as a source of transmission, but also forms *in vivo* biofilms in extracellular compartments that provide protection against host antimicrobials and

produce ECM rich in vesicles containing the polyketide toxin mycolactone (173-175). *In vivo* biofilms of *M. ulcerans* increased the transmissibility from the host *Naucoris cimicoides* to humans by colonizing the water bug's salivary glands, and also formed biofilms on its legs in later stages of infection (174-176).

1.6.2 Genetics of Mycobacterial Biofilms

Similar to other biofilms, mycobacterial biofilms develop through distinct stages: attachment, aggregative growth, and maturation. Development is controlled through sequential regulation of genetic expression for each stage (107). This is exemplified by identification of some of the genetic requirements for each stage in the rapidly growing model organism *M. smegmatis*. Transposon disruption of the gene *mps* in *M. smegmatis* results in loss of sliding motility and biofilm formation on PVC substrates. Lipid analysis revealed a lack of glycopeptidolipids (GPLs), a component of the outermost layer of the cell wall, in the *mps* mutant (177). Inactivation of the nucleoid-associated protein Lsr2 in *M. smegmatis* had pleiotropic effects including increased "hyper" sliding motility, changes to a smooth, shiny colony morphology, and loss of biofilm formation (178, 179). A suppressor mutation in the GPL biosynthesis gene *mps* in an *lsr2* knockout background results in hyper aggregation and restoration of biofilm formation free of GPLs (107). This indicates GPLs, and sliding motility, have a role in attachment, but are not required for the aggregation phase of biofilm development. GroEL1, a chaperonin protein involved in the synthesis of mycolic acids, is required for maturation of biofilms in *M. smegmatis*, but not attachment (116). Additionally, mutation of *mps* in a *groEL1* mutant background does not rescue the immature biofilm phenotype, further demonstrating the distinct genetic requirements for different stages of biofilm development (107).

Furthermore, GPL is also required for biofilm development in *M. avium* (180). GPL modulates the host immune system during infection linking biofilm and virulence requirements (181). Biofilm defective mutants of *M. avium* are also unable to translocate across bronchial epithelial cells and fail to colonize the host (167, 182). Whether biofilms of *M. avium* directly play a role in pathogenesis *in vivo* is not understood.

While free mycolic acids (FM) are an abundant extracellular component of mature biofilms of both *M. smegmatis* and MTB biofilms (116), regulation of FM synthesis appears to be different in the two species. FM synthesis in *M. smegmatis* biofilms is dependent of GroEL1, but the chaperone is dispensable for FM synthesis in MTB (183, 184). FM produced by *M. smegmatis* and MTB in biofilms differ structurally, with alpha- and epoxy-FM predominating in *M. smegmatis* and methoxy-FM in MTB, indicating similar yet distinct structural component in each species' biofilms (183). FM of MTB biofilms are further structurally differentiated from planktonic cells which predominately synthesizes FM esterified to trehalose and other sugars (185). Mutation of *mmaA4*, a gene in the mycolic acid biosynthetic pathway in MTB, disrupts the formation of antibiotic tolerant biofilms by the pathogen, further demonstrating the importance of FM in the structural development of MTB biofilms (186). Mycolyl diacyl glycerol (MDAG) has also been reported as a required product of *M. smegmatis* biofilms in mutagenesis studies (179). Genetic disruption of polyketide synthase genes *pks16* and *pks1/15* result in loss of MTB biofilm formation (184, 187). Polyketide synthase genes are required for production of immunomodulatory phenolic glycolipids (PGL). Deletion of lipid transporter Mmpl11 in MTB resulted in morphologically altered biofilm formation with less FM, loss of survival in nutrient and oxygen depleted conditions, and loss of persistence in an *in vitro* granuloma (188). These studies together link genetic requirements for biofilms to virulence in mycobacteria. Consistently across species, mycobacterial

biofilms require the genetically regulated synthesis of lipid-containing molecules for structural development and maturation.

Transcriptomic analysis of *M. smegmatis* colony biofilms in the *lsr2* mutant compared to the *mps* suppressor showed an indirect role in biofilm formation for Lsr2 by negative regulation of a set of genes whose increased expression in the *lsr2* mutant was restored in the double mutant. A group of genes dedicated to importing iron, a required nutrient for mycobacterial biofilm formation (189), were induced in the double mutant in the early aggregation stage, while 83 of the genes restored by the *mps* suppressor mutant were induced in late stage biofilm development after establishment of Lsr2-dependent aggregated growth (107, 189). A set of 51 of those 83 genes are under the control of the nitrogen-starvation sensing regulator GlnR (107). A group of 8 ORFs (open reading frames) under the control of GlnR confer resistance to peroxide upon induction during biofilm growth, and thus have been termed the "GlnR-dependent peroxide resistance" *gpr* cluster. Conserved across several NTM species, *gpr* provides a potential explanation for mycobacteria's resistance to peroxide-based sterilization in nosocomial settings (190). Induction of three genes encoding ammonium transporters under the control of GlnR were not induced in the *groEL1* mutant in a biofilm-specific manner, indicating nitrogen import requirements of late stage biofilms occur after a GroEL1-depdendent checkpoint (107). This illustrates the sequential pattern of gene expression between early and late stage maturation in *M. smegmatis* biofilms. This pattern is presumably driven by dynamic changes in nutritional demands and environmental conditions.

1.6.3 MTB Biofilms Harbor Drug Tolerant Persister Cells

In vitro mycobacterial biofilms exhibit increased phenotypic tolerance to multiple antibiotics (162). When grown in pellicles at the air-medium interface, MTB biofilms harbor drug-tolerant persisters (184). Comparing MTB WT to a biofilm defective *pks16* mutant, and exposing cultures to INH and RIF in both planktonic and pellicle cultures revealed that WT biofilms harbored significantly more persisters than planktonic: a difference of ten-fold and 10^4-fold to each antibiotic, respectively. For the *pks16* mutant strain, which fails to form a pellicle, this biofilm-dependent phenotypic tolerance was abrogated.

Biofilm-dependent phenotypic tolerance to antibiotics is most likely due to a combination of extrinsic factors and physiological changes in the constituent bacteria. The structure of the biofilm itself may provide some protection from antibiotic penetration, although supporting evidence is yet to be obtained. Lipid-rich ECM of MTB biofilms also likely protects bacteria from exposure. Mutants that form structurally deficient biofilms in both MTB and *M. smegmatis*, even when the genetic source of the defect are functionally unrelated, are more sensitive to antibiotic exposure (184). This indicates that the maturation of the mycobacterial biofilm architecture is a key component to developing phenotypic tolerance. Heterogeneous microenvironments within the biofilm also produce a gradient of nutrient and oxygen availability. This could create fluctuations in gene expression and changes in growth rate and metabolism that are often associated with phenotypic tolerance. Asymmetric growth has also been associated with phenotypic tolerance to antibiotics in mycobacteria (191), and deletion of non-conserved divisome component LamA in MTB results in less phenotypic heterogeneity and more rapid killing by RIF and cell wall targeting antibiotics (192). Hypothetically, mycobacteria responding to biofilm microenvironments could

develop an increased phenotypic tolerance through multiple mechanisms described, though this has yet to be specifically investigated.

1.7 Possibility of Clinical MTB Biofilms

As early as 1955, researchers noted extracellular MTB aggregates in infected host tissues (193). In guinea pigs infected with MTB and treated with an experimental compound, persisters predominantly survived in the acellular rim of granulomas in multicellular aggregates (27). MTB forms pellicle biofilms *in vitro* that demonstrate a typical biphasic killing pattern and harbor antibiotic tolerant persisters (184). This pattern of phenotypic tolerance is similar to that observed in clearance of bacterial burden in clinical isolates from sputa demonstrated by Jindani et. al (37), raising the question as to if MTB forms persistent biofilms in the host. While latent TB has been characterized as dormant, non-growing cells, immunological studies demonstrate TB at the latent end of the spectrum actively engages with host immune cells, contains actively replicating bacteria, and displays heterogeneity in lesion structure and response to antibiotics (54, 194-196). Aggregation of MTB is a potential long-term persistence strategy against the stress of host defenses that needs to be further investigated. The FM and lipid rich ECM produced by MTB biofilms could hypothetically shield replicating or non-dormant persistent bacteria from host defenses by not eliciting inflammatory responses from host immune cells. Whether or not MTB biofilms form *in vivo* remains unproven, but *in vitro* biofilms provide an insightful model for studying the generation of phenotypically tolerant subpopulations.

1.8 Practical Challenges of Investigating MTB Biofilms

As noted above, MTB naturally clumps together during *in vitro* culturing without the addition of surfactants due its lipid-rich cell wall and hydrophobic properties. While single-cell planktonic suspensions are convenient for enumerating bacterial quantity, the growth conditions change the surface properties of MTB, and differ sharply from the conditions encountered by bacteria in the host. Biofilm growth methods overlap with some of these conditions including heterogenic microenvironments, nutrient and oxygen availability gradients, and cell-to-cell attachment and communication. Culturing MTB in biofilms does carry several complications, however. With a doubling time of 18-24 hours under ideal conditions, it takes 3-5 weeks for MTB to form the three-dimensional architecture that constitutes a significant portion of its biomass depending on method. Pellicles grown at the air-medium interface represent the most robust form of biofilms, but require the longest incubation period for development. Genetic determinants of biofilms may also differ depending on substratum type, or media chosen as demonstrated previously, and in this study. Many of the traits specific to MTB biofilms are metastable (transient), and lost once the bacteria are removed from the dynamic environments of a biofilm. The spatiotemporal expression of different genetic factors during mycobacterial biofilm growth is evident from the differing genetic factors required for attachment, aggregation, and maturation stages, and sequential induction of gene sets under control of multiple regulators in *M. smegmatis* biofilms described earlier. Also, experiments involving *in vitro* biofilms of MTB must be processed mechanically to break up clumps of constituent bacteria before an accurate number of viable bacteria for comparison to planktonic cultures can be made.

High-throughput DNA sequencing circumvents some of these challenges. Our project attempted to control for these confounding elements by using a rich media in our initial genetic

screen to limit elimination of mutants due to nutritional stress alone, and by screening biofilms grown in pellicles as well as attached to PVC membranes. We focused our efforts on analyzing genetic determinants of multiple *in vitro* biofilm models compared to planktonic counterparts and utilizing CLSM to identify a biomarker for MTB biofilm formation.

2.0 Specific Aims

Infections of tuberculosis (TB), caused by the pathogen *Mycobacterium tuberculosis* (MTB), resulted in 1.6 million deaths in 2017 according to the World Health Organization (11). Treatment requires a 6-month long, multi-drug regimen that overburdens healthcare systems and can include serious side effects for patients. Antibiotics kill the majority of MTB cells early in treatment, yet an extended therapy for TB is necessitated by a subpopulation of MTB that remain recalcitrant to antibiotic exposure without acquiring resistance-associated genetic mutations. However, the mechanisms underlying this phenomenon, called phenotypic drug tolerance, remain largely unclear. Many bacterial species have the propensity to grow in sessile multicellular communities called biofilms, which are highly tolerant to antibiotics. Mycobacteria also spontaneously form biofilms *in vitro* that exhibit phenotypic tolerance to anti-TB drugs. MTB biofilms provide a relevant and useful system for analyzing the molecular mechanisms of phenotypic tolerance.

The long-term goal of our work is to identify the molecular basis of multidrug tolerance in MTB, and potential targets for therapeutics, which can be used in combination with conventional TB antibiotics to shorten the required length of treatment. Our overall goal in this study is to identify genes required for the development of MTB biofilms *in vitro* and their role in antibiotic tolerance, and to develop a biomarker to microscopically investigate the potential of MTB biofilms *in vivo*. We <u>hypothesize</u> that genes required for MTB to adapt to biofilm growth will overlap with genes that contribute to the frequency of phenotypically tolerant persisters due to changes in genetic expression in response to survival within the nutrient-limited, heterogeneous microenvironments of biofilms. Using a high-throughput genomic approach (Tn-seq) and confocal

laser scanning microscopy (CLSM). We sought to understand the molecular basis of adaption of MTB to biofilm growth and its relationship to phenotypic tolerance. We will address our central hypothesis via the following three specific aims:

Aim 1: Define the genes required for fitness of MTB in biofilms. From the Tn-seq analysis of MTB in planktonic and biofilm cultures, I will rank the mutants based on their relative fitness in biofilms. I will then construct isogenic deletion strains and assay their ability to form pellicle biofilms *in vitro.* This will allow me to distinguish between absolute and relative requirement of genes for fitness in biofilms. I will also determine each mutant's susceptibility to rifampicin and the persister frequency of specific mutants of interest.

Aim 2: Characterize the growth environment of MTB biofilms using gene expression analysis. Utilizing a combination of quantitative PCR, RNA-seq, and biochemistry analysis, I will investigate the growth environments of MTB biofilm maturation at the expression level, and nutrients necessary to adapting to MTB biofilm microenvironments.

Aim 3: Develop a fluorescent biomarker for MTB biofilms. By fusing the promoter region of a biofilm-required gene upstream of the green fluorescent protein Dendra-2, I will develop a biomarker specifically induced during biofilm maturation to be tested in multiple mycobacterial strains. If successful, this reporter could be used to investigate whether MTB forms phenotypically tolerant multicellular aggregates (biofilms) *in vivo* as a long-term survival strategy.

3.0 Materials and Methods

3.1 Bacterial Culture Conditions

Unless otherwise indicated, an attenuated strain of MTB, mc^{2}7000 (184), was used as the parent WT in the study. This auxotrophic strain is derived from the virulent laboratory strain MTB H37Rv by deletion of RD1 (Region of Difference 1; *Rv3271-Rv3279c*) and *panCD* (pantothenate biosynthesis genes), and is suitable for use in a biosafety level 2 (BSL-2) facility. For planktonic cultures of mc^{2}7000 or its recombinant strains, cells were grown at 37°C in Middlebrook 7H9 medium (Difco) supplemented with 10% (v/v) albumin dextrose catalase and oleate (OADC) (Difco), 0.05% (v/v) Tween-80 (Sigma), and 100 µg/mL pantothenic acid (Sigma). For plate cultures, Middlebrook 7H11 agar supplemented with 10% OADC, and 100 µg/mL pantothenic acid were primarily used. In experiments to assess the colony morphology, Sauton's medium with 1% agarose and 100 µg/mL pantothenic acid were used. As necessary, zeocin, kanamycin, and hygromycin were added at concentrations of 25 µg/mL, 20µg/mL, and 50µg/mL, respectively while selecting the recombinant strains. For pellicle biofilms, logarithmic phase planktonic cultures of the tested strains were washed twice and then re-suspended in detergent-free 7H9 or Sauton's media and diluted 1:100 into the corresponding detergent-free medium. Pellicles were grown at 37 °C with 4 mL per well in 12-well polystyrene tissue culture plates wrapped in parafilm for 5 weeks. For colonies grown for the Tn-seq, 1:10 dilutions of washed and re-suspended cultures were spotted onto 13mm Whatman polycarbonate membranes (Millipore Sigma, Cat. No. WHA110407), which were then dried for 1 hour to allow cells to attach to the surface. Inoculated membranes were placed on sterilized stacks of cardstock soaked in a pool of either detergent-free

7H9 medium or Sauton's medium inside of a 100 x 35 mm polystyrene culture plate, and then grown at 37 °C for the indicated period of time. Medium was replenished as needed. For *M. smegmatis*, the parental WT mc^{2}155 strain was grown at 37 °C in Middlebrook 7H9 medium supplemented with 10% (v/v) albumin, dextrose, and catalase (ADC) (Difco), and 0.05% (v/v) Tween-80, or in detergent-free Sauton's medium. Agar plates of these medium were used to obtain colonies. For selection of *M. smegmatis*, 150 μg/mL of hygromycin or 25 μg/mL of zeocin was used as necessary. *M. smegmatis* pellicle biofilms were grown in Sauton's medium, as previously described (107). 10 μL of a saturated planktonic culture were inoculated into 10 mL of detergent-free Sauton's medium in 60mm polystyrene culture plates and incubated at 37 °C for 4 days. For molecular cloning, *E. coli* GC5 cells were grown at 37 °C in Luria Broth or on LB agar under antibiotic selection conditions; 100 μg/mL of carbenicillin, 50 μg/mL of kanamycin, 150 μg/mL of hygromycin or 25 μg/mL of zeocin. A complete list of strains, plasmids, and oligonucleotide primers used in this work are listed in Table1, Table 2, and Table 3, respectively.

Table 1 List of bacterial strains used in this study

Name	Remarks	Origin
mc^{2}7000	Auxotrophic, attenuated BSL-2 strain of MTB w/ deletions of RD1 and *panCD*	(184)
mc^{2}7000 Tn-Library	*Himar-1* transposon mutant library in mc^{2}7000, *kan^r*	This study
Δ*fadA2*	deletion of *Rv0243* in mc^{2}7000, *zeo^r*	This study
Δ*ansP2*	deletion of *Rv0346c* in mc^{2}7000, *zeo^r*	This study
Δ*phoT*	deletion of *Rv0820* in mc^{2}7000, *zeo^r*	This study
Δ*pstC2-A1*	deletion of *Rv0929-30* in mc^{2}7000, *zeo^r*	This study
Δ*Rv1111c*	deletion of *Rv1111c* in mc^{2}7000, *zeo^r*	This study
Δ*glgP*	deletion of *Rv1328* in mc^{2}7000, *zeo^r*	This study
Δ*Rv1516c*	deletion of *Rv1516c* in mc^{2}7000, *zeo^r*	This study
Δ*ansA*	deletion of *Rv1538c* in mc^{2}7000, *zeo^r*	This study
Δ*bioA*	deletion of *Rv1568* in mc^{2}7000, *zeo^r*	This study

Table 1 Continued

$\Delta bioF1$	deletion of *Rv1569* in mc^{2}7000, *zeo*^{r}	This study
$\Delta bioB$	deletion of *Rv1589* in mc^{2}7000, *zeo*^{r}	This study
$\Delta Rv2041c$	deletion of *Rv2041c* in mc^{2}7000, *zeo*^{r}	This study
$\Delta cysQ$	deletion of *Rv2131c* in mc^{2}7000, *zeo*^{r}	This study
$\Delta Rv2224c$	deletion of *Rv2224c* in mc^{2}7000, *zeo*^{r}	This study
$\Delta cobC$	deletion of *Rv2231c* in mc^{2}7000, *zeo*^{r}	This study
Δdgt	deletion of *Rv2344c* in mc^{2}7000, *zeo*^{r}	This study
$\Delta hrcA$	deletion of *Rv2374c* in mc^{2}7000, *zeo*^{r}	This study
$\Delta nuoD$	deletion of *Rv3148* in mc^{2}7000, *zeo*^{r}	This study
$\Delta nuoN$	deletion of *Rv3158* in mc^{2}7000, *zeo*^{r}	This study
$\Delta ponA2$	deletion of *Rv3682* in mc^{2}7000, *zeo*^{r}	This study
$\Delta glpK$	deletion of *Rv3696c* in mc^{2}7000, *zeo*^{r}	This study
$\Delta Rv3779$	deletion of *Rv3779* in mc^{2}7000, *zeo*^{r}	This study
$\Delta phoTcomp$	$\Delta phoT$ with pJR14, *zeo*^{r}, *kan*^{r}	This study
$\Delta pstC2\text{-}A1comp$	$\Delta pstC2\text{-}A1$ with pJR15, zeo^r, *kan*^{r}	This study
$\Delta dgtcomp$	Δdgt with pJR08, *zeo*^{r}, *kan*^{r}	This study
$\Delta inlps$	deletion of Rv0096-0101 in mc^{2}7000, *zeo*^{r}	This study
$\Delta inlps\_$comp	$\Delta inlps$ with cosmid 3D11.2.cm5, *zeo*^{r}, *hyg*^{r}, *CB*^{r}	This study
mc^{2}155	High-Frequency Transformation strain of *M. smegmatis*	(197)
$\Delta lsr2$	deletion of *lsr2* in mc^{2}155, *zeo*^{r}	(107)
$\Delta lsr2/\Delta mps$	deletion of *mps* in unmarked Δlsr2, zeo^r	(107)

Table 2 List of plasmids used in this study

Name	Remarks	Origin
PhiMycoMarT7	Temperate mycobacteriophage carrying *himar-1* transposon, *kan*^{r}	(198)
pJV53sacB	Recombineering plasmid carrying inducible proteins gp60 gp61 from phage Che9c and SacB cassette, *kan*^{r}	(107)
pJL37	extrachromosomal vector containing P$_{hsp60}$, *kan*^{r}	(199)
pMH94	L5-attp-based integrative vector, *kan*^{r}	(197)
pJR14	*phoT* cloned in pMH94$_{hsp60Pr}$ @ NdeI and EcoRI, *kan*^{r}	This study
pJR15	*Rv0928-30* with natural promoter region cloned in pMH94 @ SacI and XbaI, *kan*^{r}	This study
pJR08	*dgt* cloned in pMH94$_{hsp60Pr}$ @ NdeI and EcoRI, *kan*^{r}	This study
pEM2	P*hsp60* -mCherry cloned in pMH94 @ XbaI, *kan*^{r}	(107)

Table 2 Continued

| pJR36 | P*Rv0096* cloned in pYL026 (Phsp60-Dendra2) @ XbaI and BamHI, *hygʳ* | This study |
| Cosmid 3D11.2.cm5 | integrative cosmid carrying *M. tuberculosis H37Rv* genomic fragment from *Rv0096* to *Rv0115*, *hygʳ*, *CBʳ* | Gift from Dr. William Jacobs, Albert Einstein College of Medicine |

Table 3 List of oligonucleotides used in this study

Name	Sequence	Remarks
Adapter 1.2	TACCACGACCA-NH$_2$	Tn-seq Library Preparation
Adapter 2.2 BarB	ATGATGGCCGGTGGATTTGTGTGGTCGTGGTAT	Tn-seq Library Preparation
ShortPrimer_T7	ATGATGGCCGGTGGATTTGTG	Tn-seq Library Preparation
ShortPrimer_JEL_AP1	TAATACGACTCACTATAGGGTCTAGAG	Tn-seq Library Preparation
Primer_Sol_Mar	AATGATACGGCGACCACCGAGATCTACACTCTTTCCCTAC ACGACGCTCTTCCGATCTCGGGGACTTATCAGCCAACC	Tn-seq Library Preparation
Primer_Sol_Mar_1b	AATGATACGGCGACCACCGAGATCTACACTCTTTCCCTAC ACGACGCTCTTCCGATCTTCGGGGACTTATCAGCCAACC	Tn-seq Library Preparation
Primer_Sol_Mar_4b	AATGATACGGCGACCACCGAGATCTACACTCTTTCCCTAC ACGACGCTCTTCCGATCTGATACGGGGACTTATCAGCCAA CC	Tn-seq Library Preparation
Primer_Sol_Mar_5b	AATGATACGGCGACCACCGAGATCTACACTCTTTCCCTAC ACGACGCTCTTCCGATCTATCTACGGGGACTTATCAGCCA ACC	Tn-seq Library Preparation
Sol_AP1_1	CAAGCAGAAGACGGCATACGAGATATCACGGTGACTGGA GTTCAGACGTGTGCTCTTCCGATCTGTCAATGATGGCCGGT GGATTTGTG	Tn-seq Library Preparation
Sol_AP1_3	CAAGCAGAAGACGGCATACGAGATTTAGGCGTGACTGGA GTTCAGACGTGTGCTCTTCCGATCTGTCAATGATGGCCGGT GGATTTGTG	Tn-seq Library Preparation
Sol_AP1_6	CAAGCAGAAGACGGCATACGAGATGCCAATGTGACTGGA GTTCAGACGTGTGCTCTTCCGATCTGTCAATGATGGCCGGT GGATTTGTG	Tn-seq Library Preparation
Sol_AP1_9	CAAGCAGAAGACGGCATACGAGATGATCAGGTGACTGGA GTTCAGACGTGTGCTCTTCCGATCTGTCAATGATGGCCGGT GGATTTGTG	Tn-seq Library Preparation
Illumina_Seq1	ACACTCTTTCCCTACACGACGCTCTTCCGATCT	Tn-seq Library Sequencing
Δ*Rv0243* PrA	GTCAGTGGCGGTTCGCCTGCTCGA	For isogenic deletion of *Rv0243*
Δ*Rv0243* PrB	TGGTGAGGGAGATGAGGTCTGAAGTGTTTTCTCCGTTGAT CA	For isogenic deletion of *Rv0243*
Δ*Rv0243* PrC	GTTGAGGTGTGAGGTGTGCTGAAGCGCTGACGGCTCGGTA AG	For isogenic deletion of *Rv0243*

Table 3 Continued

Δ*Rv0243* PrD	ACGGGTTACTCGCACTTTTGCGTG	For isogenic deletion of *Rv0243*
Δ*Rv0346c* PrA	CTACGACCGCGGCTACGACACCCT	For isogenic deletion of *Rv0346c*
Δ*Rv0346c* PrB	TGGTGAGGGAGATGAGGTCTGAAGTGAGCTCCCTGGGATGGT	For isogenic deletion of *Rv0346c*
Δ*Rv0346c* PrC	GTTGAGGTGTGAGGTGTGCTGAAGGGTCCACGTCGACATCGC	For isogenic deletion of *Rv0346c*
Δ*Rv0346c* PrD	GTCACCGCGATTACCGCGCCGGAC	For isogenic deletion of *Rv0346c*
Δ*Rv0820* PrA	CGATCGGTATCGTCTCGCT	For isogenic deletion of *Rv0820*
Δ*Rv0820* PrB	TGGTGAGGGAGATGAGGTCTGAAGCTTGGCCACTTAAGCTCCTG	For isogenic deletion of *Rv0820*
Δ*Rv0820* PrC	GTTGAGGTGTGAGGTGTGCTGAAGCTTCGGCTAGGCCCGAT	For isogenic deletion of *Rv0820*
Δ*Rv0820* PrD	CATTTGTTCACCGTGCTGATG	For isogenic deletion of *Rv0820*
Δ*Rv0929-30* PrA	ACGACCTGGTGCTCGACACGGACT	For isogenic deletion of *Rv0929-30*
Δ*Rv0929-30* PrB	TGGTGAGGGAGATGAGGTCTGAAGCGGCTTTGTGAGCGGCTCGGTGAC	For isogenic deletion of *Rv0929-30*
Δ*Rv0929-30* PrC	GTTGAGGTGTGAGGTGTGCTGAAGCGACGGCGGCGACTCCCGTTATGA	For isogenic deletion of *Rv0929-30*
Δ*Rv0929-30* PrD	TTGTCAAGCTAGAGGCCGAGTCGA	For isogenic deletion of *Rv0929-30*
Δ*Rv1111c* PrA	CACGAAGGTGACCGGCGCGGGTAC	For isogenic deletion of *Rv1111c*
Δ*Rv1111c* PrB	TGGTGAGGGAGATGAGGTCTGAAGACGTCGACCGTACCGGCA	For isogenic deletion of *Rv1111c*
Δ*Rv1111c* PrC	GTTGAGGTGTGAGGTGTGCTGAAGCGTGAGCGGATGTGCTCA	For isogenic deletion of *Rv1111c*
Δ*Rv1111c* PrD	GGTTCGGCTGGTCGAGGTGGCGCT	For isogenic deletion of *Rv1111c*
Δ*Rv1328* PrA	CGCTGACCGGGACCACCTCGCCGA	For isogenic deletion of *Rv1328*
Δ*Rv1328* PrB	TGGTGAGGGAGATGAGGTCTGAAGTCCTTACCTTACTGAGGA	For isogenic deletion of *Rv1328*
Δ*Rv1328* PrC	GTTGAGGTGTGAGGTGTGCTGAAGGAGAAGACGCAAAAGCTC	For isogenic deletion of *Rv1328*
Δ*Rv1328* PrD	CTTCATGACGGTCGCCGCCAGCCA	For isogenic deletion of *Rv1328*
Δ*Rv1516c* PrA	AATGGCTATTGACCAGCTAAGATA	For isogenic deletion of *Rv1516c*
Δ*Rv1516c* PrB	TGGTGAGGGAGATGAGGTCTGAAGCGTCGGCCCTTTTCCTGC	For isogenic deletion of *Rv1516c*
Δ*Rv1516c* PrC	GTTGAGGTGTGAGGTGTGCTGAAGCCATGTCGACAAACCCAG	For isogenic deletion of *Rv1516c*
Δ*Rv1516c* PrD	ATGCGCGCGAACCCGACCGCGTAC	For isogenic deletion of *Rv1516c*
Δ*Rv1538c* PrA	AGAGTCCAGGTCACCGTGTCGCCG	For isogenic deletion of *Rv1538c*
Δ*Rv1538c* PrB	TGGTGAGGGAGATGAGGTCTGAAGTCTGGGCGGGCCATATCG	For isogenic deletion of *Rv1538c*

Table 3 Continued

ΔRv1538c PrC	GTTGAGGTGTGAGGTGTGCTGAAGACCGATAGCTGGCCGATG	For isogenic deletion of Rv1538c
ΔRv1538c PrD	ACGTCGAAACACCGGGAGCGGTCG	For isogenic deletion of Rv1538c
ΔRv1568 PrA	GTGATGGCCAGCTAGTCATCGTGA	For isogenic deletion of Rv1568
ΔRv1568 PrB	TGGTGAGGGAGATGAGGTCTGAAGGGAGATCGAGGGTAATGC	For isogenic deletion of Rv1568
ΔRv1568 PrC	GTTGAGGTGTGAGGTGTGCTGAAGACGCAGGCACGGATCGAC	For isogenic deletion of Rv1568
ΔRv1568 PrD	CTGGGCCTCGAATTGCTGGTGCAG	For isogenic deletion of Rv1568
ΔRv1569 PrA	ACCGAACTGGCCGCCGGGCTGACC	For isogenic deletion of Rv1569
ΔRv1569 PrB	TGGTGAGGGAGATGAGGTCTGAAGGGCAGTGAGCCTACGAGC	For isogenic deletion of Rv1569
ΔRv1569 PrC	GTTGAGGTGTGAGGTGTGCTGAAGCGATCCTGGTCGTCACCG	For isogenic deletion of Rv1569
ΔRv1569 PrD	CGCACGATCTGATCGCGGGCGGGC	For isogenic deletion of Rv1569
ΔRv1589 PrA	GCATAACCCCCGCCGGTGAACCGC	For isogenic deletion of Rv1589
ΔRv1589 PrB	TGGTGAGGGAGATGAGGTCTGAAGCAGGTACTCCCCTGCATC	For isogenic deletion of Rv1589
ΔRv1589 PrC	GTTGAGGTGTGAGGTGTGCTGAAGATGGTGGAAATCGTGGCT	For isogenic deletion of Rv1589
ΔRv1589 PrD	AGGCTCGGACGGTCCGCCAAAACC	For isogenic deletion of Rv1589
ΔRv2041c PrA	CAAGTCCGCTGCGTATCACGCGTT	For isogenic deletion of Rv2041c
ΔRv2041c PrB	TGGTGAGGGAGATGAGGTCTGAAGCTGTGGTACAACGACCGT	For isogenic deletion of Rv2041c
ΔRv2041c PrC	GTTGAGGTGTGAGGTGTGCTGAAGTCGTCGCGCCGAACTTGG	For isogenic deletion of Rv2041c
ΔRv2041c PrD	ACGGCAAGAAGACGACCGTCCGAA	For isogenic deletion of Rv2041c
ΔRv2131c PrA	ATCGCGTCGCCGATGTTGGAGTAG	For isogenic deletion of Rv2131c
ΔRv2131c PrB	TGGTGAGGGAGATGAGGTCTGAAGTCGCCGAGCTGAACGCAG	For isogenic deletion of Rv2131c
ΔRv2131c PrC	GTTGAGGTGTGAGGTGTGCTGAAGGCTGCTCAGAAAGGCTCG	For isogenic deletion of Rv2131c
ΔRv2131c PrD	TAGTGCAATTCATGACCGAGATCC	For isogenic deletion of Rv2131c
ΔRv2224c PrA	CATCGGGGATCGCCCTCGGGCGAT	For isogenic deletion of Rv2224c
ΔRv2224c PrB	TGGTGAGGGAGATGAGGTCTGAAGAATGCTGCCAGAGCAGAC	For isogenic deletion of Rv2224c
ΔRv2224c PrC	GTTGAGGTGTGAGGTGTGCTGAAGCGGGGCGAAGAAACGAAG	For isogenic deletion of Rv2224c
ΔRv2224c PrD	TGCAGTGCGAATTTCGCTGGTGTC	For isogenic deletion of Rv2224c
ΔRv2231c PrA	GGAGATCGCGATCAACTACCGCCT	For isogenic deletion of Rv2231c

Table 3 Continued

Δ*Rv2231c* PrB	TGGTGAGGGAGATGAGGTCTGAAGCGCCGACGCGTTGTCTAC	For isogenic deletion of *Rv2231c*
Δ*Rv2231c* PrC	GTTGAGGTGTGAGGTGTGCTGAAGGTGTGCGGCTGGCCGATG	For isogenic deletion of *Rv2231c*
Δ*Rv2231c* PrD	CGACCGGTCCGGATCAGGCGGTGC	For isogenic deletion of *Rv2231c*
Δ*Rv2344c* PrA	ACCACCCACAGTCGGATGCGGCGA	For isogenic deletion of *Rv2344c*
Δ*Rv2344c* PrB	TGGTGAGGGAGATGAGGTCTGAAGCGACCCACAGTCTGCCAG	For isogenic deletion of *Rv2344c*
Δ*Rv2344c* PrC	GTTGAGGTGTGAGGTGTGCTGAAGGCCGATGTCCGGCCGGAT	For isogenic deletion of *Rv2344c*
Δ*Rv2344c* PrD	AAGCAACTCAACCGCCTCGACGAA	For isogenic deletion of *Rv2344c*
Δ*Rv2374c* PrA	ACTCGTCGAGCCGGATCTGTTGCG	For isogenic deletion of *Rv2374c*
Δ*Rv2374c* PrB	TGGTGAGGGAGATGAGGTCTGAAGCGACTGCTCACCTCACTT	For isogenic deletion of *Rv2374c*
Δ*Rv2374c* PrC	GTTGAGGTGTGAGGTGTGCTGAAGACGCGCACCTGCTGCAGG	For isogenic deletion of *Rv2374c*
Δ*Rv2374c* PrD	CCAGGTCGACGATGCGACGTTTGT	For isogenic deletion of *Rv2374c*
Δ*Rv3148* PrA	ACAACCGTCGCCTCCGGTTGGAAG	For isogenic deletion of *Rv3148*
Δ*Rv3148* PrB	TGGTGAGGGAGATGAGGTCTGAAGCAGTTGTAGCCCCTCCGC	For isogenic deletion of *Rv3148*
Δ*Rv3148* PrC	GTTGAGGTGTGAGGTGTGCTGAAGCACAGCCACCCGGTCAGC	For isogenic deletion of *Rv3148*
Δ*Rv3148* PrD	GCCGACACCTCGGCCCCGGTCAGC	For isogenic deletion of *Rv3148*
Δ*Rv3158* PrA	TTACATGCTGTGGCTCTACCAGCG	For isogenic deletion of *Rv3158*
Δ*Rv3158* PrB	TGGTGAGGGAGATGAGGTCTGAAGGGTGCGGTCCTTCGGCTG	For isogenic deletion of *Rv3158*
Δ*Rv3158* PrC	GTTGAGGTGTGAGGTGTGCTGAAGATCCGTTAGGGCTGACCG	For isogenic deletion of *Rv3158*
Δ*Rv3158* PrD	CAGGCTTCTTTAACACGGGCAATG	For isogenic deletion of *Rv3158*
Δ*Rv3682* PrA	GGTGTTACCTGTATCTCACTGATC	For isogenic deletion of *Rv3682*
Δ*Rv3682* PrB	TGGTGAGGGAGATGAGGTCTGAAGGCGTACTACAGTAGCGAC	For isogenic deletion of *Rv3682*
Δ*Rv3682* PrC	GTTGAGGTGTGAGGTGTGCTGAAGGCCCTCCCAATCGGCCTC	For isogenic deletion of *Rv3682*
Δ*Rv3682* PrD	TGTTTGCGGTGCTGGTTGGGCAGC	For isogenic deletion of *Rv3682*
Δ*Rv3696c* PrA	GAGCAATTCACCTCACGACCGCAC	For isogenic deletion of *Rv3696c*
Δ*Rv3696c* PrB	TGGTGAGGGAGATGAGGTCTGAAGTGCATCTAATCGTCCATG	For isogenic deletion of *Rv3696c*
Δ*Rv3696c* PrC	GTTGAGGTGTGAGGTGTGCTGAAGCTTTCGCTGTGCGCCTGA	For isogenic deletion of *Rv3696c*
Δ*Rv3696c* PrD	GTTGCGACTGCGTCCCACGCTGCC	For isogenic deletion of *Rv3696c*

Table 3 Continued

Δ*Rv3779* PrA	ACCGCCGCGCTACGCCGCGCCGAC	For isogenic deletion of *Rv3779*
Δ*Rv3779* PrB	TGGTGAGGGAGATGAGGTCTGAAGTCGATTAGTATGGCTGGC	For isogenic deletion of *Rv3779*
Δ*Rv3779* PrC	GTTGAGGTGTGAGGTGTGCTGAAGAAGGTGCGTAAGAGGATG	For isogenic deletion of *Rv3779*
Δ*Rv3779* PrD	CTTCGAGTTCGCGGATGCTGGTGG	For isogenic deletion of *Rv3779*
Zeo_In_CF	GTCTCCACCAACTTCAGGGATGC	For PCR confirmation of isogenic deletions
Zeo_in_BR	ACCTGCAAAGTCATCCTCCACA	For PCR confirmation of isogenic deletions
*Rv2344c*_hsp60_F	GACTGTGGGTCGCATATGAGCGCGAGTGAGCACGAC	For Plasmid pJR08
*Rv2344c*_hsp60_R	CCGGACATCGGCGAATTCTCAGTCTAAAGCGTTCCT	For Plasmid pJR08
*Rv0820*_hsp60_F	GCAGGAGCTTAACATATGGCCAAGCGGTTGGACCTC	For Plasmid pJR14
*Rv0820*_R2	CCGTGGAAGTGAATTCGGCACGACGCGTGATCTT	For Plasmid pJR14
*Rv0928-30*_NPr_F	GCGGATCTGAGCTCGTTCGGCGACAG	For Plasmid pJR15
*Rv0928-30*_NPr_R	CATCGCGGTGGATCTAGACGAAGCCGGAACCGTCTA	For Plasmid pJR15
*SigA*_rtpcr_F	TGCAGTCGGTGCTGGACAC	For RT-PCR: mc^{2}7000 *sigA*
*SigA*_rtpcr_R	CGCGCAGGACCTGTGAGCGG	For RT-PCR: mc^{2}7000 *sigA*
rt_*Rv0096*F	TTCTGATCGCCACCAACTTC	For RT-PCR: mc^{2}7000 *Rv0096*
rt_*Rv0096*R	AGCCACATGCGGACATAATC	For RT-PCR: mc^{2}7000 *Rv0096*
PrF_*Rv0096*_F	TCGCCAGTGAGCTCTAGAGCCCGACGTTGCCCTAAG	For plasmid pJR36
PrF_*Rv0096*_R	TGGTATAGCCATGGATCCCCATATCGTGGCCGCCAG	For plasmid pJR36
Δ*Rv0096-0101* PrA	CCTCGTCCAAGCGGTCCAGGTCGG	For isogenic deletion of *Rv0096-0101*
Δ*Rv0096-0101* PrB	TGGTGAGGGAGATGAGGTCTGAAGCCATATCGTGGCCGCCAG	For isogenic deletion of *Rv0096-0101*
Δ*Rv0096-0101* PrC	GTTGAGGTGTGAGGTGTGCTGAAGTTGCTCGGCGATAAAGAG	For isogenic deletion of *Rv0096-0101*
Δ*Rv0096-0101* PrD	CCAGCAGGCCAATTGCCAGCCGTA	For isogenic deletion of *Rv0096-0101*

3.2 Tn-seq

3.2.1 Growth Conditions and Library Preparation

A transposon insertion mutant library of mc^{2}7000 consisting of approximately 100,000 isolated mutant colonies was constructed using PhiMycoMarT7 bacteriophage carrying the *Himar-1* transposon. The library was grown in 7H9OADC either as planktonic suspension to mid-logarithmic phase, in pellicle biofilms for 5-weeks, or as colonies attached to polycarbonate membranes for 18 days. Cells from each growth model, including planktonic suspension, were harvested and resuspended in 1xPBS with 0.25% (v/v) Tween-80, vortexed for 30 seconds to disperse biomass, and sonicated in a Bath Sonicator (Branson) for 10 minutes. Ten-fold dilutions of bacteria from each sample were then plated out on ten 100mm 7H11OADC plates per replicate and incubated for 21 days. Colonies were harvested with a cell scraper and genomic DNA was extracted by ethanol extraction (200) and prepared for further processing as described (201). Briefly, 2-5 μg of genomic DNA was sheared with a Covaris M220 Focused-ultrasonicator (Covaris) into 400-600bp fragments, which were resolved by gel electrophoresis. The resolved fragments were gel-extracted (Qiagen Cat. No. 28606), and end-blunted using the Epicentre End Repair kit (Cat. No. ER0720). The fragments were then adenylated at the 3' sequence end and custom adapter oligonucleotides ligated using the Epicentre FastLink DNA Ligation kit (Cat. No. LK6201H). Two-step, hemi-nested PCR-amplification of DNA fragments with a mixture of four staggered primers with homology to the end region of the transposon insertion resulted in a library of PCR amplicons at the junction site of transposon insertion and genomic DNA. Primers used for hemi-nested PCR and DNA sequencing are listed in Table 3. PCR with a set of short primers was performed with settings: 95 °C for 5 minutes; 20 cycles of 95 °C for 30 seconds, 58 °C for 30

seconds, and 72 °C for 45 seconds; 72 °C for 5 minutes. This was followed by hemi-nested PCR with a staggered primer set at 95 °C for 5 minutes; 10 cycles of 95 °C for 30 seconds, 58 °C for 30 seconds, and 72 °C for 45 seconds; 72 °C for 5 minutes. A comprehensive list of oligonucleotides used in this study is listed in Table 3. The library, prepared from a pool of three biologically independent sources of genomic DNA for every growth model, were sequenced at the transposon junction site using the Illumina Hi-Seq 2500 platform (Tn-seq). Two biologically independent sets of libraries were sequenced for each growth model.

3.2.2 Tn-seq Data Analysis

The sequencing results were analyzed by the TRANSIT data analysis pipeline (202) to identify ORFs with significant mutant underrepresentation in either pellicle or colony biofilms, relative to planktonic cultures. TRANSIT's own pre-processor TPP was used to prepare DNA sequencing .fastq files for analysis by TRANSIT. TPP identifies reads containing the library barcode and Tn terminus sequence (ACTTATCAGCCAACCTGTTA), trims the reads to only the genomic sequence, and maps reads to the T-A dinucleotide insertion site on the MTB H37Rv Genbank reference genome (NC_000962) using a Burrows-Wheeler Aligner (BWA) (203). TRANSIT then uses the TPP output .wig files to determine conditional genes that confer fitness advantage between growth conditions. This method determines conditional essentiality by a resampling permutation test that randomly reshuffles observed T-A counts across datasets to determine a null hypothesis that difference in read counts at a locus is due to chance. Genes are determined to confer statistically significant fitness advantage if q-value < 0.05 (p-value < 0.05 after comparisons by Benjamini-Hochberg procedure to correct type I error) following the permutation test. Read numbers were normalized across samples by default Total Trimmed Reads

(TTR) reads across datasets. Because transposon insertions in the carboxyl terminus region are less likely to result in a non- or dysfunctional protein, insertions in dinucleotides in the 20 percent of each locus in the 3' were excluded from statistical analysis to apply a more stringent comparison between growth conditions.

3.3 Plasmids and Mutant Constructions

A modified recombineering method, as described previously (107), was used for constructing isogenic deletions in the indicated genes. For allelic exchange substrates (AES) of a target gene, 250bp PCR amplicons corresponding to upstream and downstream of the gene were joined to the either side of a loxP-flanked zeocin-resistance cassette by sewing-PCR. Oligonucleotides used for AES generation are listed in Table 3. The AES were electroporated into a recombineering strain of mc^{2}7000 carrying the plasmid pJV53-SacB (107), and plated on 7H11 agar with 25 μg/mL of zeocin and 20 μg/mL kanamycin. The genotype of zeocin resistant colonies was confirmed by PCR. The recombineering plasmid, pJV53-SacB, was removed by selecting the mutant strains on 7H11 agar with 15% sucrose and 25 μg/mL zeocin. The sucrose-resistant colonies were screened for kanamycin sensitivity by plating recombinant strains on kanamycin-containing plates. A second PCR was performed to confirm gene deletion gene using primers homologous to upstream and downstream ends of AES and to the zeocin resistance cassette. As necessary, mutants were complemented by the corresponding gene cloned along with a 500bp upstream promoter region, or fused to hsp60 promoter, on an integrative plasmid (pMH94). For a reporter strain of a mutant, an integrative plasmid expressing mCherry from the constitutive hsp60 promoter was electroporated into the mutant and transformants were selected on 7H11OADC

plates with 25 µg/mL zeocin and 20 µg/mL kanamycin. For construction of INLP expression reporter, the putative promoter and regulator elements of INLP harbored in the 500bp upstream of the gene cluster were amplified using the primers listed in Table 3 and cloned upstream of Dendra2 at XbaI and NdeI restriction sites in the plasmid pYL026 (72). The resulting plasmid, pJR36, was electroporated into *M. smegmatis* mc^{2}155, MTB mc^{2}7000 strains, and the virulent MTB (Erdman) strains for analysis of the reporter expression. Mutants and their complete genotypes are listed in Table 1.

3.4 Analysis of Planktonic Growth Rates of Mycobacterial Strains

mc^{2}7000 and derivative mutant strains were grown to mid-logarithmic phase planktonically, normalized to an OD$_{600}$ (optical density 600nm) of 0.1, and then 1 mL was inoculated in 19 mL of either Sauton's or 7H9 media, with or without detergent in triplicate. OD readings were measured using a Thermo Scientific Genesys 20 Spectrophotometer. Growth was monitored by measurement of OD$_{600}$ at the time points indicated. For growth in detergent-free media, 1 mL of culture was placed in a cuvette, 2.5 µL of 20% Tween-80 detergent was added to the cuvette and bacteria were dispersed by inverting the cuvette prior to obtaining the OD$_{600}$ reading. Data were plotted using Prism GraphPad 7 software. The Student's t-test was used to calculate statistical significance.

3.5 Microscopy: Image Acquisition and Analysis

For imaging on a wide field fluorescent microscope, Nikon Eclipse TE2000-E microscope with a 20x (NA: 0.75) dry objective was used. Images were captured with a 600 ms exposure time with a Photometrics HQ 1280x1024 monochrome camera. Transmitted light was used for phase contrast imaging and X-Cite 120 Fluorescence Illumination System with an Eclipse E800 Epi filters [blue GFP(R)-BP filter (Excitation: 460-500nm; BA: 510-560nm) for Dendra2 fluorescence or a yellow Y-2E filter (Excitation: 540-580nm; BA:600-660nm) for mCherry fluorescence]. Images were captured using Media Cybernetics ProImage Plus 7.0 software. CSLM imaging was done with a Leica SP5 confocal microscope using a 20x water immersion or 60x oil immersion objective. Fluorophores were excited with a 488 nm argon laser for Dendra2 and a 593 nm laser for mCherry, and detected by photo multiplier tube at 495-560 nm and 600-665 nm ranges, respectively. CSLM images were captured with Leica SP5 camera using Leica Microsystems Confocal LAS AF software. All post-acquisition analysis was done using FIJI image analysis software. All microscopes settings during image acquisition for a given experiment, as well as post-acquisition editing in FIJI, were maintained across compared samples. For pJR36 expression assay bacteria was fixed in 10% formalin for 2 hour for *M. smegmatis* and overnight for MTB strains. *M. smegmatis* slides were mounted on 1.0 cover slip glass in 50% glycerol and 80% glycerol for MTB strain slides.

3.6 Competitive Biofilm Assay

mc^{2}7000 WT cells carrying a pJL37-derived plasmid with the green fluorescent reporter GFP under expression of the constitutive hsp60 promoter were mixed with an isogenic mutant strain (or WT for control) carrying a pMH94-derived plasmid with the fluorescent reporter red mCherry under expression of the constitutive hsp60 promoter (pEM2) (107) at a 20:1 ratio of WT-GFP: mutant-mCherry in an effort recapitulate the competitive environment of the Tn-seq screen. A ten-fold dilution of the 20:1 mixture was inoculated onto a polycarbonate membrane and dried for 1 hour to allow for bacterial attachment. Membranes were placed inoculated side down in microscope coverslip glass-bottomed dishes (Mattek Cat. No. P35G-0.170-14-C). 1 mL of either 7H9 or Sauton's mixed with 0.85% agar was used to hold the membrane in place and 3 mL of liquid media was then added to the culture plate. Biofilms were incubated at 37 °C for the indicated time. Biofilms were imaged by CLSM as described at day 1 and day 12 for 7H9 and day 14 for Sauton's medium to determine the distribution of each strain. The count of red cells at day 1 compared to count of red microcolonies at endpoint was enumerated to assay each mutant's ability to compete with WT during biofilm formation. Five fields of view per membrane were counted at each time point. Data were plotted using Prism GraphPad 7 software. The Student's t-test was used to calculate statistical significance.

3.7 Microcolony Formation in Microfluidic Flow Cell

The Cellasic ONIX2 (MilliporeSigma Cat. No. CAX2-S0000) microfluidics system with mammalian culture plates (M0S04, MilliporeSigma Cat. No. M04S-03-5PK) was used to inoculate

approximately 1000 cells of mc^{2}7000 or derivative strains in 6 µL (obtained by diluting from a known OD$_{600}$) carrying mCherry expressing plasmid, pEM2 (107) into each microfluidic chamber, which then rested for 1 hour that allowed cells to attach to the chamber's surface. After attachment, fresh Sauton's medium was constantly perfused across the microfluidic chamber's surface at pressure of 3.4 kPa, and temperature of 37 °C for the indicated time period. Growth was analyzed by wide field fluorescent microscopy as described.

3.8 Rifampicin Sensitivity Testing

mc^{2}7000 and derivative mutant strains were grown to mid-logarithmic phase as described, and 10 µL of ten-fold serial dilutions in 1xPBS 0.05% (v/v) Tween-80 were plated on 7H11OADC agar plates containing 50 ng/mL of RIF in duplicate to determine sensitivity of each mutant strain to RIF at sub WT MIC levels. Plates were incubated at 37 °C for 21 days. Bacterial number was enumerated by counting cfu/mL. Data were plotted using Prism GraphPad 7 software.

3.9 Analysis of Persisters in Pellicle Biofilms

Pellicle biofilms of the indicated strains were grown in Sauton's medium as described above, and then exposed to 50 µg/mL of RIF (or an equal volume of DMSO as a control) for 7 days. RIF and DMSO were administered by micropipette at the side of the pellicle and allowed to diffuse throughout the well to minimize disruption. After exposure, pellicles were collected and washed 3 times with 1xPBS with 0.25% tween-80 to remove residual antibiotic, and then left on a

shaker at 4 °C overnight in the presence of sterile 10 mm glass beads. Serial dilutions were plated on 7H11 agar to enumerate the viable colonies in cfu/mL. Data were plotted using Prism GraphPad 7 software. The Student's t-test was used to calculate statistical significance.

3.10 Phosphate Starvation Viability Analysis

Parent mc^{2}7000 and its recombinant strains were cultured to mid-logarithmic phase as described in 7H9 medium, washed twice with, and then re-suspended in phosphate-free 7H9 medium buffered with MOPS (3-(N-morpholino) propanesulfonic acid). Cultures were diluted to an OD$_{600}$ of 0.05 and incubated at 37 °C in phosphate-free 7H9 medium buffered with MOPS and supplemented with 10% OADC, 0.05% (v/v) Tween-80 and 100 µg/mL pantothenic acid. Viability under phosphate starvation was enumerated by plating out serial dilutions in 1xPBS and 0.05% (v/v) Tween-80 on 7H11 agar at days 0, 3, 9, 14, 21 and 30 after transition to phosphate-free media and enumerating cfu/mL Data were plotted using Prism GraphPad 7 software. The Student's t-test was used to calculate statistical significance.

3.11 Inorganic Phosphate Importation Assay

Malachite Green Phosphate Assay Kit (Cayman Cat. No. 10009325) was used to measure the amount of inorganic phosphate uptake by cells that were starved for phosphate for 24 hours in a phosphate-free medium, and re-exposed to a known quantity of potassium phosphate at 0, 12, 24, 36, and 48 hours after the re-exposure. A standard curve was prepared using two-fold dilutions

of 7H9 medium with 25 µM potassium phosphate into phosphate-free, MOPS-buffered 7H9 medium. The standard curve confirmed the concentrations of 25µM to 2.5µM were within the linear range of the assay. mc^{2}7000 and its derivative strains were cultured to mid-logarithmic phase in 7H9 medium, washed twice with, and then re-suspended in phosphate-free 7H9 medium buffered with MOPS and without OADC supplement. Cultures were incubated in phosphate-free 7H9 medium at 37° C for 24 hours, followed by the addition of potassium phosphate to the medium at a final concentration of 25 µM. For measuring phosphate uptake, 500 µL from the phosphate-starved cultures was centrifuged at 4000 rpm for 10 minutes using a Thermo Scientific Sorvall Legend XTR (Cat. No. 75004521) centrifuge. The supernatant was collected and malachite green assay was performed following the manufacturer's instructions. The Cayman malachite green phosphate assay works by measuring the amount of molybdophosphoric acid complex formed between free inorganic phosphate in solution and the malachite green molybdate (present in the blue solution) under acidic conditions. Green molybdophosphoric acid complex can be measured at 620-640 nm absorbance. Briefly, 50 µL of supernatant for each sample was aliquoted into a 96-well polystyrene tissue culture plate along with a set of two-fold dilutions of 7H9 medium with 100 µM to 1.5 µM potassium phosphate to calculate a standard curve. 5 µL acidic solution was added to each well and incubated for 10 minutes at room temperature to produce acidic conditions. 15 µL of blue solution containing malachite green molybdate was then added to each well and incubated for 20 minutes at room temperature for complex to form. A microplate reader was used to determine the absorbance of each well at 620 nm. A linear regression was performed with the standard curve to calculate the volume of inorganic phosphate in each sample at 12, 36, and 48 hours post addition of potassium phosphate. Values were subtracted from the 0-hour reading for each sample to determine the percentage of phosphate uptake at each time point. Data were plotted

using Prism GraphPad 7 software. The Student's t-test was used to calculate statistical significance.

3.12 Hypoxia Viability Analysis

mc^{2}7000 and its derivative strains were cultured to mid-logarithmic phase as described in 7H9 medium, diluted to an OD$_{600}$ of 0.05 in 50 mL of 7H9 medium in 50 mL Falcon tubes and parafilm-sealed around the cap to produce temporal hypoxic conditions (204), and incubated at 37 °C. Viability under phosphate starvation was enumerated cfu/mL by plating out serial dilutions in 1xPBS and 0.05% (v/v) Tween-80 on 7H11 agar at days 0, 7, 14, 21, and 30 days after transition to hypoxic conditions. Data were plotted using Prism GraphPad 7 software. The Student's t-test was used to calculate statistical significance.

3.13 Gene Expression Analysis by RNA-seq and RT-qPCR

Using a Qiagen RNeasy kit (Cat. No. 74104), total RNA of the indicated strains of MTB were isolated from 20 mL cultures obtained from mid-logarithmic growth phase in 7H9OADC medium. For biofilm transcriptomics, mc^{2}7000 was grown planktonically to mid-logarithmic phase in detergent-free Sauton's medium, or into pellicles for 5 weeks in detergent-free Sautons's medium as described above. The pellicle biomass portion was scooped out of the liquid medium using parafilm. RNA was extracted from the pellicles using RNAEasy kit (Qiagen Inc.). Contaminating genomic DNA from the RNA preparations was removed with the Thermo Fisher

Scientific Turbo DNA-free Kit (Cat. No. AM1907). The ribosomal RNA from a total of 5 μg RNA was removed with the Illumina RiboZero Kit (now discontinued). Strand-specific cDNA libraries were prepared from 100 ng mRNA of each sample using the Illumina Scriptseq v2 Complete Kit (Cat. No. SSV21106). Libraries were sequenced on the Illumina NextSeq500 platform at the Wadsworth Center, and results were analyzed by Rockhopper (205) at the default settings using the Genbank MTB H37Rv reference genome (NC_000962). All oligonucleotides used for RT-qPCR are listed in Table 3. For RT-qPCR, DNA-free RNA was extracted from desired bacterial cultures as described above for RNA-seq. Using the Fisher Maxima First Strand cDNA Synthesis Kit (Cat. No. K1641), cDNA was generated from 200 ng of total RNA from each specified sample. RT-qPCR reactions were prepared using 2 μL of cDNA reaction mixture, 0.5 μL from 10 μM stock for each gene-specific primer per reaction, and Applied Biosystems SYBR Green Master Mix (Cat. No. A25742) as per the manufacturer's instruction. RT-qPCR was performed on an Applied Biosystems 7500 Fast Real-Time PCR System (Cat. No. 4351106) using the cycle conditions: 95°C for 10 minutes; followed by 40 cycles of 95°C for 20 seconds, and then 60°C for 1 minute. Primers corresponding to SigA transcripts were used as an endogenous control. Reactions without the cDNA were used as no-template negative control. Expression of a target gene (tgene) in pellicles relative to planktonic was calculated as $2^{-[\Delta Ct(\text{pellicle\_tgene} - \text{pellicle\_sigA}) - \Delta Ct(\text{plnk\_tgene} - \text{plnk\_sigA})]}$.

3.14 INLP Biochemical Analysis

3.14.1 Crude Lipid Extraction from MTB Biofilms and Planktonic Cultures

Pellicle biofilms or planktonic cultures were grown in detergent-free Sauton's medium prior to crude lipid extraction. 1 mM of 2-^{13}C-Gly (Sigma) was included in selective biofilm cultures for isotope incorporation. Cells from planktonic cultures were transferred to glass tubes and an equal volume of chloroform:methanol (2:1) was added to each culture, followed by intermittent vortexing for 30 seconds every 15 minutes for 2 hours. The mixture was then centrifuged at 2000 rpm for 10 minutes on a Thermo Scientific Sorvall Legend XTR (Cat. No. 75004521) centrifuge. The lower, organic phase was separated by Pasteur pipette and dried under N$_2$ gas. Pellicle biomass was separated from the liquid portion of the cultures using parafilm. The biomass was washed and resuspended in 5 mL 1xPBS. Equal volume of chloroform:methanol (2:1) was added to the suspension and the lipid in organic phase was collected and dried as described above. Dried crude extracts were dissolved in methanol to final concentration 0.1 mg/mL. Samples were centrifuged at 12,000 rpm for 5 minutes, and the supernatant was used for liquid chromatography mass spectrometry (LC-MS) analysis.

3.14.2 LC-MS (Orbi-trap)

All MS-based analytical experiments on INLP were performed in the laboratory of Dr. Wenjun Zhang at the University of California Berkeley. Samples of extracted metabolites were analyzed using a liquid chromatography system (LC; 1200 series, Agilent, Santa Clara, CA) that was connected in-line with an LTQ-Orbitrap-XL mass spectrometer equipped with an electrospray

ionization source (Thermo Fisher Scientific, Waltham, MA). The LC was equipped with a reversed-phase analytical column (length: 150 mm, inner diameter: 1.0 mm, particle size: 5 μm, Viva C18, Restek, Bellefonte, PA). Acetonitrile, formic acid (Optima grade, 99.5+%, Fisher, Pittsburgh, PA), and water purified to a resistivity of 18.2 MΩ·cm (at 25 °C) using a Milli-Q Gradient ultrapure water purification system (Millipore, Billerica, MA) were used to prepare mobile phase solvents. Solvent A was 99.9% water/0.1% formic acid and solvent B was 99.9% acetonitrile/0.1% formic acid (v/v). The elution program consisted of isocratic conditions at 5% B for 2 minutes, a linear gradient to 98% B over 25 minutes, isocratic conditions at 98% B for 10 minutes, at a flow rate of 150 μL/minute. Full-scan, high-resolution mass spectra were acquired over the range of mass-to-charge ratio (m/z) = 70 to 1000 using the Orbitrap mass analyzer, in the positive ion mode and profile format, with a mass resolution setting of 100,000 (measured at full width at half-maximum peak height, FWHM, at m/z = 400). For tandem mass spectrometry (MS/MS or MS^2) analysis, precursor ions were fragmented using higher energy collisional dissociation (HCD) under the following conditions: MS/MS spectra acquired using the Orbitrap mass analyzer, in centroid format, with a mass resolution setting of 7500 (at m/z = 400, FWHM), 554 isolation width: 5 m/z units, normalized collision energy: 38%, default charge state: 1+, activation time: 30 ms, and first m/z value: 100. Mass spectrometry data acquisition and analysis were performed using Xcalibur software (version 2.0.7, Thermo). Comparative metabolomics analysis was performed using MS-DIAL (206).

3.14.3 LC-MS QTOF

Liquid chromatography-mass spectrometry (QTOF): LC-MS analysis was performed using an Agilent Technologies 6520 Accurate-Mass Q-TOF LC-MS instrument and an Agilent Eclipse

Plus C18 column (4.6 x 100 mm). A linear gradient of 2-98% acetonitrile (v/v) over 30 minutes in H2O with 0.1% formic acid (v/v) at a flow rate of 0.5 mL/minute was used. HRMS/MS analysis was conducted using targeted MS/MS with collision energy of 20V.

3.14.4 Click Chemistry Analysis

Compound 1 and 2 were partially purified from the WT culture extract using high performance liquid chromatography (HPLC). This was conducted using an Agilent 1200 HPLC with a Waters Atlantis T3 OBD column (10 X 250 mm) using a linear gradient of 5-95% CH_3CN (v/v) over 30 minutes in H_2O without formic acid at a flow rate of 3.5 mL/minute Fractions were screened using LC-MS as described above. Fractions containing 1 and 2 were combined, dried, and re-dissolved in methanol, followed by addition of 100 μM of 3,6-Di-2-pyridyl-1,2,4,5-tetrazine and incubated at room temperature for 4.5 hours before LC-MS analysis.

4.0 Results

4.1 53 Candidate Genes Identified by Tn-seq Confer Fitness Advantage in MTB Biofilms

To determine the genes necessary for adaptive fitness of MTB in biofilms, we used a Tn-seq approach, which is a high-throughput genomics based screen of a saturated transposon mutant library of MTB (201). The MTB Tn-library was cultured planktonically, in pellicle biofilms, and in colony biofilms (Fig. 2). Biofilms for the Tn-seq screen were cultured in nutrient-rich 7H9-OADC medium to avoid growth bias by more selective Sauton's medium, which was originally used for characterization of wild-type biofilms (184). Sauton's medium was used for culturing all subsequent biofilms of isogenic deletion strains, unless noted otherwise. In *M. smegmatis* biofilms, there is significant overlap in gene expression profiles of pellicles and colonies (107). Here, we analyzed both of these *in vitro* biofilm growth models in our Tn-seq screen to identify any similarities and differences in fitness requirements between these different forms of aggregative growth in MTB. To recover surviving mutants from any given growth condition, the Tn-seq protocol requires outgrowth of individual mutants as colonies on agar plates (201). Mutants in the library unable to form colonies on agar plates are therefore eliminated from this screen. Because of the similarities between colony growth and our *in vitro* colony biofilms, this means our screen is limited to identifying mutants that can form colonies in monoculture, but are out-competed when cultured among more fit members of the Tn-library. Additionally, mutants that may be biofilm deficient, but are trans-complemented by WT bacteria in mixed biofilms will likely not be identified by our screen. Despite these limitations, Tn-seq is still a powerful screen for identifying genetic factors in MTB.
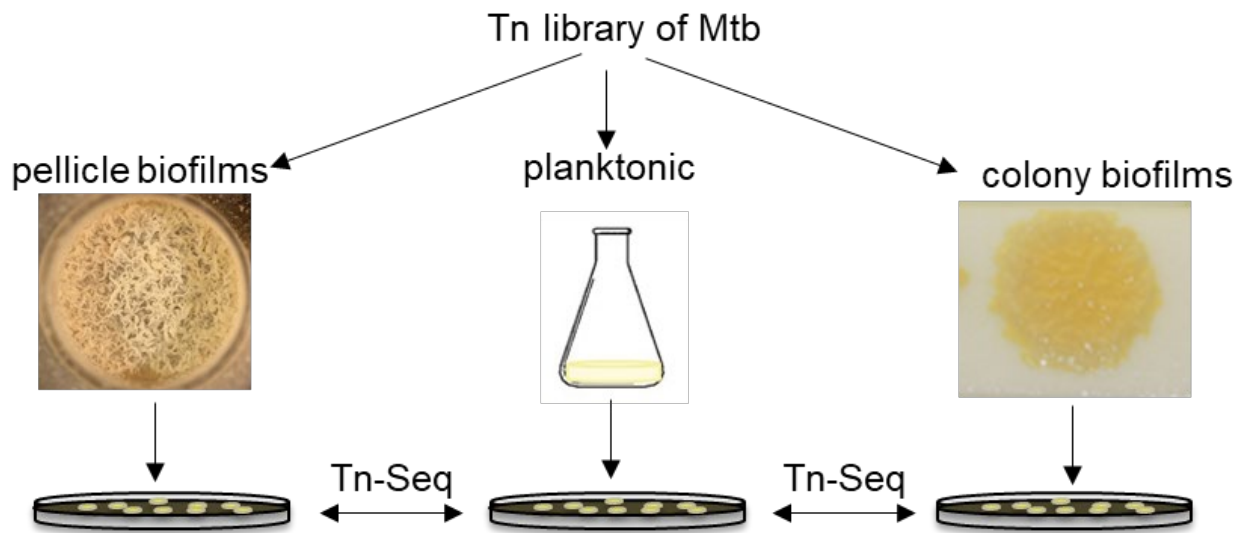
Figure 2: A schematic of Tn-seq screen to identify genes required for fitness of MTB (mc^{2}7000) in colonies or pellicle biofilms, relative to planktonic culture

4.1.1 Quality of Tn-seq Sequencing Results

Using Tn-seq, we compared the frequency of Tn insertions per gene in colony and pellicle biofilms compared to planktonic suspension. The TRANSIT analysis pipeline (202) was used to identify transposon insertion junctions to genomic DNA, trim read to the genomic sequence, map them to their T-A dinucleotide insertion sites, and determine which genes were significantly underrepresented in either biofilm growth condition. A summary of total read numbers, read numbers with transposon homology ('TTGTA' reads), mapped read numbers, and library density for the replicates of each growth condition are listed in Table 4. Of the total of 74,605 potential transposon insertion sites (T-A), insertion density ranged from 29.5% to 55.7% (Table 4). A library density of at least 35% is recommended by TRANSIT (202). Only one sample, Colony-2, had a

density below this threshold, and also returned significantly less reads than the other sequencing libraries, possibly due to high content of primer dimer in the sequencing library. Discarding this replicate from TRANSIT did not increase the number of loci significantly underrepresented in colony biofilms. Pearson r correlation coefficients of sequencing replicates for each growth condition (determined by plotting the number of mapped reads at each insertion site across replicates, excluding insertion sites with zero or only one read mapped to that insertion site in both replicates) were calculated to determine consistency in each of the growth conditions in our screen. Pearson r values in each condition (planktonic: 0.9035, pellicle biofilm: 0.7912, and colony biofilm: 0.8506) showed correlation with a p-value < 0.001 for all three growth conditions (Fig. 3A-C).

Table 4 Summary of Tn-seq data

Sample	Total Reads	TGTTA Reads	Mapped Reads	TA Sites Hit	TA Density
Planktonic-1	26,331,067	25,663,360	24,864,949	41,374	0.555
Planktonic-2	13,407,734	13,013,629	12,677,859	40,858	0.548
Pellicle-1	14,447,654	14,069,087	13,711,465	26,620	0.357
Pellicle-2	17,236,054	16,657,573	4,681,786	34,874	0.467
Colony-1	21,582,313	21,067,582	20,406,692	41,518	0.557
Colony-2	372,574	355,283	343,496	22,002	0.295
PellicleRIF-1	19,624,674	19,125,489	18,717,680	29,467	0.395
PellicleRIF-2	16,844,987	16,240,754	12,332,896	28,933	0.388

"TGTTA Reads" refers to the reads containing the Tn junction sequences; "Mapped Reads" refers to the number of reads successfully mapped to the H37Rv genome; "TA Sites Hit" refer to the number of TA sites in the genome where at least one event of transposon insertion occurred in a given sample. "TA Density" refers to the percentage of TA sites hit to the total number of TA sites in the H37Rv genome (74,605).
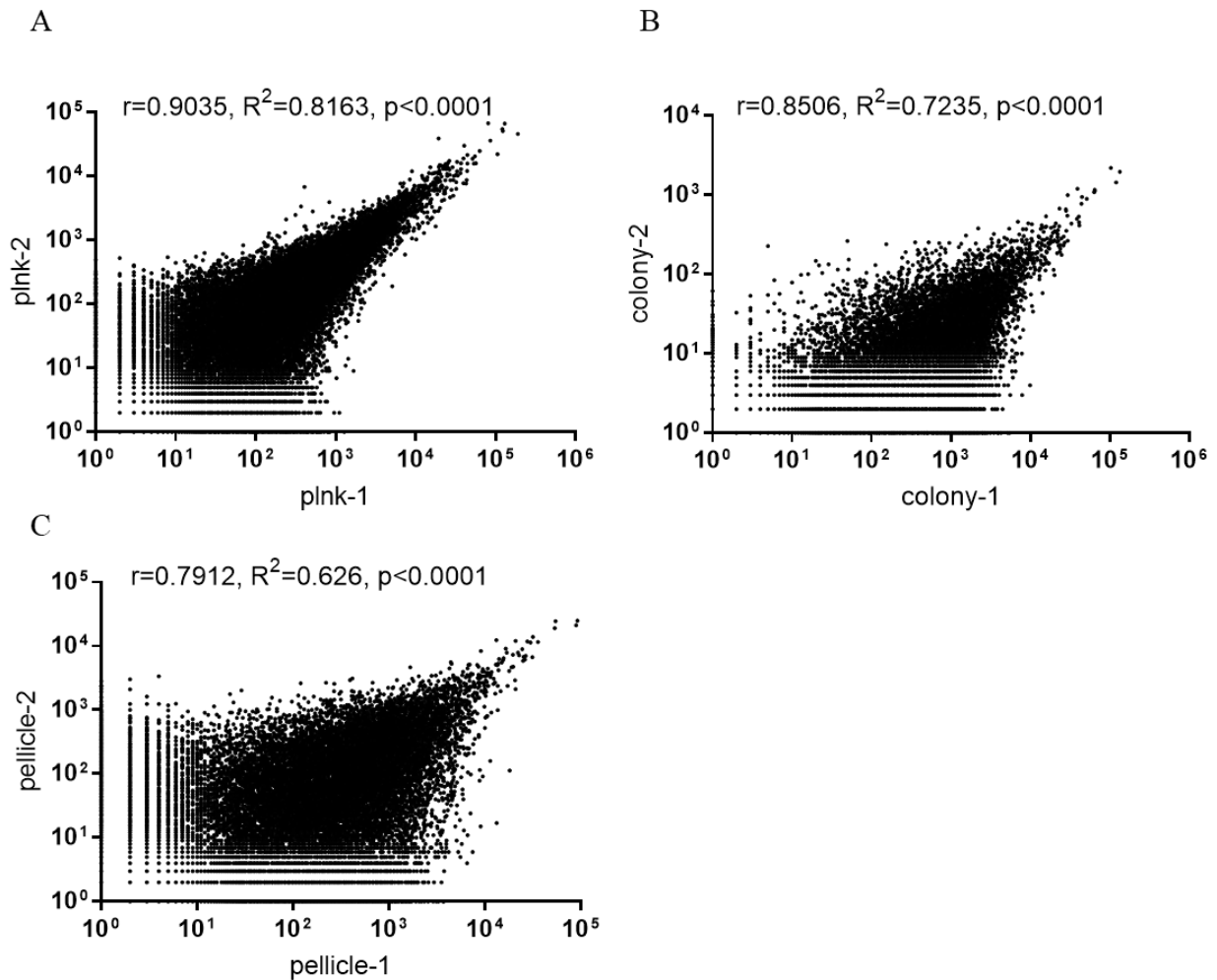
Figure 3: Tn-seq library sequencing results for each growth condition show significant correlation between replicates

A-C. Correlation between two Tn-Seq replicates of planktonic (plnk) (A), colonies (B), and pellicle biofilms (C). Number corresponding to sequencing reads mapped to each transposon insertion site in a sample is plotted against its replicate. Potential insertion sites (T-A dinucleotides) that contained zero or only one mapped read in both replicates were excluded from the correlation analysis. Any remaining insertion sites that had zero mapped reads in one of the replicates was converted to one, to allow for log-scale plotting. The Pearson coefficient (r), R-squared values, and statistical significance of correlation were calculated in GraphPad Prism 7. See Table 4 for the summary of metadata.

4.1.2 Identification of Genes Required for Fitness in MTB Biofilms

Tn-Seq identified 53 candidate genes for conferring fitness advantage during biofilm growth by statistically significant (q-value < 0.05) underrepresentation in either the pellicle and/or colony biofilm screens (Fig. 4A-B). The full dataset of read counts for each sequencing replicate and analysis by TRANSIT are available in Appendix B Tables B1 and B2. Among the 53 genes, 48 genes were exclusively identified in the pellicle biofilm, while 11 genes were identified by the colony biofilm screen. This suggests distinct genetic requirements for growth in each condition. Three genes previously implicated in biofilm development of MTB, *mmaA4* (186), *relA* (69), and *pks16* (184), were among the 53 gene set identified in our Tn-seq screen (Fig. 4A-B). Consistent with altered morphology of Δ*mmaA4* colonies, and its deficiency in pellicle biofilm formation, *mmaA4 :*Tn mutants were underrepresented in both screens. In addition to *mmaA4*, Tn mutants in five other loci – *fadA2*, *cysQ*, *ponA2*, *glpK*, and *Rv3779* – were significantly underrepresented in both the pellicle and colony biofilm screens (Fig. 4A-B).

To determine if any genes in MTB pellicle biofilms confer fitness under exposure to RIF, another Tn-seq screen was performed by exposing pellicles to 5 µg/mL of RIF for 24 hours before processing for outgrowth. Sequencing reads of RIF-exposed Tn-library pellicles were compared to unexposed pellicle sequence reads in TRANSIT as described previously (202). Metadata for the RIF-exposed pellicle replicates is listed in Table 4, and complete Tn-Seq results from RIF-exposed pellicles are compiled in Appendix B Table B3. Tn-seq identified Tn-mutants of only one gene as being significantly underrepresented (q-value < 0.05) in RIF-exposed pellicles relative to unexposed pellicles, a putative drug ATP-binding transporter gene *Rv1272c* that may be involved in long chain fatty acid import or drug efflux (207, 208). Interestingly, though not statistically significant, *Rv1273c*, which is directly upstream and also a putative drug-efflux pump that may be
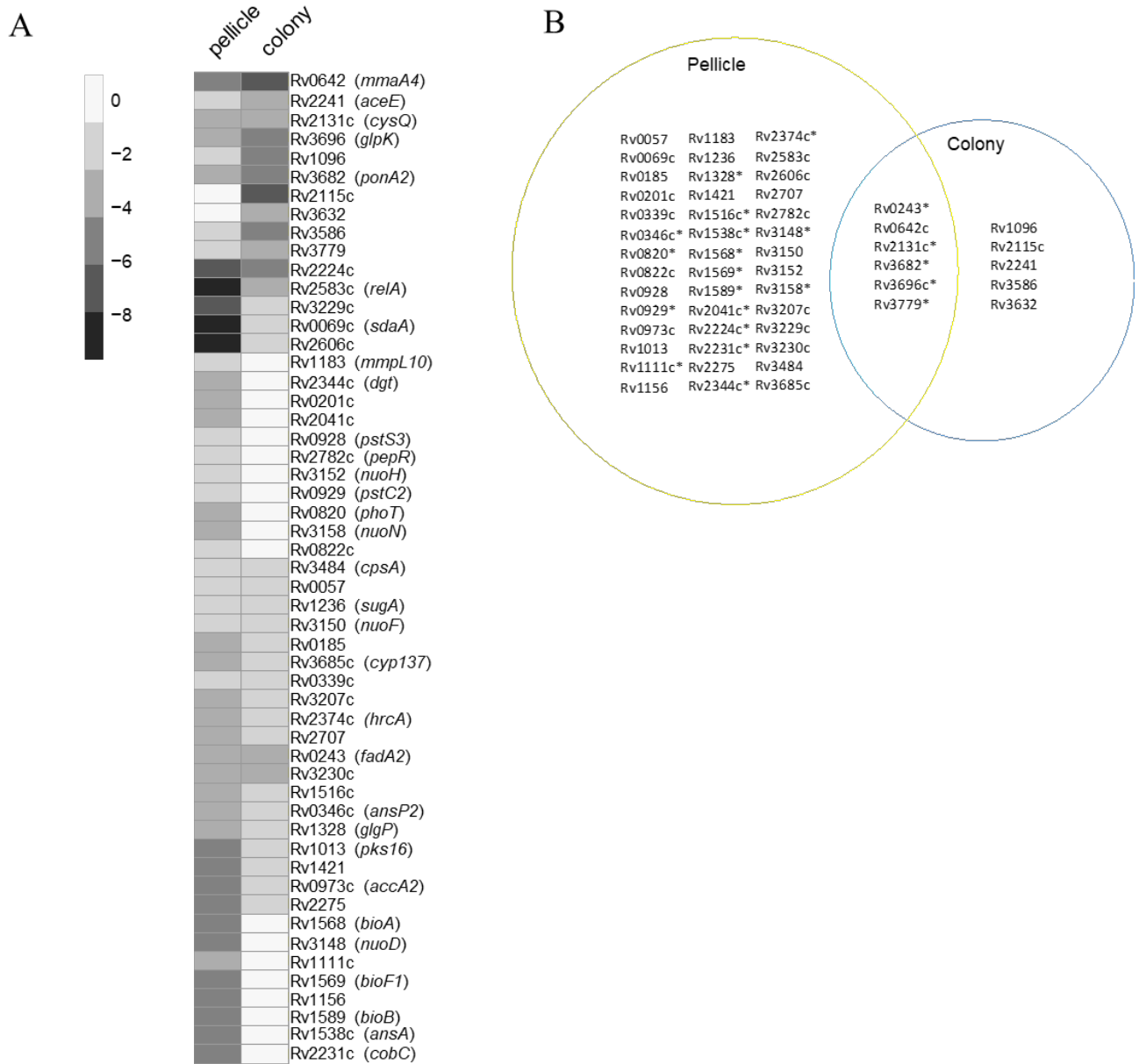
Figure 4: Genes necessary for fitness within MTB biofilms

Heat map (A) and Venn diagram (B) of 53 genes, mutations in which cause significant underrepresentation of clones either in pellicle biofilms or colonies. While the heat map depicts fold-change in the reads, the Venn diagram depicts statistically significant read counts in each of the two growth models. The scale bar for the heat map represents log2(fold-change). Fold changes of six genes (*Rv# 0057*, *0339*, *1236*, *2131c*, *3150* and *3484*), depicted by the heat map as similar in both colonies and pellicles (A), are statistically significant only in the pellicle model (B). The metadata summary of Tn-seq is provided in Table 4, whereas complete dataset obtained from biofilm TRANSIT analysis is in Appendix B. Asterisks indicate genes that were followed-up in this study.

part of an operon with *Rv1272c*, was also one of the few genes to decrease in representation under RIF exposure: log$_2$ fold change = -4.18 (Appendix B Table B3).

4.2 Monocultures of Mutants Distinguish Absolute from Relative Fitness Deficiency in Biofilms

Because Tn-seq identified mutants previously reported to be required for biofilm formation, we began evaluating the isogenic mutant strains by investigating their ability to form pellicle biofilms in monoculture. We selected 22 candidates for investigation into their role in biofilm formation (indicated in Fig. 4B). Selection was mostly based on previous indication of genes significance in persistence or pathogenesis (201, 209, 210). We hypothesized that genes identified in the biofilm Tn-seq screen that were also previously identified in Tn-seq screens for requirements in mouse and macrophage infection models were more likely to be relevant to persister formation. We constructed isogenic deletion mutants in 22 strains and assayed them for their ability to form pellicle biofilms in Sauton's medium monoculture. We also performed growth curve analyses on mutants that displayed an altered pellicle phenotype to determine if a nutritional deficit or slow growth rate was responsible for the pellicle phenotype (Fig. 5A-C).

This experiment revealed three distinct categories of mutants. Sixteen mutant strains were able to form pellicle biofilms in monoculture that were indistinguishable from WT, suggesting that the fitness disadvantage of these mutants is observable only when they are in direct competition with WT in biofilms. In the second category, Δ*ansA* and Δ*bioA* mutants were growth retarded in both pellicles and planktonic culture (Fig. 5A-C). Growth in Sauton's medium, which contains L-asparagine as the primary source of nitrogen and lacks biotin, presumably requires the activity of

L-asparaginase (*ansA*) and biotin synthase genes (*bioA*) in cells. The initial Tn-seq screen, however, was performed in nitrogen- and biotin-rich 7H9-OADC medium, suggesting *ansA* and *bioA* activity is of greater consequence during biofilm growth, possibly due to nutrient-limiting conditions. Four mutants of the last category either failed to form a pellicle at all (Δ*dgt*), was delayed in pellicle formation (Δ*phoT*), or formed a pellicle with an altered morphology (Δ*Rv2224c* and Δ*ponA2*) compared to WT, but remained growth competent planktonically through late logarithmic phase (Fig. 5A-B). The Δ*dgt* (a probable dGTPase based on sequence identity) strain was unable to form a pellicle in Sauton's medium, with growth only occurring on the bottom of the well and no biofilm forming at the air-media interface (Fig. 5A). A plasmid expressing *dgt* under the control of constitutive promoter of the *hsp60* gene (pJR08), partially complemented pellicle formation without full restoration of biofilms maturation (Fig. 5A) suggesting that additional genomic elements are necessary to fully restore biofilm formation. *dgt* is directly upstream of the essential gene *dnaG*, which encodes DNA primase that synthesizes RNA primers for Okazaki fragments during DNA replication. It is possible that deletion of *dgt* disrupts normal expression of *dnaG*, and full complementation of the pellicle formation phenotype would require proper expression of *dnaG*. Δ*phoT* (ATP-binding phosphate transporter) grew slower in pellicles than WT, and did not mature in biomass and texture until ~6 weeks of growth (Fig. 6), compared to ~5 weeks for mature WT biofilms (Fig. 5A). A plasmid constitutively expressing *phoT* under the *hsp60* promoter (pJR14) was able to restore pellicle biofilm development to a WT-level timeline (Fig. 5A). Altered texture and morphology of mature biofilms of two mutants, Δ*Rv2224c* and Δ*ponA2* (Fig. 5A). *Rv2224c* and *ponA2* have been implicated in modulation of the host innate immune system and peptidoglycan biosynthesis respectively (211, 212), compared to WT. Colonies of all four mutants from this class grown on Sauton's agar showed altered morphological

61

phenotypes (Fig. 7), and growth retarded mutants Δ*ansA* and Δ*bioA* showed defect forming colonies on Sauton's agar.
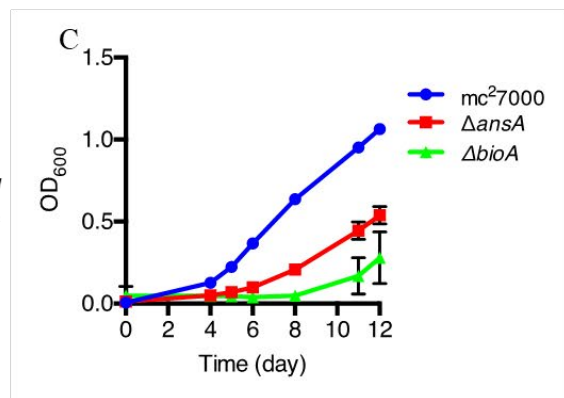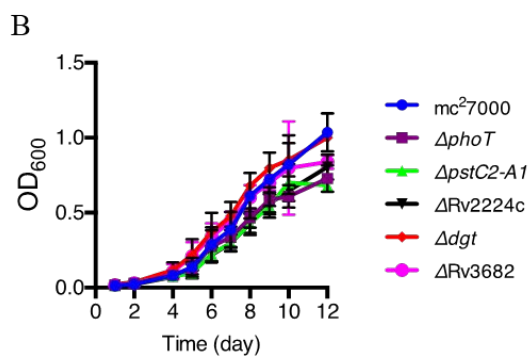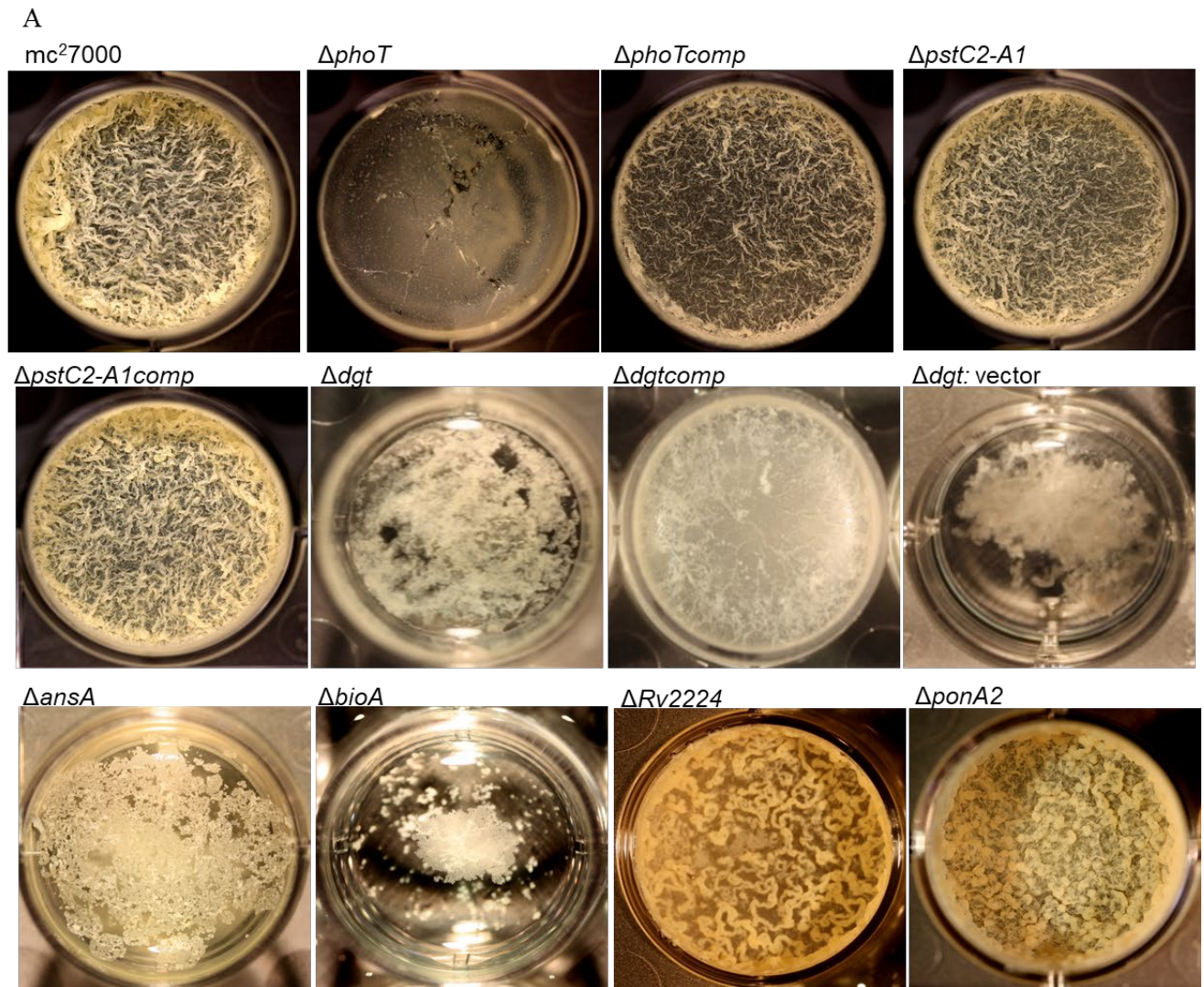
Figure 5: Genes required for growth of MTB in pellicle biofilms

A. Top down view of pellicles of mc²7000 (WT) and mutant strains carrying isogenic deletion of the indicated genes, identified in the Tn-seq based screen (see Table B1 and B2). Complemented strains of Δ*phoT* (Δ*phoTcomp*), Δ*pstC2-A1* (Δ*pstC2-A1comp*), Δ*dgt* (Δ*dgtcomp*) carrying a plasmid expressing the corresponding genes under the control of either its natural promoter (Δ*pstsC2A1*) or the *hsp60* promoter are also shown. The strain Δ*dgt* carrying the empty vector pMH94 was control for Δ*dgtcomp*. Pellicles were grown at the air-medium interface in 12-well tissue culture plates in Sauton's medium for 5 weeks at 37°C. The strain Δ*phoT* formed normal pellicle upon further incubation (see Figure 6). B-C. Planktonic growth of mc²7000 and the mutants cultured in detergent-free Sauton's medium. Cultures were shaken once daily, and their optical density were measured after dispersion of 1 mL aliquots in detergent at 600 nm. Data represent mean ± SD (n= 3).

Δ*phoT*   Δ*phoT*comp

Figure 6: Pellicle development in Δ*phoT* upon extended incubation

A top-down view of pellicles of Δ*phoT* and Δ*phoT*comp in Sauton's medium at the liquid-medium interface after six weeks of incubation.

Figure 7: Morphologies of colonies formed by the indicated mutants after six weeks of incubation on Sauton's medium based agar plates

4.3 Δ*phoT* and Δ*pstC2-A1* Are Outcompeted by WT in Hypoxic Microcolony Formation

Attempts to recapitulate the competitive growth environment of the Tn-seq screen by mixing WT with isogenic deletion strains in pellicles at a 7500:1 ratio (estimate of average mutant representation in Tn-seq) resulted in a surprising number of spontaneous zeocin-resistant mutants (the antibiotic marker used for selection of successful mutants) complicating efforts to obtain an accurate ratio of WT to mutants in mixed pellicle biofilms. To quantitatively determine the

magnitude of biofilm deficiency of mutants when part of a mixed population, we grew different

fluorescent reporter strains of WT and mutant strains in direct competition to form microcolonies

in Sauton's medium when attached to a polycarbonate membrane in cover glass-bottom culture

dishes as described in Chapter 3.6. An approximated 20:1 ratio of WT to either Δ*phoT*, Δ*pstC2-*

A1, Δ*Rv2224c*, Δ*dgt*, or Δ*ponA2* cells were mixed and spotted on a polycarbonate membrane.

While WT constitutively expressed GFP, the mutants expressed mCherry (a WT strain expressing

mCherry was used as a control). At day 1, cells expressing mCherry were counted by CLSM in

five independent fields of view per membrane to obtain an average value of population

distribution. The membranes were incubated at 37 °C and after 14 days of growth of cells,

microcolonies expressing mCherry were counted in five independent fields of view per membrane.

Of the five mutant strains compared, only Δ*phoT* and Δ*pstC2-A1* were significantly outcompeted

by the WT strain in microcolony formation (Fig 8A-D). The Δ*phoT* mutant produced no detectable

microcolonies when in competition with WT (p-value < 0.001), and Δ*pstC2-A1* was significantly

outcompeted by WT (p-value < 0.01) albeit to a lesser degree than Δ*phoT* (Fig. 8B). To test

whether this result was media specific, the same competition assay was performed with the two

phosphate-sensing mutant strains Δ*phoT* and Δ*pstC2-A1* in 7H9OADC medium. Similar to

Sauton's medium, Δ*phoT* was unable to form microcolonies in 7H9OADC medium when in

competition with WT (p-value < 0.001), while Δ*pstC2-A1* was significantly outcompeted by WT

(p-value < 0.05), but to a lesser degree (Fig. 8C-D). This indicates that though deletion of *pstC2-*

A1 transporters does not exhibit any phenotype in monoculture pellicles, that phosphate

homeostasis via expression of the *pstS3C2A1* operon, as well as *phoT*, is required for adaptive

fitness at WT levels in biofilm formation. An alternative explanation however, is that these due to

the logistics of this experimental setup, membrane-bound microcolonies are likely growing in
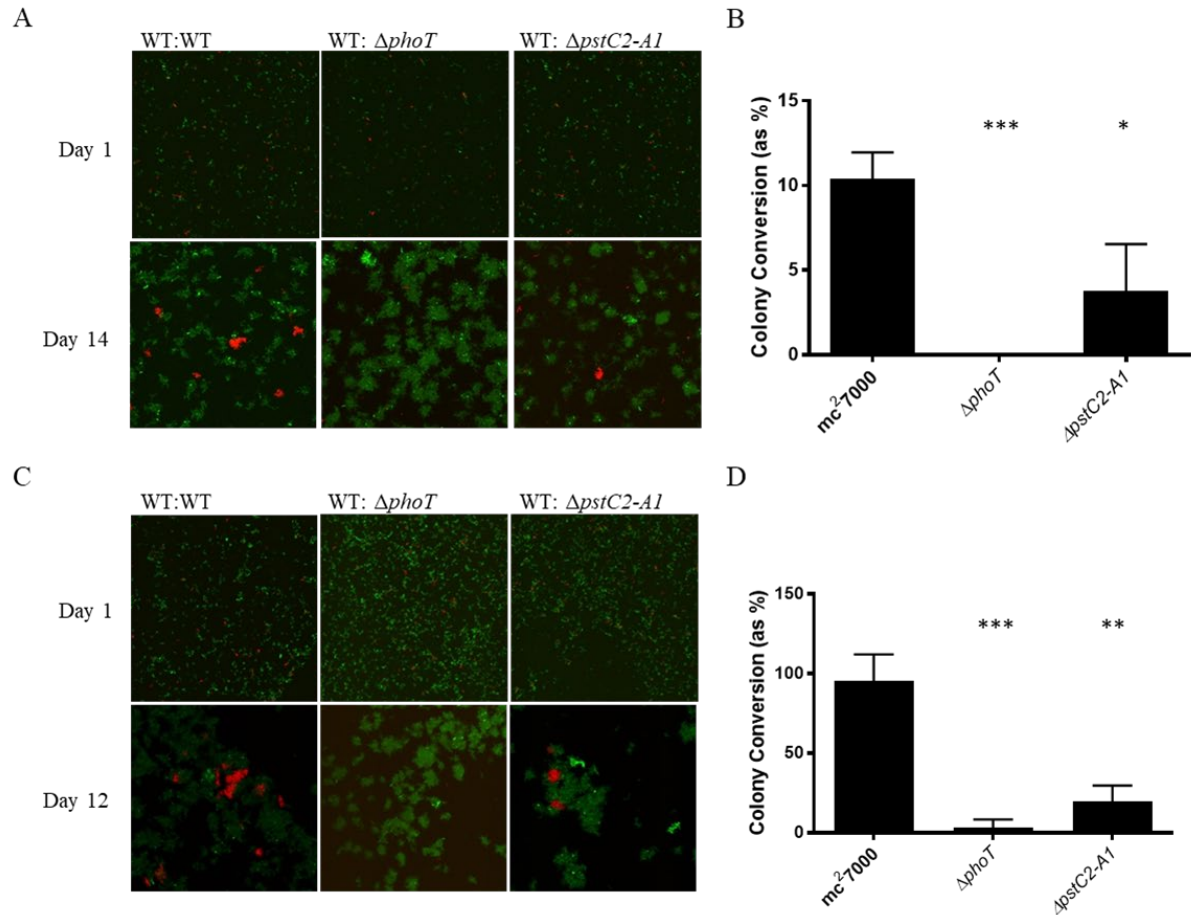
Figure 8: ΔphoT and ΔpstC2-A1 is out competed by WT in formation of microcolonies in hypoxic conditions
A and C. Representative max projections from CLSM micrographs showing outgrowth of mCherry (red) expressing wild-type (mc^{2}7000)as a control, and its isogenic mutants ΔphoT or ΔpstC2-A1 on a solid substratum in a glass bottomed tissue culture dish. An internal control (wild-type expressing GFP) at a ratio of 20:1 was seeded with each of mCherry expressing strains. The reporters in their corresponding strains were expressed by the *hsp60* promoters. Cells were mixed and spotted on a polycarbonate membranes, which were placed in cover glass-bottomed dishes sealed with agarose and submerged in Sauton's (A) or 7H9 (C) medium. The membranes were imaged by CSLM with a 488 nm laser for GFP and 594 nm laser for mCherry after the indicated incubation period. Imaged at 20x magnification. B and D. Plot showing colony conversion frequency, defined as ratio of average number of red colonies observed at 14 days post inoculation for Sauton's and 12 days post inoculation for 7H9 from 5 fields of view per membrane to average number of red cells observed at day 1 from 5 views of the same membrane the later time point. Data represent mean of three biologically independent experiments. Scale bars = S.D. ; * indicates a p-value < 0.05; ** indicates a p-value < 0.01; *** indicates a p-value < 0.001. Statisitcal significance determined by student's t-test using GraphPad Prism 7.0 software.

oxygen-limited conditions, and that lack of sufficient oxygen is driving the observed decrease in colony conversion in the phosphate-sensing strains when in competition with WT, however under a modified Wayne model of hypoxia, both Δ*phoT* and Δ*pstC2-A1* survived at rates comparable to WT (Fig. 12B). In an alternative *in vitro* biofilm model using microfluidic flow cells, Δ*phoT* showed an observable deficiency in aggregative growth relative to WT by day 6 post-inoculation (Fig. 9) as well. It is possible that lack of Δ*phoT* microcolony formation in hypoxic conditions (Fig.8) is due to Δ*phoT* exhibiting a slower biofilm growth rate similar to its behavior in pellicle (Fig. 5A) and microfluidic (Fig. 9) biofilm models, rather than by direct competition with WT. These findings however still validate Tn-seq identification of *phoT* as conferring a fitness advantage in biofilm growth. Because *dgt*, *Rv2224c*, and *ponA2* mutants had colony conversion rates comparable to WT, the pellicle-specific fitness advantages that caused them to be identified in the Tn-seq screen may apply only to that growth model or only be important at later a developmental point in biofilm maturation, and may not apply to microcolony formation.
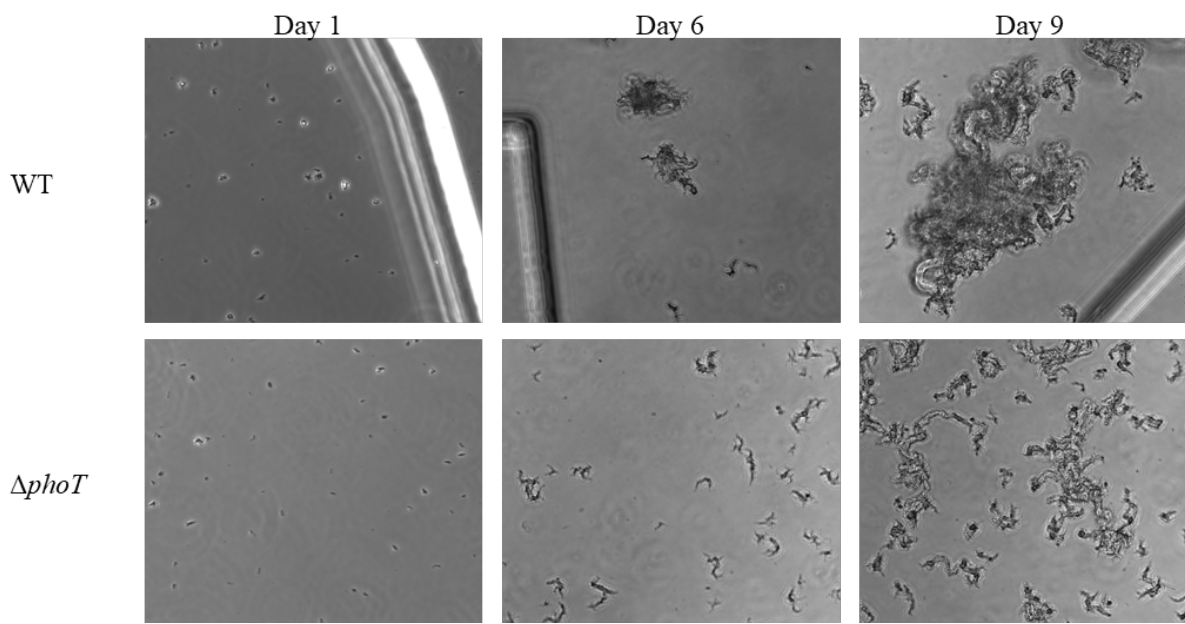
Figure 9: Δ*phoT* is deficient in aggregative growth in a microfluidic flow cell

Representative phase contrast micrographs of MTB mc^{2}7000 strains WT (top row) and Δ*phoT* (bottom row). Bacteria were grown in the CellASICS Onix2 microflufidic plates as described and imaged using widefield microscopy at 20x magnification on days 1, 6 and 9 of growth.

4.4 Relationship Between Fitness in Biofilms and Persistence Against Antibiotics

4.4.1 Biofilm Deficient Mutants Identified in Tn-seq Exhibit Hypersensitivity to RIF

Biofilms are phenotypically more tolerant to exogenous stresses than single cells or planktonic cultures of bacteria suspended in liquid medium (98). MTB biofilms have been shown to harbor antibiotic-tolerant cells *in vitro* (184). We sought to test our hypothesis that genes conferring a fitness advantage in MTB biofilms also facilitate antibiotic tolerance. To test if mutations in biofilm fitness genes would make MTB hypersensitive to a frontline TB antibiotic, we plated serial dilutions of the 22 isogenic deletion strains on 7H11OADC agar plates containing a sub-inhibitory concentration (50 ng/mL) of RIF and compared them to WT cfu to assay for hyper susceptibility (Fig. 10). Six of the mutant strains (Δ*phoT*, Δ*pstC2-A1*, Δ*cysQ*, Δ*Rv2224c*, Δ*dgt*, and Δ*ponA2*) formed less colonies than WT on the RIF-containing plates (Fig 10). The mutant Δ*cysQ* formed smaller colonies than WT even in the absence of antibiotics, indicating their slow growth in this medium. The mutant therefore was excluded from further experiments. The Δ*Rv2224c* and Δ*ponA2* mutants have been previously reported to be hypersensitive to RIF in addition to isoniazid (INH), low pH, oxidative stress, and cell wall stress (213). Deletion of *pstA1* is also found to result in RIF hypersensitivity (214), although such a phenotype for Δ*phoT* and Δ*dgt* have not been previously reported. Three of these genes, *pstA1*, *Rv2224c*, and *ponA2*, are required for persistence in mouse infections (210), and *phoT* is essential for virulence in primary

murine macrophages based on previously published microarray data (209). Together, these data suggest that genes required for fitness in biofilms are also important for survival under antibiotics and other stresses.
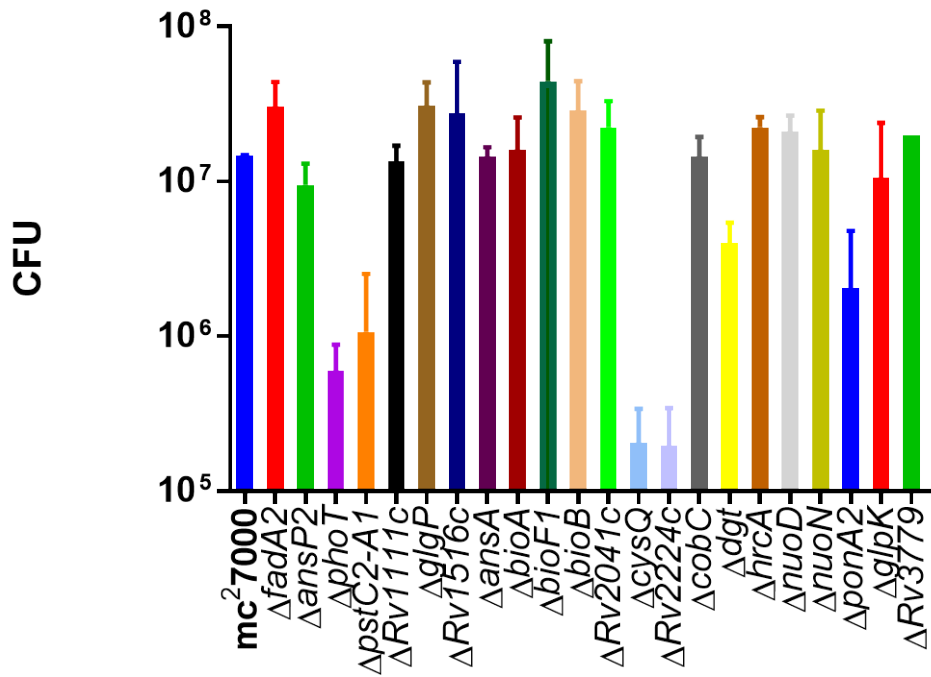
Figure 10: Hypersensitivity to RIF of isogenic mutant strains

Hypersensitivity to RIF was tested by plating ten-fold serial dilutions of mc^{2}7000 and isogenic deletion strains on 7H11OADC agar plates containing 50 ng/mL RIF. Colony forming units were enumerated after 21 days of colony growth. Dilutions were plated from mid-exponential phase planktonic cultures of equal OD_{600}. Data represent mean of two biologically independent experiments performed in triplicate; error bars = S.D.

4.4.2 Increase in Intrinsically Antibiotic Tolerant Cells in MTB Biofilms Produces an Increase in Persister Frequency

The strong overlap in mutants with a biofilm phenotype and RIF hypersensitivity suggests that environmental conditions within biofilms favor cells with fitness to tolerate both endogenous and exogenous stressors. This would mean that there is reasonable expectation that biofilms harbor more cells that are *intrinsically* tolerant to antibiotics than planktonic suspension. There is also a link between intrinsically antibiotic cells and persister frequency (89, 214). We hypothesized that enrichment of intrinsically tolerant cells in MTB biofilms would correlate with increased persister frequency (Fig. 11A). A corollary to this hypothesis is that biofilms of cells that are intrinsically hypersensitive to antibiotics would also harbor fewer persisters than those present in wild-type biofilms. To test this hypothesis, we exploited Δ*phoT* and Δ*pstC2-A1* mutants that are both RIF-hypersensitive but exhibit biofilm development. The ability of the mutants to form mature pellicles indistinguishable from WT allowed us to circumvent potentially compounding results of RIF sensitivity displayed by biofilm-defective mutants like *ponA2* and *mmaA4 and pks16* mutants. We grew pellicle biofilms of WT, Δ*phoT* and Δ*pstC2-A1*, and their complementing strains, to maturation (6 weeks for Δ*phoT*) and exposed them to 7 days of 100xMIC 50 µg/mL RIF (or DMSO as a control), processed pellicles as described, and plated serial dilutions onto 7H11OADC agar to assay the number of persisters in each strain. Both mutants, Δ*phoT* and Δ*pstC2-A1*, produced approximately 20-fold less persisters compared to WT (p-value < 0.01) (Fig. 11B-C). This phenotype was partially rescued by expression of *pstC2-A1* on a complementing plasmid, but was not rescued by expression of *phoT* on a complementing plasmid (Fig. 11B-C). Lack of complementation in Δ*phoT* may be due to continued activation of *pstSCAB* module (Appendix B Table B4), or inability of an extrachromosomal phoT to fully restore gene dysregulation caused

by its deletion. Δ*pstA1* also produces less persisters in planktonic cultures (214) indicating that regardless of growth conditions, intrinsic antibiotic tolerance is a central determinant of persister frequency. It is reasonable to conclude that growth limiting conditions in MTB biofilms act as a self-selecting environment for more drug tolerant cells than in planktonic cultures and results in increase of persister frequency.
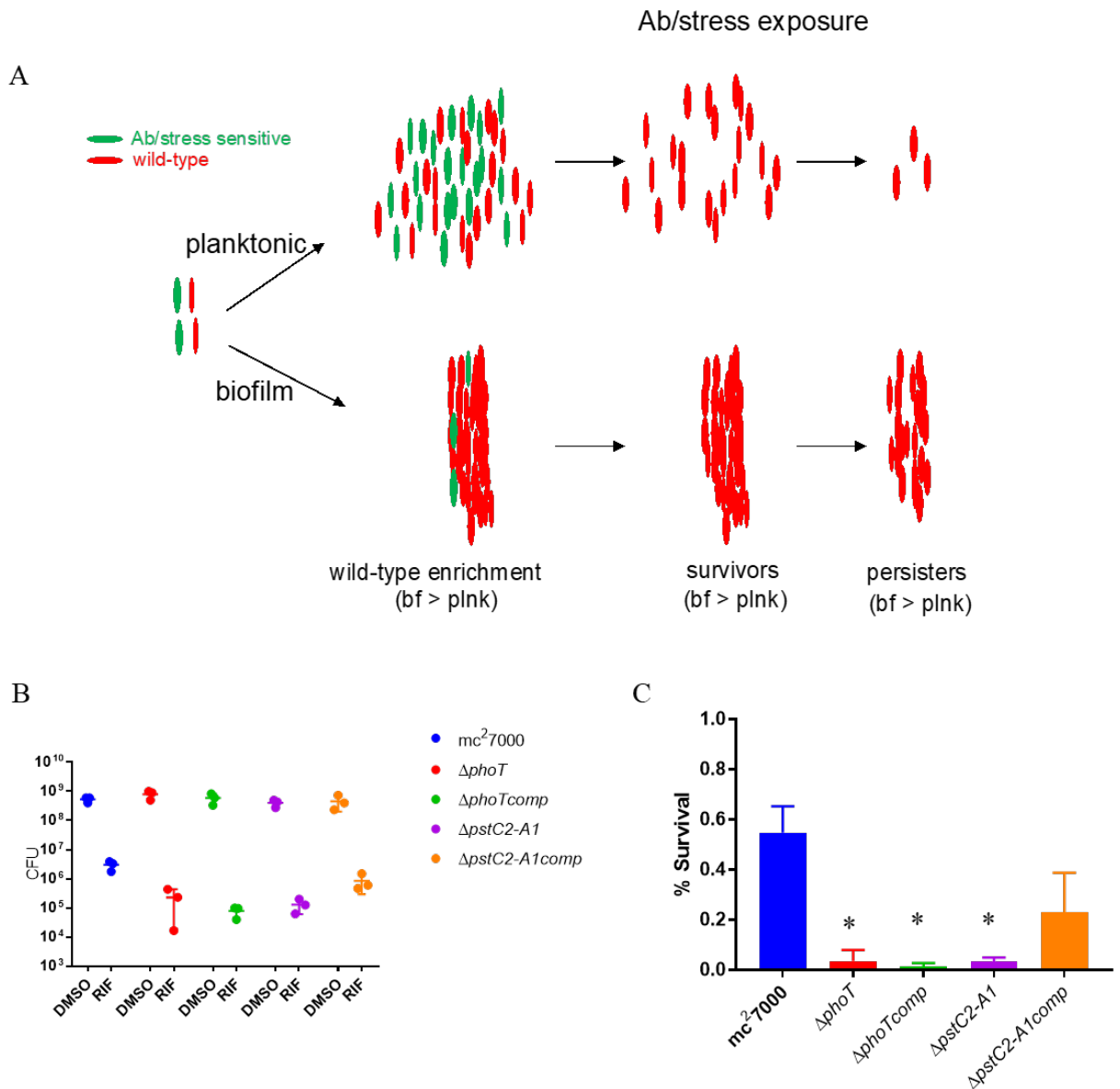
Figure 11: Intrinsic resistance of individual cells determine persister frequency in MTB biofilms

A. A schematic explanation of biofilm-associated drug tolerance in MTB. The model hypothesizes that enrichment of WT clones in biofilms is the crucial determinant for high frequency of survivors and eventual persisters, thus predicting that a monoculture biofilms of a hypersensitive mutant will harbor fewer persisters than WT. B-C. Frequency of RIF tolerant persisters in biofilms of mc²7000, and RIF sensitive Δ*phoT* and Δ*pstC2-A1* and Δ*photcomp* and Δ*pstC2-A1comp*. Five week pellicles were exposed to 50 µg/mL RIF for 7 days, then solubilized with Tween-80 and dilutions were plated on 7H11OADC agar plates to enumerate the the surviving cfu. Cells exposed to DMSO (solvent for rifampicin) were used as untreated control (Ctrl). Data represent three biologically independent experiments. average percentage (%) survival calculated from panel B are shown in panel C (n= 3; p < 0.01; unpaired t-test).

4.5 Gene Dysregulation in Δ*phoT* and Δ*pstC2-A1*

Tn-seq identified underrepresentation of *pst* and *phoT* Tn mutants under pellicle conditions, both members of the phosphate specific transport (*pst*) module in the phosphate-sensing pathway (215). This indicates an importance for phosphorous homeostasis for fitness of MTB cells in biofilm microenvironments. However, the difference in biofilm phenotypes in Δ*phoT* and Δ*pstC2-A1* was unexpected. Because regulation of phosphate homeostasis has been linked to persistence in the host and antibiotic tolerance in MTB (214, 216), we attempted to understand the basis of the difference between Δ*phoT and ΔpstC2-A1* phenotypes in biofilms.

In bacteria, PstSCAB complexes are part of the superfamily of ATP-binding cassette (ABC) transporters, and thought to function as sensors that respond to environmental phosphate concentrations leading to downstream regulation of gene expression (217). PstS is the periplasmic component of the complex and directly binds phosphate to present it to the transmembrane transporters PstC and PstA. PstC and PstA complex together to form a channel into the cell. PstB is a cytoplasmic protein which dimerizes and contains nucleotide-binding domains. PstB hydrolyzes ATP to power the PstSCAB complex (218). Recent studies suggest that PstB (dependent on whether or not inorganic phosphate is bound to PstS) interacts with PhoU directly, or frees it to activate genetic regulators downstream, coupling environmental phosphate concentrations with genetic regulation (219, 220).

MTB has several paralogs of genes encoding components of the pstSCAB complex: three pstS paralogs, two each of transporters PstC and PstA, and two pstB paralogs. The *pst* operon at *Rv0928-30* (*pstS3C2A1*) in particular has been shown to be induced under phosphate starvation and regulate gene expression through the two component regulators RegX3/SenX3 (216, 221). RegX3 is a transcriptional regulator that responds to inorganic phosphate depletion via its cognate

sensor SenX3 (222). Notably, this operon lacks a gene for a dedicated PstB ATP-binding protein. MTB encodes a PstB at *Rv0933* located within a genomic region encoding an additional Pst module (*Rv0932c*, *Rv0931-36*), which is not induced during phosphate starvation and does not seem to be linked to gene regulation or virulence (215, 221). Located at *Rv0820* and *Rv0821* is *phoT*—a probable paralog of *pstB*—and one of MTB's two *phoU* orthologs, *phoY2*. *phoT* has shown minor induction under phosphate starvation (221), and *phoY2* has been shown to play a role in persister formation in a RegX3-dependent manner (214). We hypothesized that the difference in the phenotype of Δ*phoT* and Δ*pstC2-A1* was due to their differential response to conditions that likely prevail in biofilms, including phosphate starvation. To test this hypothesis, we analyzed the ability of the two mutants to survive under phosphate-starvation and hypoxia. We also studied their ability to import inorganic phosphate.

4.5.1 Δ*phoT* and Δ*pstC2-A1* Have Comparable Viability in Phosphate-starved Conditions

We grew planktonic cultures of WT, Δ*phoT*, Δ*pstC2-A1*, and their complementing strains to mid-logarithmic phase in 7H9OADC medium, washed them twice in phosphate-free 7H9 medium buffered with MOPS, and then re-suspended them in phosphate-free 7H9 medium buffered with MOPs for 30 days and plated serial dilutions from the phosphate-starved cultures on 7H11OADC agar at 0, 3, 9, 14, 21, and 30 days to enumerate surviving cfu (Fig. 12A). Despite a modest decrease in viable Δ*phoT* cells at day 14 of phosphate starvation, no significant changes in viability of either mutant was observed during phosphate starvation.

4.5.2 Import of Inorganic Phosphate is Not Affected in Δ*phoT* and Δ*pstC2-A1*

To determine if Δ*phoT* or Δ*pstC2-A1* mutants exhibited a deleterious effect on import of inorganic phosphate, we used the Malachite Green Phosphate Assay Kit (Cayman Cat. No. 10009325) to determine the percentage of a known quantity of potassium phosphate (KH_2PO_4) imported by cells in WT, Δ*phoT*, and Δ*pstC2-A1* planktonic cultures after 24 hours of phosphate starvation. Mid-exponential cultures of each strain were grown in 7H9OADC medium, phosphate-starved for 24 hours as described, and then potassium phosphate was added to a concentration of 25μM. Phosphate content was recorded by colorimetric assay at 0, 12, 24, 36 and 48hr after the addition of potassium phosphate. Neither Δ*phoT* nor Δ*pstC2-A1* were observably deficient at importing inorganic phosphate within the range of this assay (Fig. 12B). Because neither of the mutant strains were significantly less viable under phosphate starvation, or deficient at importing inorganic phosphate, the difference in pellicle formation rate between Δ*phoT* and Δ*pstC2-A1*, is unlikely caused by low levels of intracellular phosphate in the later stages of biofilm development.

4.5.3 Δ*phoT* and Δ*pstC2-A1* Are Comparably Tolerant to Hypoxia

It has been previously demonstrated that deletion of the *phoY2*, one of the two PhoU orthologs of MTB, results in premature growth arrest under hypoxic conditions (214). In MTB, *phoY2* is located genomically at *Rv0821*, directly downstream of *phoT* (*Rv0820*). Because Δ*phoT* shows a delayed pellicle maturation phenotype compared to normal development to Δ*pstC2-A1*, and Δ*phoT* shows greater deficiency than Δ*pstC2-A1* in a submerged, membrane-attached biofilm model, we decided to investigate the tolerance to hypoxic conditions as a possible mechanism of the Δ*phoT* specific defect. Using a modified Wayne model (204) of cultures in parafilm-sealed

75

tubes with no headspace, we assayed the viability of WT, Δ*phoT*, and Δ*pstC2-A1* under *in vitro*

hypoxic conditions and enumerated cfu at 0, 7, 14, 21, and 30 days after the exposure to hypoxic

conditions. Neither of the mutant strains displayed a loss of viability relative to WT under hypoxic

exposure for up to 30 days, indicating that greater inability to survive under hypoxic conditions is

not the cause of biofilm deficiency in Δ*phoT* (Fig. 12C).

4.5.4 Transcriptome Signatures of Δ*phoT* and Δ*pstC2-A1* Are Similar

We next pursued an alternative hypothesis that disruption of the two loci may produce

different extent of dysregulation in global gene expression pattern in MTB cells. Deletion of *pstA1*

leads to constitutive activation of the RegX3-Senx3 two-component system that regulates the

expression of a broad range of genes in MTB (216, 223). Although the precise mechanism driving

the activation of RegX3 is unknown, the activation of PstSCAB transporter complex appears to be

a determinant. To determine differences in gene expression in Δ*phoT* or Δ*pstC2-A1*, we performed

RNA-seq based transcriptomic profiling of the two mutants compared to WT. Cultures were grown

planktonically in 7H9OADC to mid-logarithmic phase, whole RNA was extracted, and RNA-seq

libraries were prepared, sequenced, and analyzed (205) as described above. The transcriptomic

profiles of Δ*phoT* and Δ*pstC2-A1* were very similar in their gene dysregulation relative to WT

(Fig. 12D). Notably, *regX3* was induced five-fold more in Δ*phoT*, and four-fold more in Δ*pstC2-*

A1 compared to WT. While deletion of *phoT* leads to induction of the *pstS3C2A1* operon, deletion

of *pstC2-A1* does not correspondingly result in induction of *phoT* (Fig. 12D). Expression levels

of MTB paralog *pstB* (*Rv0933*) are constitutively higher than *phoT* in all the strains. Deletion in

Δ*phoT* results in induction of *pstS3C2A1* and therefore likely increases the level of functional

PstSCAB complexes, dysregulating phosphate homeostasis. This is impossible in the Δ*pstC2-A1*

strain as its inducible phosphate transporters are not present. This suggests that the biofilm formation defects observed in Δ*phoT* are the result of more severe dysregulation of phosphate homeostasis by constitutive activation of *pstSCAB* complexes via RegX3-SenX3 two component system.
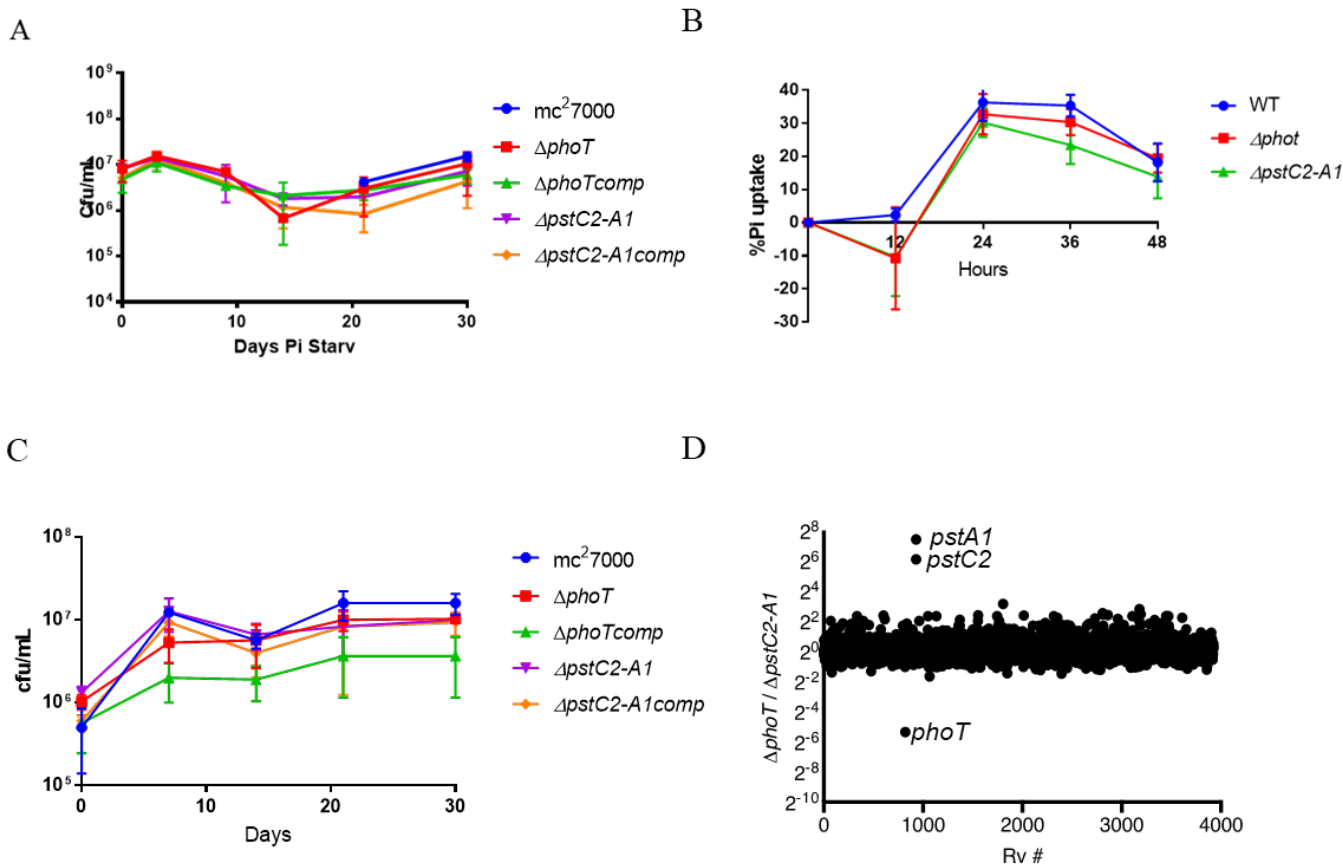
Figure 12: Analysis of Δ*phoT* and *ΔpstC2-A1* response to microenvironment conditions

A. Survival of mc^{2}7000, deletion, and complementing strains during phosphate starvation. OD$_{600}$: 0.05 cultures were washed and resuspended in phosphate-free 7H9 medium buffered with MOPS. Serial dilutions were plated on 7H11OADC agar plates to enumerate the surviving cfu/mL at the indicated time points. B. Inorganic phosphate importation of mc^{2}7000, deletion strains was measured at the indicated timepoints using Cayman malachite green phosphate assay and absorbance was measured at 620 nm. C. Survival of mc^{2}7000, deletion, and complementing strains during hypoxic conditions. Using a modified Wayne model of *in vitro* hypoxia, strains were incubated in parafilmed 50 mL tubes with no headspace. At the indicated timepoints, some tubes were opened and serial dilutions were plated on 7H11OADC agar plates to enumerate the surviving cfu/mL. A-C. Data represent three biologically independent experiments; error bars = S.D.; Student's t-test was used to calculate significance. D. Ratio of the reads corresponding to each Rv # between Δ*phoT* and *ΔpstC2-A1* indicate a broad similarity in transcriptomes of the two mutants, while each being similarly different from the wild type. The only significant differences (> 4-fold) are in the mutated genes. The RNA-seq data are provided in Appendix B Table B4.

4.6 Unique Growth Environment of MTB Biofilms is Marked by INLPS Induction

We hypothesized that the enrichment of stress and antibiotic tolerant cells in biofilms likely originates from their complex microenvironments that emerge from the uniquely stratified architecture. To determine the response to unique growth environment of biofilms, we sought to identify the distinctive gene-expression pattern specific to MTB growth in mature biofilms. We compared transcriptomic analysis of planktonic and biofilm cultures (Appendix B Table B5). The most notable finding was co-induction of a 6-gene operon (*Rv0096-0101*), which is involved in the synthesis of a putative isonitrile lipopeptide (INLP), and thus called INLP synthase (INLPS) complex (224) (Fig. 13A) (Table B5). The transcript levels of the first gene in the cluster, *Rv0096*, coding for PPE1, was 187 times greater in biofilms compared to planktonic cultures (Table B5). By RT-qPCR, we confirmed induction of *Rv0096* in pellicles at 4 weeks growth, which was not evident during an earlier (2-week) stage (Fig. 13B). Such a high level of induction in biofilms makes *inlps* a strong candidate for a biomarker of MTB biofilm formation. The gene of Dendra2 fluorescent reporter fused to the *inlps* promoter (P*inlps*) region fused to the Dendra2 reporter was used for microscopic demonstration of biofilm-specific expression. Dendra2 induction was detected at the 4-week stage in pellicle (Fig. 13C). By contrast, the reporter expression was not observed at an earlier stage of biofilm development (2 weeks), in high-density, detergent-free planktonic culture, or in colonies grown on an agar surface (Fig. 13C and Fig. 15). Reporter expression was further confirmed in 4-week biofilms of the virulent strain of MTB (Erdman) (Fig. 14). Based on this microscopic analysis, INLPS induction appears to be

A

PPE1 Oxy FcoT AAL ACP NRPS

Rv0096-0101 (INLPS)

B

Rv0096 fold change (relative to plnk)

p = 0.06

2wk   4wk

C

mCherry   Dendra-2   merged

2wk pellicle

4wk pellicle

D

Rv0096 fold change (relative to plnk)

*

ΔphoT_4wk   ΔphoTcomp_4wk   ΔphoT_5wk   ΔphoTcomp_5wk

E

mc²7000   Δinlps   Δinlps_comp
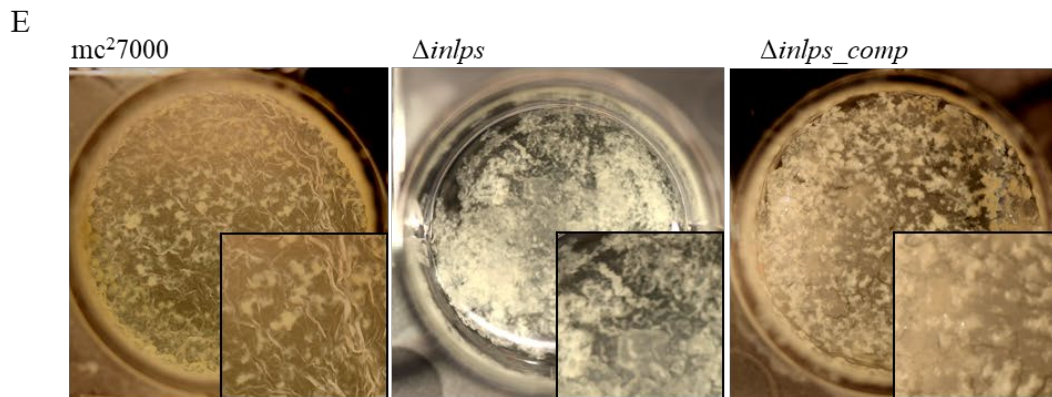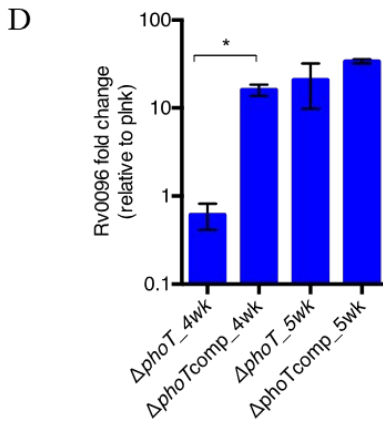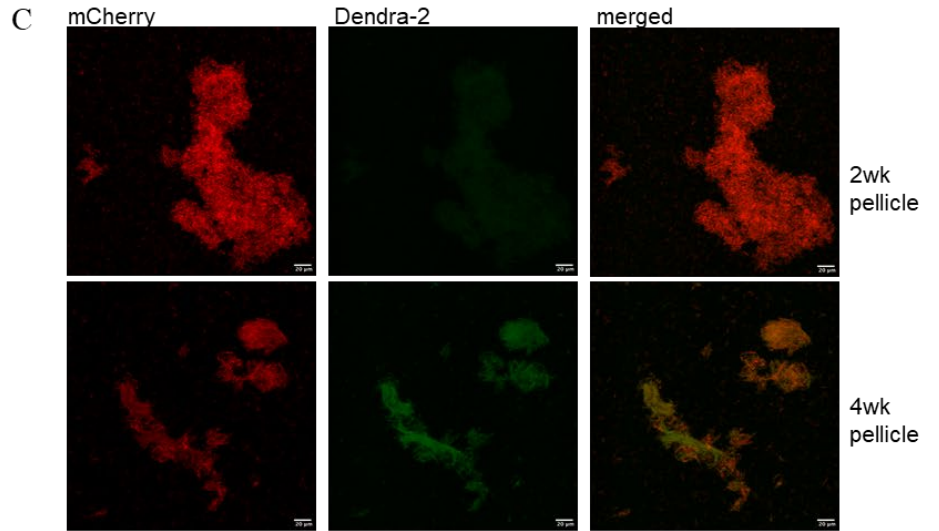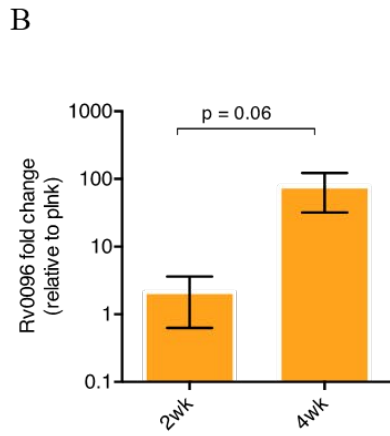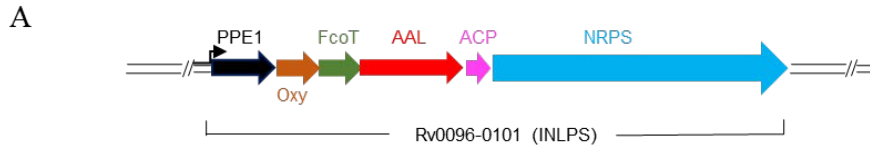
Figure 13: Induced expression of INLPS is required for biofilm development

A. Schematic representation of inlps gene cluster comprising of six ORFs organized in an operon. Except for *Rv0096*, which has the conserved Pro-Pro-Glu (PPE) motif, likely function of other genes have been assigned based on previous studies (224). Oxy: oxidase, FcoT: thioesterase, AAL: acyl ACP ligase, ACP: Acyl Carrier Protein and NRPS: Non-ribosomal peptide synthase. The arrow indicates the promoter region. B. RT-qPCR based expression analysis of *Rv0096* in mc²7000 biofilms at 2-week and 4-week stages, relative to planktonic (plnk) culture. C. Microscopic analysis of Dendra-2 expression from the promoter of INLPS in 2- and 4-week stages of mc²7000. Cells were constitutively expressing mCherry from the *hsp60* promoter. D. An RT-qPCR analysis of *Rv0096* expression in the Δ*phoT* mutant and a complemented (Δ*phoTcomp*) strains at 4- and 5-week stages of pellicle biofilm development. SigA transcripts were used as endogenous control for normalization. Data in panels B and C represent average of two (for 5-week biofilms in panel C) or three (in panel B and for 4-week biofilms in panel C) biologically independent experiments. * $p < 0.05$ (paired t-test). E. A top-down view of 4-week pellicle biofilms of mc²7000, its isogenic Δ*inlps* mutant, and a complemented strain carrying cosmid-borne *inlps*. While the parent wild-type and the complemented strains had visible texture development at the air-medium interface, the biomass of the mutant was predominantly at the bottom of the well.

specifically limited to later developmental stages of pellicle biofilms, but not any other forms of growth. This pellicle-specific INLPS induction further highlights the distinction between pellicle biofilms and colony growth as suggested by the Tn-seq results.

Expression of *inlps* is negatively regulated by RegX3 (223), suggesting that the reduced induction of *inlps* by constitutive activation of RegX3 may contribute to the delayed biofilm formation of Δ*phoT*. While *Rv0096* induction was not apparent in pellicles of Δ*phoT* at 4 weeks growth, the expression was fully restored upon further incubation (Fig. 13D). The Δ*pstC2-A1* mutant, which also induces RegX3, exhibited induction of *inlps* similar to WT levels (Fig. 13D). This implies that additional factors, beyond RegX3 regulate *inlps*. Such factors could potentially be responsive to signals generated during maturation of biofilms. The correlation between *inlps* induction and timing of biofilm maturation further suggested an important role of INLP during biofilm maturation stages. A severe defect in pellicle biofilm formation of isogenic Δ*inlps* mutant strain was confirmed (Fig. 13E), without any growth defect in planktonic culture (Fig. 15). The

pellicle deficient phenotype was partially restored upon complementation with a cosmid bearing *inlps* and its upstream promoter region (Fig. 13E). The Δ*inlps* mutant formed relatively smooth and shiny colonies, in contrast to dry and rugose textured WT colonies (Fig. 14), indicating that the basal level of INLP also has important functional significance.

RNA-seq based transcriptomic analysis identified a total of 27 genes significantly up-regulated and 30 genes significantly down-regulated in mature MTB biofilms. To determine significance, we used a p-value < 0.05 and fold change over five as cut offs. Differentially expressed genes in MTB pellicle biofilms are listed in Appendix B Table B5. Multiple genes of the Zur regulon were highly induced in biofilms, including genes coding for alternative ribosomal proteins, Mrf, PPE3, polyketide synthase PapA, MmpL8 and MmpL10. This is consistent with the zinc-depleted activation of alternative ribosomes during biofilm maturation in *M. smegmatis* (72). The *kdp* potassium transporter system and *mce1* operon both uniformly had increased levels of transcripts, although not all genes were above the statistical threshold.
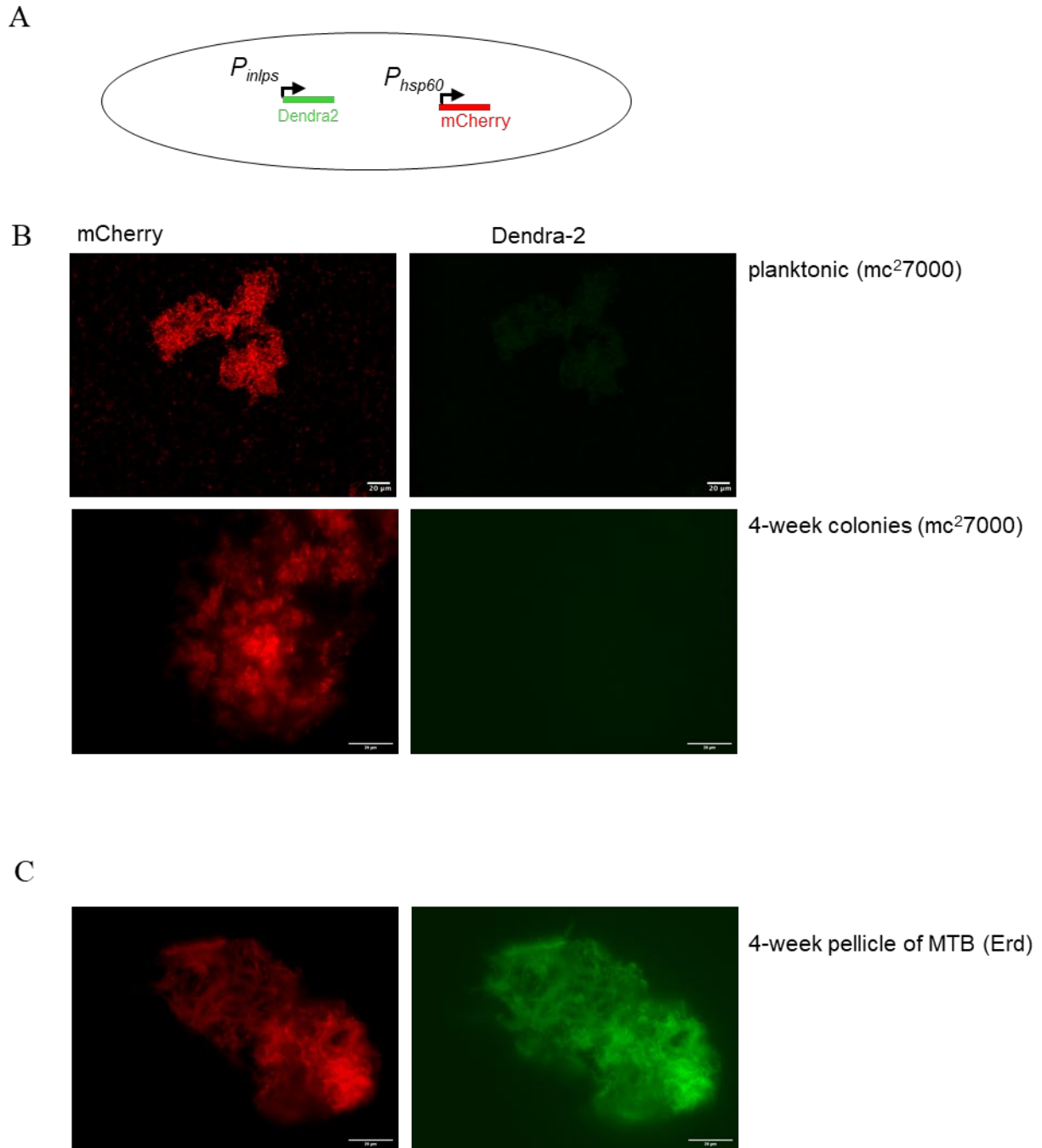
Figure 14: INLP expression in MTB pellciles

A. A schematic of the reporter construction for strains used in panels B, C, and in Figure 13C. B. Lack of *inlps* expression in detergent-free planktonic mc^{2}7000 cells after 2-weeks of incubation, and in 4-week colonies. C. Expression of *inlps* in 4-week pellicles of MTB (Erdman). Clump of cells of the indicated strains from either colonies or pellicles were collected, fixed, smeared on slides and visualized under wide field fluorescence microscopy. Scale bar represents 20 μm.

A

B
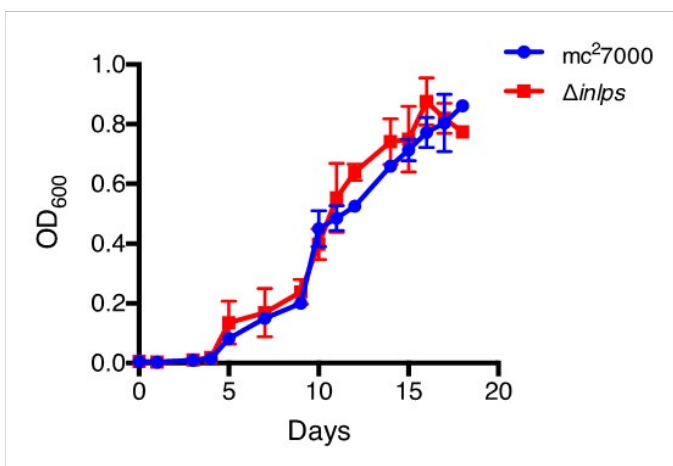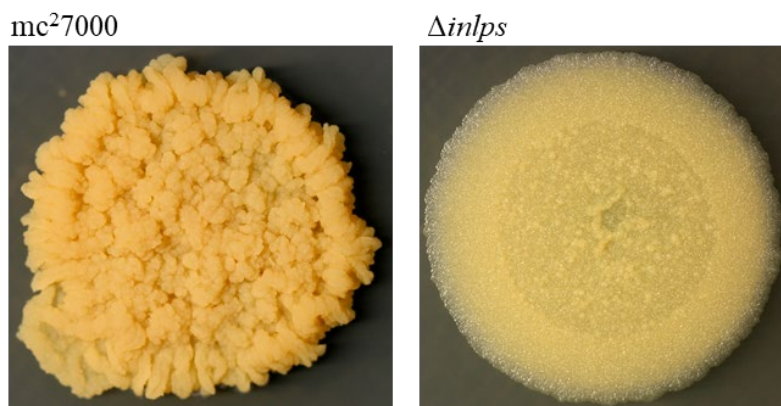
| mc²7000 | Δinlps |

Figure 15: Growth of mc^{2}7000 and its isogenic Δ*inlps* in planktonic culture and colonies

A. Planktonic growth of mc^{2}7000 and Δ*inlps* cultured in detergent-free Sauton's medium. Cultures were shaken once daily, and their optical density were measured after dispersion of 1 mL aliquots in detergent at 600 nm. Data represent mean ± SD (n= 3). B. Colonies of mc^{2}7000 and Δ*inlps* inoculated on Sauton's agar plates following 6 weeks of growth.

4.7 Chemical Evidence of INLP Accumulation of Biofilms

Next, we attempted to determine if *inlps* expression correlates with accumulation of new metabolites in MTB biofilms. Originally, identification of INLP was elucidated upon

overexpression of *Rv0097-0101* and its homologues in *E. coli* (224), but MTB-native structure of INLP is unknown. Therefore, we used an unbiased approach and compared lipid profiles of crude organic extract from planktonic and biofilm cultures of WT MTB. $\Delta inlps$ null-biofilm cultures were included for comparison. Analysis of comparative profiling by Liquid Chromatography-High Resolution Mass Spectrometry (LC-HRMS) detected an increased abundance of more than two hundred small molecules in WT biofilm extracts relative to other extracts (data not shown), complicating the identification of metabolic products of the *inlps* gene cluster. Four compounds with identical masses (m/z: 717.5612, proposed molecular formulas $C_{40}H_{73}N_6O_5^+$), which are likely synthesized by the *inlps* cluster were identified, though. (Fig. 16; 1-4, and Fig. 17). The following three criteria were used to identify these compounds as products of *inlps*. First, these four compounds were detected exclusively in WT biofilm extracts, and were not detected in either planktonic WT or in $\Delta inlps$ cultures (Fig. 16A). Identical fragmentation patterns by LC-MS/MS analysis of these metabolites were observed (Fig. 17) indicating that these compounds are isomers. Second, click reactions with tetrazine confirmed the presence of unique isonitrile functionality in the compounds (225) (Fig. 16B-C). Tetrazine treatment of partially purified 1 and 2 caused disappearance of their mass signals with concomitant appearance of the predicted reaction product. Third, weak but noticeable incorporation of ^{13}C- glycine was observed in these four metabolites (Fig. 18). Glycine is a direct precursor utilized by INLPS (224, 225). Therefore its incorporation in 1-4 is in agreement with the characterized biosynthetic mechanism for INLP synthesis. We note that the structure of these molecules remains to be determined, largely due to the difficulty in purification of these molecules in sufficient quantity necessary for NMR analysis. Nonetheless, our data provide substantial evidence that compounds 1-4 are isonitrile lipopeptides, and their accumulation in biofilms is a direct consequence of induced expression of *inlps*.
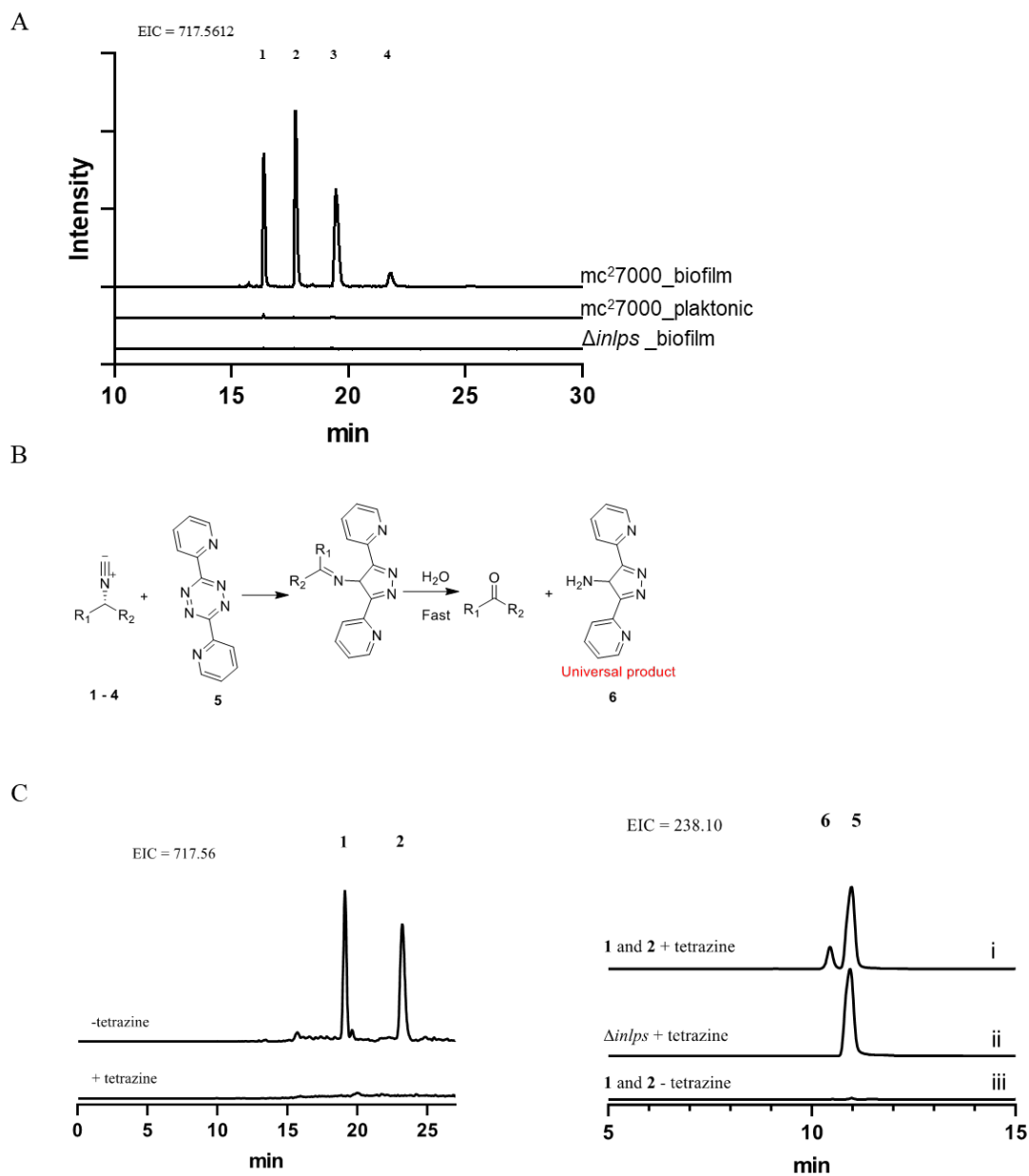
Figure 16: Accumulation of INLP in biofilms of MTB

A. Extracted ion chromatograms (EICs) show presence of four isomers of INLP (1-4; m/z = 717.5612) exclusively in the wild-type biofilm extract, but neither in planktonic wild-type nor in $\Delta inlps$ cultures. A 10-ppm mass error tolerance was used for each trace. B. Scheme of click reaction of INLP with tetrazine showing [4+1] cycloaddition between 1-4 and tetrazine. The product rapidly hydrolyzes in a trace amount of water to generate a primary amine 6. C. Extracted ion chromatograms show disappearance of partially purified 1 and 2 after reaction with 5 and concomitant appearance of the predicted reaction product 6. Control reactions without 5, and 5-treated $\Delta inlps$ mutant extract are also shown.
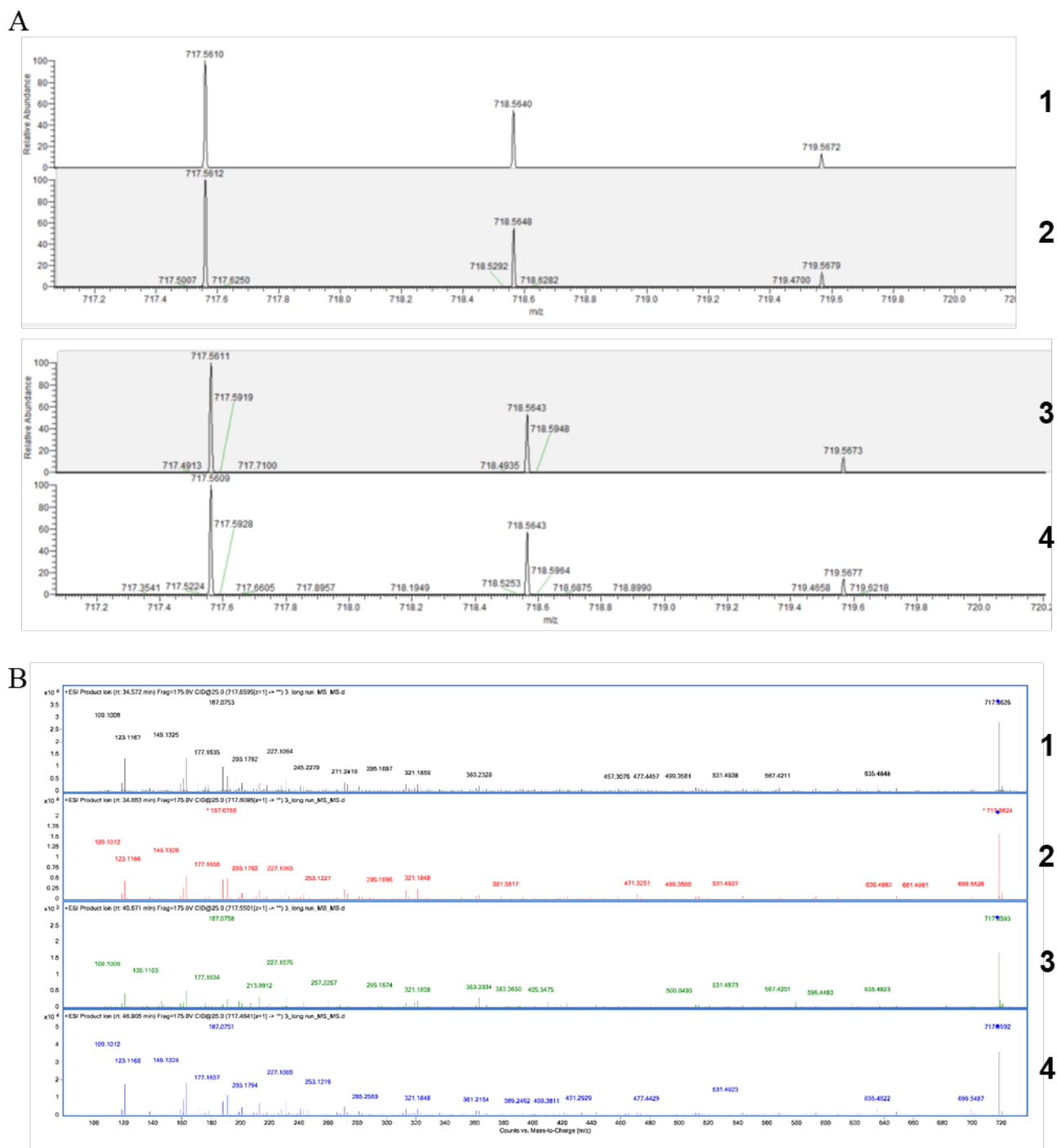
Figure 17: High-resolution mass spectrometric (HRMS) analysis of INLP isomers

A. HRMS analysis of metabolites 1-4 shown in figure 16 (proposed molecular formulas $C_{40}H_{73}N_6O_5^+$, Δ = -3.4 ppm). B. MS/MS fragmentation spectra of 1-4 showing nearly identical patterns. The presence of lipid chains are also suggested from these MS/MS spectra.
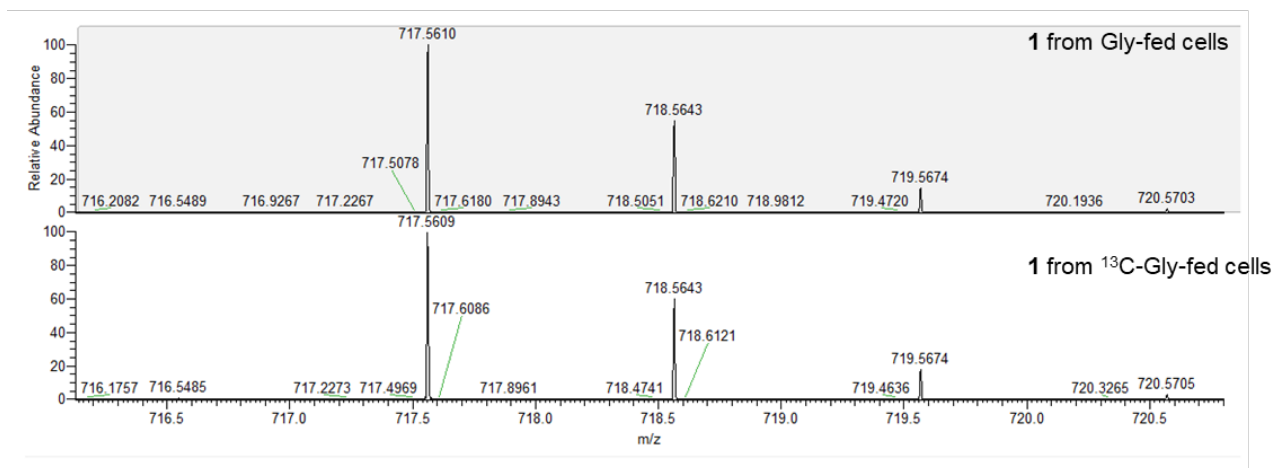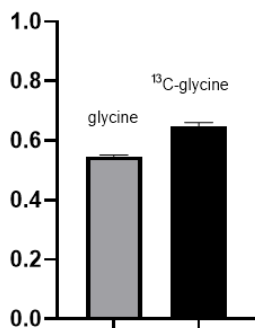
Figure 18: HRMS analysis of INLP isomer 1 upon Gly feeding

A. Feeding of 2-^{13}C-Gly to the culture of MTB demonstrated that C(2) of Gly was weakly but consistently (~10%) incorporated into 1 during biofilm formation. B. Isotopic incorporation was calculated using the ratios of integrated area under curve (AUC) of [M+2] over [M+1]. The ratios were 55% and 65% for Gly and 2-^{13}C-Gly feeding samples, respectively. Similar incorporation was observed for INLP isomers 2-4.

4.8 Signal Inducing INLPS Originates in Biofilm Architecture

We next sought to determine the likely origin of signal that regulates induction of *inlps* gene cluster in biofilms. RegX3-SenX3 transcript levels were unchanged in mature pellicles compared to WT (Table B5), disqualifying our previous hypothesis that changes in phosphorous homeostasis in biofilm microenvironments signaled *inlps* induction. Furthermore, reported induction of *inlps* in a *regX3* mutant (223) is roughly an order of magnitude less than that observed in mature pellicles (Table B5). Therefore, we hypothesized that regulation of *inlps* induction is dependent on specific environmental cues within mature pellicle biofilms that cannot be replicated in other growth conditions such as agar-attached colonies or high-density, detergent-free planktonic cultures. Our approach to test this hypothesis utilized a hyper-aggregative suppressor mutant strain of *M. smegmatis* whose gene regulation is responsive to biofilm microenvironments cell-surface properties (107). The strain is a double mutant of negative regulator *lsr2* and GPL biosynthesis gene *mps*. Deletion of *lsr2* in *M. smegmatis* results in pleiotropic changes that include deficiencies in biofilm formation and cell-to-cell adhesion with smooth colony morphology. Suppressor mutation of *mps* in the Δ*lsr2* background fails to restore expression of genes under negative regulation by *lsr2*, but rescues biofilm formation. This indicates that independent gene responses in the suppressor mutation are likely responding to environmental changes during biofilm development rather than being directly repressed by *lsr2* (107). We reasoned that if *M. smegmatis* encodes regulators that recognize the *inlps* promoter, then *inlps* expression should be induced in *M. smegmatis* biofilms. By implication, the levels of the reporter would remain diminished in biofilm-deficient Δ*lsr2*, and be restored in biofilms of the Δ*lsr2*/Δ*mps* double mutant. The expression of pJR36 (P$_{inlps}$-Dendra2) was similar to what was observed in MTB. In pellicles, Dendra2 expression was observed at 4-days or later in pellicles, but
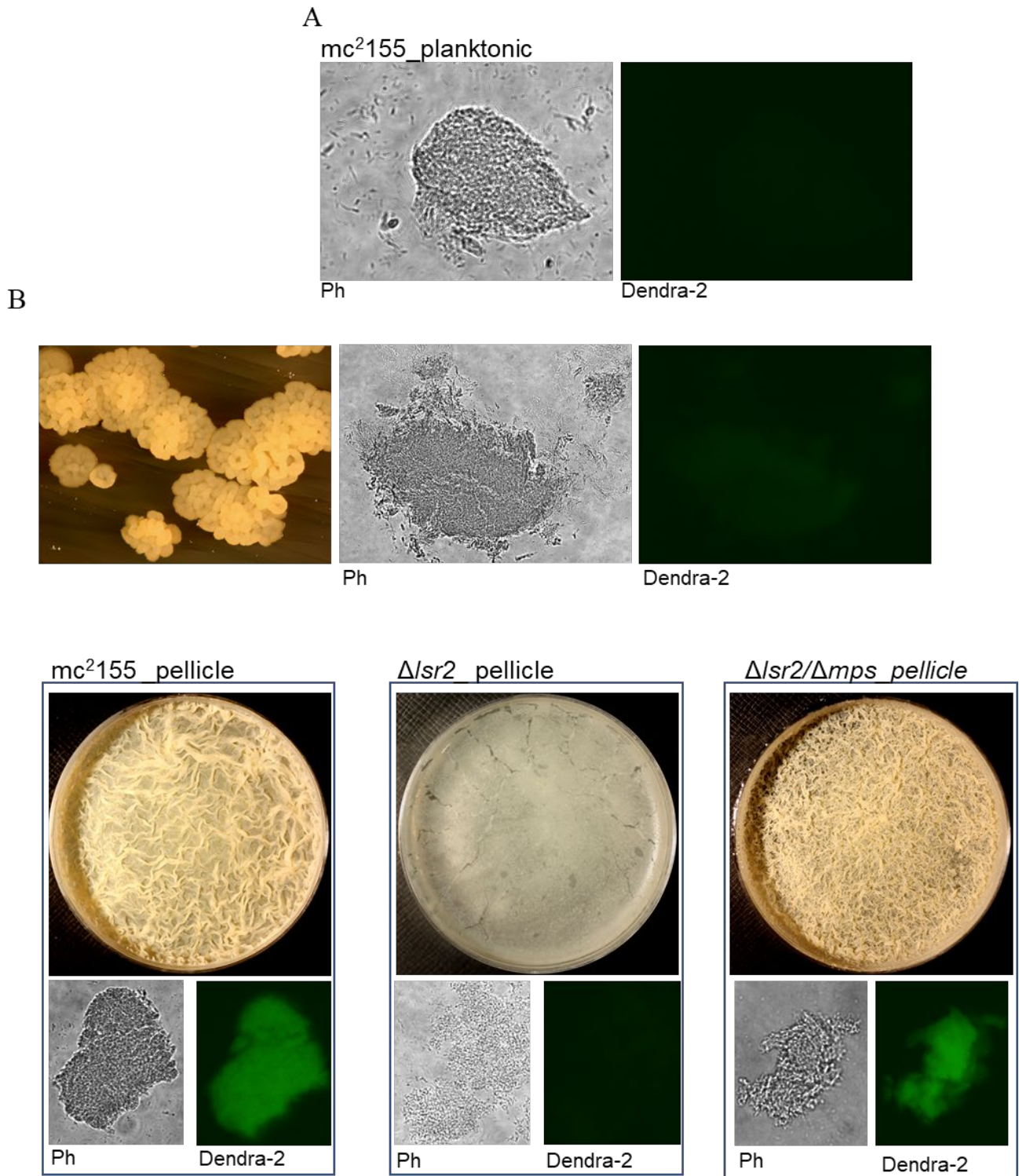
Figure 19: Biofilm-specific signals induce INLP induction in a heterologous spcies *M. smegmatis*

A-C. Microscopic analysis of Dendra-2 expression from the promoter of INLPS on an extrachromosomal plasmid

transformed in *M. smegmatis* (mc²155) and cultured either planktonically shaken in detergent-free Sauton's medium

(A), or as colonies on Sauton's medium agar plate (B), or as pellicle biofilms in static Sauton's medium (C). Reporter strains of a biofilm-defective mutant Δ*lsr2* and its extragenic suppressor Δ*lsr2* /Δ*mps* were also examined for the Dendra-2 expression. Loopful of cells from each culture were smeared on a slide and imaged under fluorescent-light microscope at 20X magnification with phase contrast (Ph) and green-filter (Dendra-2). Morphologies of pellicles and colonies from which cells were collected are also shown. Note that cells in detergent-free shaken culture contain predominantly microscopic clumps (panel A).

not in planktonic cultures or colonies (Fig. 19A-C). Likewise, in Δ*lsr2* null-pellicle culture, no induction of Dendra2 expression was observed, while induction of Dendra2 signal was restored in late (day 4) pellicle development in the suppressor double mutant Δ*lsr2*/Δ*mps* (Fig. 19C). This suggests that the signal of induction of *inlps* expression in *M. smegmatis* is a response to pellicle biofilm environmental conditions and validates Pr$_{inlps}$-Dendra2 as a biomarker for biofilm development. This biomarker could be used for investigation of MTB biofilms *in vivo*.

5.0 Discussion

5.1 Significance of Tn-seq Results to MTB Drug Tolerance

We sought to identify genes that confer a fitness advantage to MTB during biofilm growth, and their connection to the establishment of drug tolerance. The overlapping genetic requirements for growth and fitness of MTB in biofilms and its persistence under stressful conditions imply demanding growth conditions within biofilms. Resident cells growing in biofilms as they mature and produce ECM and complex architecture must adapt to limitation in various nutrients, oxygen availability, and mechanical stress from the structure itself. Therefore, identification of genes involved in MTB's stringent response (*relA*), cell wall integrity (*mmaA, ponA2, mmpL10, fadA2, and pks16*), and nutrient homeostasis (*sugA*, *Rv2606c*, *sdaA*, *pstS3C2A1*, and *phoT*) are unsurprisingly important to MTB biofilm adaptation compared to a planktonic suspension free of such environmental constraints. The identification of several genes that have previously been described as important for antibiotic tolerance (*mmaA4* (186), *ponA2* and *Rv2224c* (213), *pstA1* (214)) indicates biofilms are also enriched for antibiotic tolerant cells relative to planktonic. Extended survival of cells within biofilms could hypothetically be the result of an increased probability in specialized persisters that emerge from intrinsic defense mechanisms against antibiotics. Previous work has identified RIF-hypersensitive mutants of MTB that also show reduced persister frequency in planktonic experiments. This includes deletion mutants of *pst* genes *pstA1* and *phoY2*, both of which reduce tolerance to RIF in a RegX3-dependent manner (214). In the case of *pstA1*, we demonstrate that this also applies to RIF-exposed biofilms. Persister formation in MTB is most likely the result of several mechanisms that include stochastic changes

in gene expression that lead to growth arrest and metabolic downshifts, but also responses to environmental stresses such as nutrient limitation, host immune factors, antibiotic exposure, and hypoxia. Strict control of genetic responses to these environmental cues is crucial to MTB's survival.

In vitro pellicle biofilms provide a unique model for investigating the effect of isogenic deletions in a heterogeneic population responding to multiple microenvironments. The lower persister frequency in both biofilms of Δ*pstC2-A1* and Δ*phoT* mutant strains that are morphologically indistinguishable from WT provides us with an experimental framework to systematically evaluate other genes identified by Tn-seq for their role in persister formation. However, additional future work that involves testing of isogenic deletion mutant of these genes in monoculture biofilms will be important. It is noteworthy that *Rv1272*-73c, the putative drug efflux pump identified as being important to RIF-tolerance in biofilms by Tn-seq, may serve as an interesting candidate for future study on persisters (Table B3). Considering that the two mutant strains tested here for persister frequencies do form pellicle biofilms (albeit one at a delayed rate), we conclude that the external protection provided by three-dimensional architecture and ECM is only partially responsible for biofilms phenotypic tolerance to antibiotics, and that intrinsic ability to tolerate drug exposure also plays a crucial role. Currently, we have not yet investigated whether isogenic mutant strains of additional Tn-seq identified genes that form pellicle similar to WT, would harbor a comparable population of drug-tolerant persisters as well.

5.2 Pellicle Growth Requirements Are More Stringent Than Colony

There are multiple *in vitro* methods of culturing biofilms (pellicle, colony, surface attached, flow cell) with potentially different genetic requirements. We attempted to be as comprehensive as possible in our investigation of genes that confer fitness in MTB biofilms. To accomplish this, we investigated two distinct forms of aggregative growth: pellicle and colony biofilms. In *M. smegmatis*, changes in genetic expression during colony and pellicle development are markedly similar (107, 190). The results of the Tn-seq screen performed here identified more genes conferring a fitness advantage in pellicle growth than colony growth (Fig 4B). This suggests that the nutritional requirements and/or environmental stresses of pellicle formation are more stringent than colony formation. Furthermore, induction of INLPS, which we identified here as a biomarker of biofilms, in pellicles but not colonies, demonstrates the distinct genetic requirements of each biofilm model. When grown in a microfluidic flow cell, MTB began to form aggregative cord-like structures by day 6 (Fig. 9). The Cellasic ONIX2 microfluidic system used here and a green fluorescent Calcein AM stain for living cells after antibiotic exposure (190), provides an additional method of assaying biofilm-associated persisters in multiple MTB strains that is conducive to live imaging.

5.3 Possible Function and Regulation of INLP

Investigation of the unique microenvironments associated with mature MTB pellicles led us to identifying the INLPS gene cluster as a requirement for and unique biomarker of biofilm formation. Five genes of the INLPS cluster (*Rv0097-0101*) are conserved among pathogenic

mycobacterial species, yet absent from non-pathogenic strains such as of *M. smegmatis*. *Rv0096*, annotated as PPE1, is unique to the MTB complex. Disruption of *Rv0096* and *Rv0097* by transposon insertion results in decreased survival in mouse lungs and spleen, yet also decreased *in vivo* killing by INH without acquiring resistance mutations (226). In *M. bovis*, disruption of the *inlps* operon altered colony morphology, decreased phthiocerol dimycocerosate (PDIM) biosynthesis, and attenuated the strain (227). A smooth colony variant of MTB H37Rv strain repressed expression of *inlps* operon (though the operon itself was intact and not mutated), and was biofilm defective, phagocytosed less often than WT in murine macrophages, and was not observed to form cords (228).

The function of INLP metabolites remains unknown, though. INLP compounds are linked to copper transport in *Streptomyces thioluteus* (229). This suggests a potential role in metal transport in MTB biofilms. Acquisition of iron (189) and zinc homeostasis (72) are both crucial to mycobacterial growth in biofilms. Mutation of *M. marinum* INLPS genes resulted in reduced intracellular levels of zinc and nickel (224) possibly relating INLP function to the zinc requirements of mycobacterial biofilms (72). Addition of high levels of zinc sulfate to Δ*inlps* pellicle cultures did not restore biofilm formation (data not shown). If INLP is required for zinc acquisition, then it is expected that supplemental zinc in the media would not rescue a zinc-dependent biofilm phenotype. Notably, INLPS genes were not identified in the Tn-seq screen despite its obvious role in biofilm development. A likely explanation is that *inlps* mutants are trans-complemented by WT clones in in mixed biofilms of Tn-library. However, a trans-complementation is inconsistent with deficiency in zinc import, an intrinsic property of the mutant, as the cause for biofilm deficiency. This suggests additional function(s) of INLP in biofilm growth.

Though INLP function remains unknown in biofilms, the unique environment of MTB biofilms is conclusively supported by its specific induction.

Regulation of *inlps* and the conditions and signals driving *inlps* induction in biofilms remains an open question. Based on literature and our transcriptomic data, SigC appears to be a strong candidate. SigC directly binds upstream of *Rv0096* based on ChIP-seq data (230), and SigC overexpression induces *Rv0096* expression (231). Importantly, other genes of the SigC regulon were also induced in mature MTB pellicles. A SigC homolog however is not encoded by the *M. smegmatis* genome, yet *inlps* promoter is regulated in *M. smegmatis* in a biofilm-specific manner (Fig. 19). A possible explanation could be that *M. smegmatis* encodes a functional equivalent of SigC that regulates biofilm maturation. When SigM was overexpressed in MTB, induction of several genes in the *inlps* operon was observed (232). Further investigations into the identity of the regulators of *inlps* will offer new insight into the mechanism of regulation and the upstream signal responsible for the regulation. The rapidly growing *M. smegmatis* offers a convenient model for identifying induction signals and regulators of *inlps*, though.

Biofilms are a common bacterial lifestyle and of high clinical relevance. It is estimated that the majority of clinical bacterial infections are biofilm-associated (92), and biofilms have been associated in the pathogenesis of the NTM's *M. abscessus* and the *M. avium* complex (182, 233). *M. abscessus* is highly intrinsically resistant to most antibiotics (233), and also encodes homologs to MTB genes *Rv0097-0101* that constitute part of *inlps*. Investigation of *M. abscessus* biofilms for induction of *inlps* gene homologs, and determination of whether or not the *inlps* fluorescent reporter is expressed in *M. abscessus* biofilms will be an important future extension of this study. Understanding the genetics of mycobacterial biofilms and drug tolerance will be crucial to developing new chemotherapies for successful health outcomes.

5.4 Possibility of MTB Biofilms *in vivo*

Analysis of our Tn-seq results also demonstrates a strong link between biofilm adaptation and survival *in vivo.* Several genes required for biofilm fitness based on Tn-seq are also required for virulence in macrophages (i.e. *mmaA4*, *phoT*, *ponA2*, *Rv2224c*, *pstC2A1*) (209-211, 213, 214, 234) or chronic phase of mouse infections (survival > 8 weeks) (i.e. *RelA*) (67). This raises the question of whether or not organized, aggregative growth could be a host survival strategy of MTB. MTB biofilms would provide a suitable mechanism of establishing a community of bacilli harboring specialized cells capable of survival host responses from both the innate and adaptive immune system. As noted, INLP has been implicated in survival of MTB *in vivo* in both early and more chronic infections in mouse models (226, 235), though the kinetics of *inlps* expression throughout infection have not been investigated. Induced expression levels of *inlps* in chronic infection could potentially have different consequences on pathogenesis than basal expression, though *inlps* roles in pathogenesis have yet to be investigated. Here, we have established an *inlps*-based fluorescent reporter to be used in investigating the questions of *in vivo* MTB biofilm formation and *inlps* expression of bacilli at different time points of infection and in varying lesion types.

If *in vivo* biofilms of MTB are identified using the biomarker described here, whether or not these biofilms would be targetable with specific drugs would need to be investigated. In this study, we demonstrated that intrinsic antibiotic tolerance of biofilm constituent cells is a determinant of persister frequency. Therefore in the event of clinical MTB biofilms, drugs aimed at disruption of *in vivo* aggregates would most likely still necessitate prolonged treatment against a subpopulation of multidrug tolerant persisters. A more successful route may require discovering drugs that prevent biofilm formation by MTB *in vitro* (using pellicles as a model) that could

97

potentially inhibit the self-selection process that enriches persister frequency during an *in vivo* infection if combined with conventional antibiotics at the outset of treatment.

5.5 Public Health Significance of This Work

Lengthy treatment time of TB with multiple antibiotics remains one of the largest obstacles to the disease's elimination. Therefore, reduction of treatment time is an attractive prospective route for easing the global disease burden of TB. Multidrug tolerant persister cells that make up only a small portion of the bacterial population are thought to be the main reason for TB's extended treatment time compared to other bacterial infections (46, 236). To accomplish shortening treatment time, novel therapies that specifically addresses the formation of persisters are needed. In this study, we have identified significant overlap between the genetic requirements for biofilm fitness and drug tolerance in MTB. We have also demonstrated that decreased intrinsic tolerance to antibiotics will result in a reduction of persister frequency in MTB biofilms. Whether MTB forms biofilms during host infection still remains unknown, but the *inlps* promoter-based fluorescent reporter system described here provides a new tool for investigating this question in animal infection models. Additionally, pellicle biofilms provide a useful *in vitro* model for drug discovery specifically aimed at targeting the formation of persisters in MTB. This study lays the groundwork for specific targeting of MTB persisters, which in turn could lead to reduced antibiotic treatment time.

Appendix A : Abbreviations Used Within This Work

ADC – albumin dextrose and catalase
AES – allelic exchange substrate
AM – alveolar macrophages
ATP – adenosine triphosphate
Bap – biofilm adhesion proteins
bp – base pairs
BSL-2 – biosafety level 2
BWA – Burrows-Wheeler Aligner
C – Celsius
Cat. No. – catalog number
c-di-GMP – cyclic diguanosine-5'-monophosphate
CD4 – cluster of differentiation 4
CD8 – cluster of differentiation 8
cDNA – complementary deoxyribonucleic acid
cfu – colony forming units
CLSM – confocal laser scanning microscopy
cm – centimeter
DNA – deoxyribonucleic acid
DMSO – dimethyl sulfoxide [(CH3)2SO]
ECM – extracellular matrix
eDNA – extracellular deoxyribonucleic acid
EIC – extracted ion chromatogram
EMB – ethambutol
EPS – exopolysaccharide
FAS-II – fatty acid synthetase II
FDA –Food and Drug Administration
FM – free mycolic acids
FWHM – full width at half maximum
GFP – green fluorescent protein
GPL – glycopeptidolipids
HCD – higher energy collisional dissociation
HGT – horizontal gene transfer
HIV – human immunodeficiency virus
HPLC – high performance liquid chromatography
HRMS/MS – high resolution tandem mass spectrometry
IFN-γ – interferon gamma
IL-12 – interleukin-12
INH – isoniazid
INLP – isonitrile lipopeptide
kPa – kiloPascals
LB – Luria broth

LC – liquid chromatography
LC-MS – liquid chromatography mass spectrometry
MDAG – mycolyl diacyl glycerol
MDR-TB – multidrug resistant tuberculosis
MIC – minimum inhibitory concentration
mg – milligram
mL – milliliter
mm – millimeter
mM – millimolar
MOPS – (3-(N-morpholino)propanesulfonic acid)
mRNA – messenger ribonucleic acid
MRSA – methicillin-resistant Staphylococcus aureus
ms – millisecond
MS – mass spectrometry
MS-DIAL – mass spectrometry data analysis software
MS-MS – tandem mass spectrometry
MTB – Mycobacterium tuberculosis
m/z – mass-to-charge ratio
NA – numerical aperture
ng – nanogram
NK – natural killer cells
nm – nanometer
NMR – nuclear magnetic resonance spectroscopy
NTM – non-tuberculosis mycobacterial species
OADC – albumin dextrose catalase and oleate
OD – optical density
ORF – open reading frame
PBS – phosphate buffered saline
PCR – polymerase chain reaction
PDIM – phthiocerol dimycoserosate
PGL – phenolic glycolipids
Pst –phosphate specific transport
PVC – polyvinyl chloride
PZA – pyrazinamide
QS – quorum sensing
Q-TOF – quadruple time-of-flight
RD1 – Region of differentiation one
RIF – rifampicin
RNA – ribonucleic acid
rpm – revolutions per minute
RT-qPCR – reverse transcriptase quantitative polymerase chain reaction
SEM – scanning electron microscopy
sRNA – small ribonucleic acids
TA – toxin-antitoxin
TB – tuberculosis
TCA – tricarboxylic acid

TNF-α – tumor necrosis factor alpha
Tn – transposon
Tn-seq – transposon junction sequencing
TPP – TRANSIT pre-processor
TTR – total trimmed reads
μg – microgram
μL – microliter
μm – micrometer
μM – micromolar
USD – United States dollars
UV – ultraviolet light
V – volts
v/v – percent as volume in mL in 100mL solution
WHO – World Health Organization
WT – wild-type

Appendix B : Supplemental Results for Tn-seq and RNA-seq Experiments

Supplementary results available at http://d-scholarship.pitt.edu/

Bibliography

1. **Daniel VS, Daniel TM.** 1999. Old Testament Biblical References to Tuberculosis. Clinical Infectious Diseases **29:**1557-1558.

2. **Brothwell D, Sandison AT.** 1967. Diseases in antiquity. A survey of the diseases, injuries and surgery of early populations. Diseases in antiquity A survey of the diseases, injuries and surgery of early populations.

3. **Brown L.** 1941. The story of clinical pulmonary tuberculosis. The Radiological Society of North America.

4. **Cave AJE, Demonstrator A.** 1939. The evidence for the incidence of tuberculosis in ancient Egypt. British Journal of Tuberculosis **33:**142-152.

5. **Thomas M.** 1997. Captain of death: The story of tuberculosis. University of Rochester Press.

6. **Dubos RJ, Dubos J.** 1987. The white plague: tuberculosis, man, and society. Rutgers University Press.

7. **Keshavjee S, Farmer PE.** 2012. Tuberculosis, drug resistance, and the history of modern medicine. New England Journal of Medicine **367:**931-936.

8. **Daniel TM.** 2006. The history of tuberculosis. Respiratory Medicine **100:**1862-1870.

9. **Chalke HD.** 2012. The impact of tuberculosis on history, literature and art. Medical History **6:**301-318.

10. **Bates JH, Stead WW.** 1993. The history of tuberculosis as a global epidemic. The Medical Clinics of North America **77:**1205-1217.

11. **Organization WH.** 2018. Global tuberculosis report 2017. 2017. Google Scholar.

12. **Fox W, Ellard GA, Mitchison DA.** 1999. Studies on the treatment of tuberculosis undertaken by the British Medical Research Council tuberculosis units, 1946–1986, with relevant subsequent publications. The international journal of tuberculosis and lung disease **3:**S231-S279.

13. **Gomez JE, McKinney JD.** 2004. *M. tuberculosis* persistence, latency, and drug tolerance. Tuberculosis **84:**29-44.

14. **Lewis K.** 2010. Persister Cells. Annual Review of Microbiology **64:**357-372.

15. **Barry CE, Boshoff HI, Dartois V, Dick T, Ehrt S, Flynn J, Schnappinger D, Wilkinson RJ, Young D.** 2009. The spectrum of latent tuberculosis: rethinking the biology and intervention strategies. Nature Reviews Microbiology **7:**845.

16. **Fennelly KP, Martyny JW, Fulton KE, Orme IM, Cave DM, Heifets LB.** 2004. Cough-generated aerosols of *Mycobacterium tuberculosis*: a new method to study infectiousness. American journal of respiratory and critical care medicine **169:**604-609.

17. **Lurie MB.** 1939. Studies on the mechanism of immunity in tuberculosis : the role of extracellular factors and local immunity in the fixation and inhibition of growth of tubercle bacilli. J Exp Med **69:**555-578.

18. **Orme IM.** 1987. The kinetics of emergence and loss of mediator T lymphocytes acquired in response to infection with *Mycobacterium tuberculosis*. J Immunol **138:**293-298.

19. **Pena JC, Ho WZ.** 2015. Monkey models of tuberculosis: lessons learned. Infect Immun **83:**852-862.

20. **McMurray DN, Collins FM, Dannenberg AM, Jr., Smith DW.** 1996. Pathogenesis of experimental tuberculosis in animal models. Curr Top Microbiol Immunol **215:**157-179.

21. **Keane J, Remold HG, Kornfeld H.** 2000. Virulent *Mycobacterium tuberculosis* Strains Evade Apoptosis of Infected Alveolar Macrophages. The Journal of Immunology **164:**2016.

22. **Rohde K, Yates RM, Purdy GE, Russell DG.** 2007. *Mycobacterium tuberculosis* and the environment within the phagosome. Immunological Reviews **219:**37-54.

23. **Kang PB, Azad AK, Torrelles JB, Kaufman TM, Beharka A, Tibesar E, DesJardin LE, Schlesinger LS.** 2005. The human macrophage mannose receptor directs *Mycobacterium tuberculosis* lipoarabinomannan-mediated phagosome biogenesis. The Journal of Experimental Medicine **202:**987.

24. **Welin A, Lerm M.** 2012. Inside or outside the phagosome? The controversy of the intracellular localization of *Mycobacterium tuberculosis*. Tuberculosis **92:**113-120.

25. **Ramakrishnan L.** 2012. Revisiting the role of the granuloma in tuberculosis. Nature Reviews Immunology **12:**352.

26. **Via LE, Lin PL, Ray SM, Carrillo J, Allen SS, Eum SY, Taylor K, Klein E, Manjunatha U, Gonzales J.** 2008. Tuberculous granulomas are hypoxic in guinea pigs, rabbits, and nonhuman primates. Infection and immunity **76:**2333-2340.

27. **Lenaerts AJ, Hoff D, Aly S, Ehlers S, Andries K, Cantarero L, Orme IM, Basaraba RJ.** 2007. Location of persisting mycobacteria in a Guinea pig model of tuberculosis revealed by r207910. Antimicrob Agents Chemother **51:**3338-3345.

28. **Peyron P, Vaubourgeix J, Poquet Y, Levillain F, Botanch C, Bardou F, Daffe M, Emile JF, Marchou B, Cardona PJ, de Chastellier C, Altare F.** 2008. Foamy macrophages from tuberculous patients' granulomas constitute a nutrient-rich reservoir for *M. tuberculosis* persistence. PLoS Pathog **4:**e1000204.

29. **Russell DG, Cardona P-J, Kim M-J, Allain S, Altare F.** 2009. Foamy macrophages and the progression of the human tuberculosis granuloma. Nature Immunology **10:**943.

30. **Wallis RS, Patil S, Cheon SH, Edmonds K, Phillips M, Perkins MD, Joloba M, Namale A, Johnson JL, Teixeira L, Dietze R, Siddiqi S, Mugerwa RD, Eisenach K, Ellner JJ.** 1999. Drug tolerance in *Mycobacterium tuberculosis*. Antimicrobial agents and chemotherapy **43:**2600-2606.

31. **Dooley KE, Lahlou O, Knudsen J, Elmessaoudi MD, Cherkaoui I, El Aouad R.** 2011. Risk factors for tuberculosis treatment failure, default, or relapse and outcomes of retreatment in Morocco. BMC public health **11:**140.

32. **Becerra M, Freeman J, Bayona J, Shin S, Kim J, Furin J, Werner B, Sloutsky A, Timperi R, Wilson M.** 2000. Using treatment failure under effective directly observed short-course chemotherapy programs to identify patients with multidrug-resistant tuberculosis. The International Journal of Tuberculosis and Lung Disease **4:**108-114.

33. **Jain A, Dixit P.** 2008. Multidrug-resistant to extensively drug resistant tuberculosis: what is next? J Biosci **33:**605-616.

34. **Marks SM, Flood J, Seaworth B, Hirsch-Moverman Y, Armstrong L, Mase S, Salcedo K, Oh P, Graviss EA, Colson PW.** 2014. Treatment practices, outcomes, and costs of multidrug-resistant and extensively drug-resistant tuberculosis, United States, 2005–2007. Emerging infectious diseases **20:**812.

35. **Diacon AH, Pym A, Grobusch M, Patientia R, Rustomjee R, Page-Shipp L, Pistorius C, Krause R, Bogoshi M, Churchyard G.** 2009. The diarylquinoline TMC207 for multidrug-resistant tuberculosis. New England Journal of Medicine **360:**2397-2405.

36. **Laughon BE, Nacy CA.** 2017. Tuberculosis — drugs in the 2016 development pipeline. Nature Reviews Disease Primers **3:**17015.

37. **Jindani A, Aber VR, Edwards EA, Mitchison DA.** 1980. The early bactericidal activity of drugs in patients with pulmonary tuberculosis. Am Rev Respir Dis **121:**939-949.

38. **Sarathy JP, Via LE, Weiner D, Blanc L, Boshoff H, Eugenin EA, Barry CE, Dartois VA.** 2018. Extreme Drug Tolerance of *Mycobacterium tuberculosis* in Caseum. Antimicrobial Agents and Chemotherapy **62:**e02266-02217.

39. **Lewis K.** 2006. Persister cells, dormancy and infectious disease. Nature Reviews Microbiology **5:**48.

40. **Mitchison DA.** 2004. The search for new sterilizing anti-tuberculosis drugs. Front Biosci **9:**1059-1072.

41. **Bigger J.** 1944. Treatment of Staphylococcal Infections with Penicillin by Intermittent Sterilisation. Lancet**:**497-500.

42. **Canetti G.** 1955. The tubercle bacillus in the pulmonary lesion of man: histobacteriology and its bearing on the therapy of pulmonary tuberculosis. Springer Publishing Company.

43. **McCune RM, Tompsett R.** 1956. Fate of *Mycobacterium tuberculosis* in mouse tissues as determined by the microbial enumeration technique: I. The persistence of drug-susceptible tubercle bacilli in the tissues despite prolonged antimicrobial therapy. Journal of Experimental Medicine **104:**737-762.

44. **Vandiviere H, Loring WE, Melvin IG, Willis H.** 1956. The treated pulmonary lesion and its tubercle bacillus. II. The death and resurrection. American Journal of Medical Sciences **232:**30-37.

45. **Ahmad Z, Klinkenberg LG, Pinn ML, Fraig MM, Peloquin CA, Bishai WR, Nuermberger EL, Grosset JH, Karakousis PC.** 2009. Biphasic kill curve of isoniazid reveals the presence of drug-tolerant, not drug-resistant, *Mycobacterium tuberculosis* in the guinea pig. The Journal of infectious diseases **200:**1136-1143.

46. **Keren I, Minami S, Rubin E, Lewis K.** 2011. Characterization and Transcriptome Analysis of *Mycobacterium tuberculosis* Persisters. mBio **2**.

47. **Shah D, Zhang Z, Khodursky AB, Kaldalu N, Kurg K, Lewis K.** 2006. Persisters: a distinct physiological state of *E. coli*. BMC microbiology **6:**53.

48. **Keren I, Shah D, Spoering A, Kaldalu N, Lewis K.** 2004. Specialized persister cells and the mechanism of multidrug tolerance in *Escherichia coli*. Journal of bacteriology **186:**8172-8180.

49. **Schumacher MA, Piro KM, Xu W, Hansen S, Lewis K, Brennan RG.** 2009. Molecular mechanisms of HipA-mediated multidrug tolerance and its neutralization by HipB. Science **323:**396-401.

50. **Dörr T, Vulić M, Lewis K.** 2010. Ciprofloxacin causes persister formation by inducing the TisB toxin in *Escherichia coli*. PLoS biology **8:**e1000317.

51.   **Teleti A, Imboden P, Marchesi F, Lowrie D, Cole S, Colston MJ, Matter L, Schopfer K, Bodmer T.** 1993. Detection of rifampicin-resistance mutations in *Mycobacterium tuberculosis*. Lancet **341:**647-650.

52.   **Boritsch EC, Khanna V, Pawlik A, Honoré N, Navas VH, Ma L, Bouchier C, Seemann T, Supply P, Stinear TP, Brosch R.** 2016. Key experimental evidence of chromosomal DNA transfer among selected tuberculosis-causing mycobacteria. Proceedings of the National Academy of Sciences **113:**9876.

53.   **Nguyen KT, Piastro K, Gray TA, Derbyshire KM.** 2010. Mycobacterial Biofilms Facilitate Horizontal DNA Transfer between Strains of *Mycobacterium smegmatis*. Journal of Bacteriology **192:**5134.

54.   **Barry CE, 3rd, Boshoff HI, Dartois V, Dick T, Ehrt S, Flynn J, Schnappinger D, Wilkinson RJ, Young D.** 2009. The spectrum of latent tuberculosis: rethinking the biology and intervention strategies. Nat Rev Microbiol **7:**845-855.

55.   **Connolly LE, Edelstein PH, Ramakrishnan L.** 2007. Why Is Long-Term Therapy Required to Cure Tuberculosis? PLOS Medicine **4:**e120.

56.   **Banerjee A, Dubnau E, Quemard A, Balasubramanian V, Um KS, Wilson T, Collins D, de Lisle G, Jacobs WR.** 1994. *inhA*, a gene encoding a target for isoniazid and ethionamide in *Mycobacterium tuberculosis*. Science **263:**227-230.

57.   **Moyed HS, Bertrand KP.** 1983. *hipA*, a newly recognized gene of *Escherichia coli* K-12 that affects frequency of persistence after inhibition of murein synthesis. Journal of bacteriology **155:**768-775.

58.   **Wayne LG, Hayes LG.** 1996. An *in vitro* model for sequential study of shiftdown of *Mycobacterium tuberculosis* through two stages of nonreplicating persistence. Infection and immunity **64:**2062-2069.

59.   **de Steenwinkel JE, Marian T, de Knegt GJ, Kremer K, Aarnoutse RE, Boeree MJ, Verbrugh HA, van Soolingen D, Bakker-Woudenberg IA.** 2012. Drug susceptibility of *Mycobacterium tuberculosis* Beijing genotype and association with MDR TB. Emerging infectious diseases **18:**660.

60.   **Deb C, Lee C-M, Dubey VS, Daniel J, Abomoelak B, Sirakova TD, Pawar S, Rogers L, Kolattukudy PE.** 2009. A novel *in vitro* multiple-stress dormancy model for *Mycobacterium tuberculosis* generates a lipid-loaded, drug-tolerant, dormant pathogen. Plos one **4:**e6077.

61.   **Potrykus K, Cashel M.** 2008. (p)ppGpp: still magical? Annu Rev Microbiol **62:**35-51.

62. **Traxler MF, Summers SM, Nguyen H-T, Zacharia VM, Hightower GA, Smith JT, Conway T.** 2008. The global, ppGpp-mediated stringent response to amino acid starvation in *Escherichia coli*. Molecular microbiology **68:**1128-1148.

63. **Barker MM, Gaal T, Gourse RL.** 2001. Mechanism of regulation of transcription initiation by ppGpp. II. Models for positive control based on properties of RNAP mutants and competition for RNAP. J Mol Biol **305:**689-702.

64. **Zhou YN, Jin DJ.** 1998. The *rpoB* mutants destabilizing initiation complexes at stringently controlled promoters behave like "stringent" RNA polymerases in *Escherichia coli*. Proc Natl Acad Sci U S A **95:**2908-2913.

65. **Korch SB, Henderson TA, Hill TM.** 2003. Characterization of the *hipA7* allele of *Escherichia coli* and evidence that high persistence is governed by (p)ppGpp synthesis. Mol Microbiol **50:**1199-1213.

66. **Amato SM, Orman MA, Brynildsen MP.** 2013. Metabolic control of persister formation in *Escherichia coli*. Mol Cell **50:**475-487.

67. **Dahl JL, Kraus CN, Boshoff HIM, Doan B, Foley K, Avarbock D, Kaplan G, Mizrahi V, Rubin H, Barry CE.** 2003. The role of Rel$_{Mtb}$-mediated adaptation to stationary phase in long-term persistence of *Mycobacterium tuberculosis* in mice. Proceedings of the National Academy of Sciences **100:**10026.

68. **Klinkenberg LG, Lee J-H, Bishai WR, Karakousis PC.** 2010. The Stringent Response Is Required for Full Virulence of *Mycobacterium tuberculosis* in Guinea Pigs. The Journal of Infectious Diseases **202:**1397-1404.

69. **Weiss LA, Stallings CL.** 2013. Essential roles for *Mycobacterium tuberculosis* Rel beyond the production of (p)ppGpp. J Bacteriol **195:**5629-5638.

70. **Dutta NK, Klinkenberg LG, Vazquez M-J, Segura-Carro D, Colmenarejo G, Ramon F, Rodriguez-Miquel B, Mata-Cantero L, Porras-De Francisco E, Chuang Y-M, Rubin H, Lee JJ, Eoh H, Bader JS, Perez-Herran E, Mendoza-Losana A, Karakousis PC.** 2019. Inhibiting the stringent response blocks *Mycobacterium tuberculosis* entry into quiescence and reduces persistence. Science Advances **5:**eaav2104.

71. **McKay SL, Portnoy DA.** 2015. Ribosome hibernation facilitates tolerance of stationary-phase bacteria to aminoglycosides. Antimicrob Agents Chemother **59:**6992-6999.

72. **Li Y, Sharma MR, Koripella RK, Yang Y, Kaushal PS, Lin Q, Wade JT, Gray TA, Derbyshire KM, Agrawal RK, Ojha AK.** 2018. Zinc depletion induces ribosome hibernation in mycobacteria. Proc Natl Acad Sci U S A **115:**8191-8196.

73. **Li XZ, Nikaido H.** 2009. Efflux-mediated drug resistance in bacteria: an update. Drugs **69:**1555-1623.

74. **Poole K, Krebes K, McNally C, Neshat S.** 1993. Multiple antibiotic resistance in *Pseudomonas aeruginosa*: evidence for involvement of an efflux operon. J Bacteriol **175:**7363-7372.

75. **Piddock LJ.** 2006. Clinically relevant chromosomally encoded multidrug resistance efflux pumps in bacteria. Clin Microbiol Rev **19:**382-402.

76. **Noguchi N, Okada H, Narui K, Sasatsu M.** 2004. Comparison of the nucleotide sequence and expression of *norA* genes and microbial susceptibility in 21 strains of *Staphylococcus aureus*. Microb Drug Resist **10:**197-203.

77. **Coll F, Phelan J, Hill-Cawthorne GA, Nair MB, Mallard K, Ali S, Abdallah AM, Alghamdi S, Alsomali M, Ahmed AO, Portelli S, Oppong Y, Alves A, Bessa TB, Campino S, Caws M, Chatterjee A, Crampin AC, Dheda K, Furnham N, Glynn JR, Grandjean L, Minh Ha D, Hasan R, Hasan Z, Hibberd ML, Joloba M, Jones-Lopez EC, Matsumoto T, Miranda A, Moore DJ, Mocillo N, Panaiotov S, Parkhill J, Penha C, Perdigao J, Portugal I, Rchiad Z, Robledo J, Sheen P, Shesha NT, Sirgel FA, Sola C, Oliveira Sousa E, Streicher EM, Helden PV, Viveiros M, Warren RM, McNerney R, Pain A, et al.** 2018. Genome-wide analysis of multi- and extensively drug-resistant *Mycobacterium tuberculosis*. Nat Genet **50:**307-316.

78. **Takiff HE, Cimino M, Musso MC, Weisbrod T, Martinez R, Delgado MB, Salazar L, Bloom BR, Jacobs WR, Jr.** 1996. Efflux pump of the proton antiporter family confers low-level fluoroquinolone resistance in *Mycobacterium smegmatis*. Proc Natl Acad Sci U S A **93:**362-366.

79. **Jiang X, Zhang W, Zhang Y, Gao F, Lu C, Zhang X, Wang H.** 2008. Assessment of efflux pump gene expression in a clinical isolate *Mycobacterium tuberculosis* by real-time reverse transcription PCR. Microb Drug Resist **14:**7-11.

80. **Gupta AK, Katoch VM, Chauhan DS, Sharma R, Singh M, Venkatesan K, Sharma VD.** 2010. Microarray analysis of efflux pump genes in multidrug-resistant *Mycobacterium tuberculosis* during stress induced by common anti-tuberculous drugs. Microb Drug Resist **16:**21-28.

81. **Adams KN, Takaki K, Connolly LE, Wiedenhoft H, Winglee K, Humbert O, Edelstein PH, Cosma CL, Ramakrishnan L.** 2011. Drug tolerance in replicating mycobacteria mediated by a macrophage-induced efflux mechanism. Cell **145:**39-53.

82. **Srivastava S, Musuka S, Sherman C, Meek C, Leff R, Gumbo T.** 2010. Efflux-pump-derived multiple drug resistance to ethambutol monotherapy in *Mycobacterium tuberculosis* and the pharmacokinetics and pharmacodynamics of ethambutol. J Infect Dis **201:**1225-1231.

83.   **Singh M, Jadaun GP, Ramdas, Srivastava K, Chauhan V, Mishra R, Gupta K, Nair S, Chauhan DS, Sharma VD, Venkatesan K, Katoch VM.** 2011. Effect of efflux pump inhibitors on drug susceptibility of ofloxacin resistant *Mycobacterium tuberculosis* isolates. Indian J Med Res **133:**535-540.

84.   **Moyed HS, Broderick SH.** 1986. Molecular cloning and expression of *hipA*, a gene of *Escherichia coli* K-12 that affects frequency of persistence after inhibition of murein synthesis. J Bacteriol **166:**399-403.

85.   **Correia FF, D'Onofrio A, Rejtar T, Li L, Karger BL, Makarova K, Koonin EV, Lewis K.** 2006. Kinase activity of overexpressed HipA is required for growth arrest and multidrug tolerance in Escherichia coli. J Bacteriol **188:**8360-8367.

86.   **Falla TJ, Chopra I.** 1998. Joint tolerance to beta-lactam and fluoroquinolone antibiotics in *Escherichia coli* results from overexpression of *hipA*. Antimicrob Agents Chemother **42:**3282-3284.

87.   **Viducic D, Ono T, Murakami K, Susilowati H, Kayama S, Hirota K, Miyake Y.** 2006. Functional analysis of *spoT*, *relA* and *dksA* genes on quinolone tolerance in *Pseudomonas aeruginosa* under nongrowing condition. Microbiol Immunol **50:**349-357.

88.   **Li Y, Zhang Y.** 2007. PhoU is a persistence switch involved in persister formation and tolerance to multiple antibiotics and stresses in *Escherichia coli*. Antimicrob Agents Chemother **51:**2092-2099.

89.   **Shan Y, Brown Gandt A, Rowe SE, Deisinger JP, Conlon BP, Lewis K.** 2017. ATP-Dependent Persister Formation in *Escherichia coli*. mBio **8:**e02267-02216.

90.   **Ramage HR, Connolly LE, Cox JS.** 2009. Comprehensive functional analysis of *Mycobacterium tuberculosis* toxin-antitoxin systems: implications for pathogenesis, stress responses, and evolution. PLoS Genet **5:**e1000767.

91.   **Sala A, Calderon V, Bordes P, Genevaux P.** 2013. TAC from *Mycobacterium tuberculosis*: a paradigm for stress-responsive toxin-antitoxin systems controlled by SecB-like chaperones. Cell Stress Chaperones **18:**129-135.

92.   **Davies D.** 2003. Understanding biofilm resistance to antibacterial agents. Nat Rev Drug Discov **2:**114-122.

93.   **Mah T-FC, O'Toole GA.** 2001. Mechanisms of biofilm resistance to antimicrobial agents. Trends in Microbiology **9:**34-39.

94.   **Hoiby N, Ciofu O Fau - Bjarnsholt T, Bjarnsholt T.** *Pseudomonas aeruginosa* biofilms in cystic fibrosis.

95.   **D. MP.** 2005. Dental plaque: biological significance of a biofilm and community life-style. Journal of Clinical Periodontology **32:**7-15.

96.   **J W Costerton, K J Cheng, G G Geesey, T I Ladd, J C Nickel, M Dasgupta a, Marrie TJ.** 1987. Bacterial Biofilms in Nature and Disease. Annual Review of Microbiology **41:**435-464.

97.   **Costerton JW, Montanaro L, Arciola CR.** 2005. Biofilm in Implant Infections: Its Production and Regulation. The International Journal of Artificial Organs **28:**1062-1068.

98.   **Hoiby N, Bjarnsholt T, Givskov M, Molin S, Ciofu O.** 2010. Antibiotic resistance of bacterial biofilms. Int J Antimicrob Agents **35:**322-332.

99.   **Fux CA, Costerton JW, Stewart PS, Stoodley P.** 2005. Survival strategies of infectious biofilms. Trends Microbiol **13:**34-40.

100.   **Stoodley P, Sauer K, Davies DG, Costerton JW.** 2002. Biofilms as complex differentiated communities. Annu Rev Microbiol **56:**187-209.

101.   **López D, Vlamakis H, Kolter R.** 2010. Biofilms. Cold Spring Harbor Perspectives in Biology **2:**a000398.

102.   **Flemming HC, Wingender J, Szewzyk U, Steinberg P, Rice SA, Kjelleberg S.** 2016. Biofilms: an emergent form of bacterial life. Nat Rev Microbiol **14:**563-575.

103.   **Islam MS, Richards JP, Ojha AK.** 2012. Targeting drug tolerance in mycobacteria: a perspective from mycobacterial biofilms. Expert Rev Anti Infect Ther **10:**1055-1066.

104.   **Lopez D, Vlamakis H, Kolter R.** 2010. Biofilms. Cold Spring Harb Perspect Biol **2:**a000398.

105.   **Petrova OE, Sauer K.** 2009. A novel signaling network essential for regulating *Pseudomonas aeruginosa* biofilm development. PLoS Pathog **5:**e1000668.

106.   **Pratt LA, Kolter R.** 1998. Genetic analysis of *Escherichia coli* biofilm formation: roles of flagella, motility, chemotaxis and type I pili. Mol Microbiol **30:**285-293.

107.   **Yang Y, Thomas J, Li Y, Vilchèze C, Derbyshire KM, Jacobs WR, Ojha AK.** 2017. Defining a temporal order of genetic requirements for development of mycobacterial biofilms. Molecular Microbiology **105:**794-809.

108.   **Geesey GG, Richardson WT, Yeomans HG, Irvin RT, Costerton JW.** 1977. Microscopic examination of natural sessile bacterial populations from an alpine stream. Can J Microbiol **23:**1733-1736.

109. **Costerton JW, Irvin RT, Cheng KJ.** 1981. The role of bacterial surface structures in pathogenesis. Crit Rev Microbiol **8:**303-338.

110. **Nickel JC, Ruseska I, Wright JB, Costerton JW.** 1985. Tobramycin resistance of *Pseudomonas aeruginosa* cells growing as a biofilm on urinary catheter material. Antimicrob Agents Chemother **27:**619-624.

111. **Lam J, Chan R, Lam K, Costerton JW.** 1980. Production of mucoid microcolonies by *Pseudomonas aeruginosa* within infected lungs in cystic fibrosis. Infect Immun **28:**546-556.

112. **Lawrence JR, Korber DR, Hoyle BD, Costerton JW, Caldwell DE.** 1991. Optical sectioning of microbial biofilms. J Bacteriol **173:**6558-6567.

113. **von Ohle C, Gieseke A, Nistico L, Decker EM, DeBeer D, Stoodley P.** 2010. Real-time microsensor measurement of local metabolic activities in *ex vivo* dental biofilms exposed to sucrose and treated with chlorhexidine. Appl Environ Microbiol **76:**2326-2334.

114. **Stoodley P, Debeer D, Lewandowski Z.** 1994. Liquid flow in biofilm systems. Appl Environ Microbiol **60:**2711-2716.

115. **Mah TF, O'Toole GA.** 2001. Mechanisms of biofilm resistance to antimicrobial agents. Trends Microbiol **9:**34-39.

116. **Ojha A, Anand M, Bhatt A, Kremer L, Jacobs WR, Jr., Hatfull GF.** 2005. GroEL1: A Dedicated Chaperone Involved in Mycolic Acid Biosynthesis during Biofilm Formation in Mycobacteria. Cell **123:**861-873.

117. **Hobley L, Harkins C, MacPhee CE, Stanley-Wall NR.** 2015. Giving structure to the biofilm matrix: an overview of individual strategies and emerging common themes. FEMS Microbiol Rev **39:**649-669.

118. **Whitchurch CB, Tolker-Nielsen T, Ragas PC, Mattick JS.** 2002. Extracellular DNA required for bacterial biofilm formation. Science **295:**1487.

119. **Rice KC, Mann EE, Endres JL, Weiss EC, Cassat JE, Smeltzer MS, Bayles KW.** 2007. The *cidA* murein hydrolase regulator contributes to DNA release and biofilm development in *Staphylococcus aureus*. Proc Natl Acad Sci U S A **104:**8113-8118.

120. **Lasa I, Penades JR.** 2006. Bap: a family of surface proteins involved in biofilm formation. Res Microbiol **157:**99-107.

121. **Yildiz FH, Schoolnik GK.** 1999. *Vibrio cholerae* O1 El Tor: identification of a gene cluster required for the rugose colony type, exopolysaccharide production, chlorine resistance, and biofilm formation. Proc Natl Acad Sci U S A **96:**4028-4033.

122. **Fong JC, Syed KA, Klose KE, Yildiz FH.** 2010. Role of Vibrio polysaccharide (*vps*) genes in VPS production, biofilm formation and *Vibrio cholerae* pathogenesis. Microbiology **156:**2757-2769.

123. **Vlamakis H, Aguilar C, Losick R, Kolter R.** 2008. Control of cell fate by the formation of an architecturally complex bacterial community. Genes Dev **22:**945-953.

124. **Branda SS, Chu F, Kearns DB, Losick R, Kolter R.** 2006. A major protein component of the *Bacillus subtilis* biofilm matrix. Mol Microbiol **59:**1229-1238.

125. **O'Toole GA, Kolter R.** 1998. Flagellar and twitching motility are necessary for *Pseudomonas aeruginosa* biofilm development. Mol Microbiol **30:**295-304.

126. **Chapman MR, Robinson LS, Pinkner JS, Roth R, Heuser J, Hammar M, Normark S, Hultgren SJ.** 2002. Role of *Escherichia coli* curli operons in directing amyloid fiber formation. Science **295:**851-855.

127. **Borlee BR, Goldman AD, Murakami K, Samudrala R, Wozniak DJ, Parsek MR.** 2010. *Pseudomonas aeruginosa* uses a cyclic-di-GMP-regulated adhesin to reinforce the biofilm extracellular matrix. Mol Microbiol **75:**827-842.

128. **Davies DG, Parsek MR, Pearson JP, Iglewski BH, Costerton JW, Greenberg EP.** 1998. The involvement of cell-to-cell signals in the development of a bacterial biofilm. Science **280:**295-298.

129. **Kolter R, Losick R.** 1998. One for all and all for one. Science **280:**226-227.

130. **Werner E, Roe F, Bugnicourt A, Franklin MJ, Heydorn A, Molin S, Pitts B, Stewart PS.** 2004. Stratified growth in *Pseudomonas aeruginosa* biofilms. Appl Environ Microbiol **70:**6188-6196.

131. **Xu KD, Stewart PS, Xia F, Huang CT, McFeters GA.** 1998. Spatial physiological heterogeneity in *Pseudomonas aeruginosa* biofilm is determined by oxygen availability. Appl Environ Microbiol **64:**4035-4039.

132. **Rani SA, Pitts B, Beyenal H, Veluchamy RA, Lewandowski Z, Davison WM, Buckingham-Meyer K, Stewart PS.** 2007. Spatial patterns of DNA replication, protein synthesis, and oxygen concentration within bacterial biofilms reveal diverse physiological states. J Bacteriol **189:**4223-4233.

133. **Moorthy S, Watnick PI.** 2005. Identification of novel stage-specific genetic requirements through whole genome transcription profiling of *Vibrio cholerae* biofilm development. Molecular Microbiology **57:**1623-1635.

134.   **Pisithkul T, Schroeder JW, Trujillo EA, Yeesin P, Stevenson DM, Chaiamarit T, Coon JJ, Wang JD, Amador-Noguez D.** 2019. Metabolic Remodeling during Biofilm Development of *Bacillus subtilis*. MBio **10**.

135.   **Fazli M, Almblad H, Rybtke ML, Givskov M, Eberl L, Tolker-Nielsen T.** 2014. Regulation of biofilm formation in *Pseudomonas* and *Burkholderia* species. Environ Microbiol **16:**1961-1981.

136.   **McDougald D, Rice SA, Barraud N, Steinberg PD, Kjelleberg S.** 2011. Should we stay or should we go: mechanisms and ecological consequences for biofilm dispersal. Nat Rev Microbiol **10:**39-50.

137.   **Stewart PS.** 1996. Theoretical aspects of antibiotic diffusion into microbial biofilms. Antimicrobial Agents and Chemotherapy **40:**2517-2522.

138.   **Walters MC, Roe F, Bugnicourt A, Franklin MJ, Stewart PS.** 2003. Contributions of Antibiotic Penetration, Oxygen Limitation, and Low Metabolic Activity to Tolerance of *Pseudomonas aeruginosa* Biofilms to Ciprofloxacin and Tobramycin. Antimicrobial Agents and Chemotherapy **47:**317-323.

139.   **Corbin A, Pitts B, Parker A, Stewart PS.** 2011. Antimicrobial Penetration and Efficacy in an *In Vitro* Oral Biofilm Model. Antimicrobial Agents and Chemotherapy **55:**3338-3344.

140.   **Boles BR, Singh PK.** 2008. Endogenous oxidative stress produces diversity and adaptability in biofilm communities. Proceedings of the National Academy of Sciences **105:**12503-12508.

141.   **Zhang L, Mah T-F.** 2008. Involvement of a Novel Efflux System in Biofilm-Specific Resistance to Antibiotics. Journal of Bacteriology **190:**4447-4452.

142.   **Liao J, Schurr MJ, Sauer K.** 2013. The MerR-Like Regulator BrlR Confers Biofilm Tolerance by Activating Multidrug Efflux Pumps in *Pseudomonas aeruginosa* Biofilms. Journal of Bacteriology **195:**3352-3363.

143.   **Nguyen D, Joshi-Datar A, Lepine F, Bauerle E, Olakanmi O, Beer K, McKay G, Siehnel R, Schafhauser J, Wang Y, Britigan BE, Singh PK.** 2011. Active starvation responses mediate antibiotic tolerance in biofilms and nutrient-limited bacteria. Science (New York, NY) **334:**982-986.

144.   **Bernier SP, Lebeaux D, DeFrancesco AS, Valomon A, Soubigou G, Coppée J-Y, Ghigo J-M, Beloin C.** 2013. Starvation, Together with the SOS Response, Mediates High Biofilm-Specific Tolerance to the Fluoroquinolone Ofloxacin. PLoS Genetics **9:**e1003144.

145. **Cao B, Christophersen L, Thomsen K, Sonderholm M, Bjarnsholt T, Jensen PO, Hoiby N, Moser C.** 2015. Antibiotic penetration and bacterial killing in a *Pseudomonas aeruginosa* biofilm model. J Antimicrob Chemother **70:**2057-2063.

146. **Moser C, Pedersen HT, Lerche CJ, Kolpen M, Line L, Thomsen K, Hoiby N, Jensen PO.** 2017. Biofilms and host response - helpful or harmful. Apmis **125:**320-338.

147. **Leid JG, Willson CJ, Shirtliff ME, Hassett DJ, Parsek MR, Jeffers AK.** 2005. The exopolysaccharide alginate protects *Pseudomonas aeruginosa* biofilm bacteria from IFN-gamma-mediated macrophage killing. J Immunol **175:**7512-7518.

148. **Thurlow LR, Hanke ML, Fritz T, Angle A, Aldrich A, Williams SH, Engebretsen IL, Bayles KW, Horswill AR, Kielian T.** 2011. *Staphylococcus aureus* Biofilms Prevent Macrophage Phagocytosis and Attenuate Inflammation *In Vivo*. The Journal of Immunology **186:**6585-6596.

149. **Leid JG, Willson CJ, Shirtliff ME, Hassett DJ, Parsek MR, Jeffers AK.** 2005. The Exopolysaccharide Alginate Protects *Pseudomonas aeruginosa* Biofilm Bacteria from IFN-γ-Mediated Macrophage Killing. The Journal of Immunology **175:**7512.

150. **Van Gennip M, Christensen LD, Alhede M, Phipps R, Jensen PO, Christophersen L, Pamp SJ, Moser C, Mikkelsen PJ, Koh AY, Tolker-Nielsen T, Pier GB, Hoiby N, Givskov M, Bjarnsholt T.** 2009. Inactivation of the *rhlA* gene in *Pseudomonas aeruginosa* prevents rhamnolipid production, disabling the protection against polymorphonuclear leukocytes. Apmis **117:**537-546.

151. **Prabhakara R, Harro JM, Leid JG, Harris M, Shirtliff ME.** 2011. Murine immune response to a chronic *Staphylococcus aureus* biofilm infection. Infect Immun **79:**1789-1796.

152. **Vaerewijck MJ, Huys G, Palomino JC, Swings J, Portaels F.** 2005. Mycobacteria in drinking water distribution systems: ecology and significance for human health. FEMS Microbiol Rev **29:**911-934.

153. **Roland Schulze-Robbecke RF.** 1989. Mycobacteria in biofilms. Zentbl Hyg Umweltmed **188:**385-390Mycobacteria in biofilms.

154. **Falkinham JO, Norton CD, LeChevallier MW.** 2001. Factors Influencing Numbers of *Mycobacterium avium*, *Mycobacterium intracellulare*, and Other Mycobacteria in Drinking Water Distribution Systems. Applied and Environmental Microbiology **67:**1225.

155. **Schulze-Röbbecke R, Janning B, Fischeder R.** 1992. Occurrence of mycobacteria in biofilm samples. Tubercle and Lung Disease **73:**141-144.

156. **September SM, Brözel VS, Venter SN.** 2004. Diversity of Nontuberculoid Mycobacterium Species in Biofilms of Urban and Semiurban Drinking Water Distribution Systems. Applied and Environmental Microbiology **70:**7571-7573.

157. **Emtiazi F, Schwartz T, Marten SM, Krolla-Sidenstein P, Obst U.** 2004. Investigation of natural biofilms formed during the production of drinking water from surface water embankment filtration. Water Research **38:**1197-1206.

158. **Angenent LT, Kelley ST, Amand AS, Pace NR, Hernandez MT.** 2005. Molecular identification of potential pathogens in water and air of a hospital therapy pool. Proceedings of the National Academy of Sciences of the United States of America **102:**4860-4865.

159. **Cook KL, Britt JS, Bolster CH.** 2010. Survival of *Mycobacterium avium* subsp. *paratuberculosis* in biofilms on livestock watering trough materials. Veterinary Microbiology **141:**103-109.

160. **Schulze-Röbbecke R, Feldmann C, Fischeder R, Janning B, Exner M, Wahl G.** 1995. Dental units: an environmental study of sources of potentially pathogenic mycobacteria. Tubercle and Lung Disease **76:**318-323.

161. **Feazel LM, Baumgartner LK, Peterson KL, Frank DN, Harris JK, Pace NR.** 2009. Opportunistic pathogens enriched in showerhead biofilms. Proceedings of the National Academy of Sciences **106:**16393.

162. **Teng R, Dick T.** 2006. Isoniazid resistance of exponentially growing *Mycobacterium smegmatis* biofilm culture. FEMS Microbiology Letters **227:**171-174.

163. **Hall-Stoodley L, Lappin-Scott H.** 2006. Biofilm formation by the rapidly growing mycobacterial species *Mycobacterium fortuitum*. FEMS Microbiology Letters **168:**77-84.

164. **Hall-Stoodley L, Keevil CW, Lappin-Scott HM.** 1998. *Mycobacterium fortuitum* and *Mycobacterium chelonae* biofilm formation under high and low nutrient conditions. Journal of applied microbiology **85 Suppl 1:**60S-69S.

165. **Dailloux M, Albert M, Laurain C, Andolfatto S, Lozniewski A, Hartemann P, Mathieu L.** 2003. *Mycobacterium xenopi* and Drinking Water Biofilms. Applied and Environmental Microbiology **69:**6946-6948.

166. **Vess RW, Anderson RL, Carr JH, Bond WW, Favero MS.** 1993. The colonization of solid PVC surfaces and the acquisition of resistance to germicides by water micro-organisms. Journal of Applied Bacteriology **74:**215-221.

167. **Carter G, Wu M, Drummond DC, Bermudez LE.** 2003. Characterization of biofilm formation by clinical isolates of *Mycobacterium avium*. Journal of Medical Microbiology **52:**747-752.

168. **Carter G, Young LS, Bermudez LE.** 2004. A Subinhibitory Concentration of Clarithromycin Inhibits *Mycobacterium avium* Biofilm Formation. Antimicrobial Agents and Chemotherapy **48:**4907-4910.

169. **Falkinham JO.** 2007. Growth in catheter biofilms and antibiotic resistance of *Mycobacterium avium*. Journal of Medical Microbiology **56:**250-254.

170. **Bardouniotis E, Ceri H, Olson ME.** 2003. Biofilm Formation and Biocide Susceptibility Testing of *Mycobacterium fortuitum* and *Mycobacterium marinum*. Current Microbiology **46:**0028-0032.

171. **Hall-Stoodley L, Brun OS, Polshyna G, Barker LP.** 2006. *Mycobacterium marinum* biofilm formation reveals cording morphology. FEMS Microbiology Letters **257:**43-49.

172. **Bosio S, Leekha S, Gamb SI, Wright AJ, Terrell CL, Miller DV.** 2012. *Mycobacterium fortuitum* prosthetic valve endocarditis: a case for the pathogenetic role of biofilms. Cardiovascular Pathology **21:**361-364.

173. **Marsollier L, Stinear T, Aubry J, Saint André JP, Robert R, Legras P, Manceau A-L, Audrain C, Bourdon S, Kouakou H, Carbonnelle B.** 2004. Aquatic Plants Stimulate the Growth of and Biofilm Formation by *Mycobacterium ulcerans* in Axenic Culture and Harbor These Bacteria in the Environment. Applied and Environmental Microbiology **70:**1097-1103.

174. **Marsollier L, Brodin P, Jackson M, Korduláková J, Tafelmeyer P, Carbonnelle E, Aubry J, Milon G, Legras P, André J-PS, Leroy C, Cottin J, Guillou MLJ, Reysset G, Cole ST.** 2007. Impact of *Mycobacterium ulcerans* Biofilm on Transmissibility to Ecological Niches and Buruli Ulcer Pathogenesis. PLOS Pathogens **3:**e62.

175. **Williamson HR, Benbow ME, Nguyen KD, Beachboard DC, Kimbirauskas RK, McIntosh MD, Quaye C, Ampadu EO, Boakye D, Merritt RW, Small PLC.** 2008. Distribution of *Mycobacterium ulcerans* in Buruli Ulcer Endemic and Non-Endemic Aquatic Sites in Ghana. PLOS Neglected Tropical Diseases **2:**e205.

176. **Marsollier L, Aubry J, Coutanceau E, André J-PS, Small PL, Milon G, Legras P, Guadagnini S, Carbonnelle B, Cole ST.** 2005. Colonization of the salivary glands of *Naucoris cimicoides* by *Mycobacterium ulcerans* requires host plasmatocytes and a macrolide toxin, mycolactone. Cellular Microbiology **7:**935-943.

177. **Recht J, Martínez A, Torello S, Kolter R.** 2000. Genetic Analysis of Sliding Motility *Mycobacterium smegmatis*. Journal of Bacteriology **182:**4348.

178. **Arora K, Whiteford DC, Lau-Bonilla D, Davitt CM, Dahl JL.** 2008. Inactivation of *lsr2* Results in a Hypermotile Phenotype in *Mycobacterium smegmatis*. Journal of Bacteriology **190:**4291.

179. **Chen JM, German GJ, Alexander DC, Ren H, Tan T, Liu J.** 2006. Roles of Lsr2 in Colony Morphology and Biofilm Formation of *Mycobacterium smegmatis*. Journal of Bacteriology **188:**633.

180. **Yamazaki Y, Danelishvili L, Wu M, Macnab M, Bermudez LE.** 2006. *Mycobacterium avium* genes associated with the ability to form a biofilm. Appl Environ Microbiol **72:**819-825.

181. **Schorey JS, Sweet L.** 2008. The mycobacterial glycopeptidolipids: structure, function, and their role in pathogenesis. Glycobiology **18:**832-841.

182. **Yamazaki Y, Danelishvili L, Wu M, Hidaka E, Katsuyama T, Stang B, Petrofsky M, Bildfell R, Bermudez LE.** 2006. The ability to form biofilm influences *Mycobacterium avium* invasion and translocation of bronchial epithelial cells. Cellular Microbiology **8:**806-814.

183. **Ojha AK, Trivelli X, Guerardel Y, Kremer L, Hatfull GF.** 2010. Enzymatic hydrolysis of trehalose dimycolate releases free mycolic acids during mycobacterial growth in biofilms. J Biol Chem **285:**17380-17389.

184. **Ojha AK, Baughn AD, Sambandan D, Hsu T, Trivelli X, Guerardel Y, Alahari A, Kremer L, Jacobs WR, Hatfull GF.** 2008. Growth of *Mycobacterium tuberculosis* biofilms containing free mycolic acids and harbouring drug-tolerant bacteria. Molecular Microbiology **69:**164-174.

185. **Takayama K, Wang C, Besra GS.** 2005. Pathway to synthesis and processing of mycolic acids in *Mycobacterium tuberculosis*. Clinical microbiology reviews **18:**81-101.

186. **Sambandan D, Dao DN, Weinrick BC, Vilcheze C, Gurcha SS, Ojha A, Kremer L, Besra GS, Hatfull GF, Jacobs WR, Jr.** 2013. Keto-mycolic acid-dependent pellicle formation confers tolerance to drug-sensitive *Mycobacterium tuberculosis*. MBio **4:**e00222-00213.

187. **Pang JM, Layre E, Sweet L, Sherrid A, Moody DB, Ojha A, Sherman DR.** 2012. The polyketide Pks1 contributes to biofilm formation in *Mycobacterium tuberculosis*. J Bacteriol **194:**715-721.

188. **Wright CC, Hsu FF, Arnett E, Dunaj JL, Davidson PM, Pacheco SA, Harriff MJ, Lewinsohn DM, Schlesinger LS, Purdy GE.** 2017. The *Mycobacterium tuberculosis* MmpL11 Cell Wall Lipid Transporter Is Important for Biofilm Formation, Intracellular Growth, and Nonreplicating Persistence. Infect Immun **85**.

189. **Ojha A, Hatfull GF.** 2007. The role of iron in *Mycobacterium smegmatis* biofilm formation: the exochelin siderophore is essential in limiting iron conditions for biofilm formation but not for planktonic growth. Molecular Microbiology **66:**468-483.

190. **Yang Y, Richards JP, Gundrum J, Ojha AK.** 2018. GlnR Activation Induces Peroxide Resistance in Mycobacterial Biofilms. Frontiers in Microbiology **9:**1428.

191. **Aldridge BB, Fernandez-Suarez M, Heller D, Ambravaneswaran V, Irimia D, Toner M, Fortune SM.** 2012. Asymmetry and aging of mycobacterial cells lead to variable growth and antibiotic susceptibility. Science **335:**100-104.

192. **Rego EH, Audette RE, Rubin EJ.** 2017. Deletion of a mycobacterial divisome factor collapses single-cell phenotypic heterogeneity. Nature **546:**153-157.

193. **Cressy NL.** 1955. The Tubercle Bacillus in the Pulmonary Lesion of Man. The Yale Journal of Biology and Medicine **28:**72-73.

194. **Ulrichs T, Kosmiadi GA, Jorg S, Pradl L, Titukhina M, Mishenko V, Gushina N, Kaufmann SH.** 2005. Differential organization of the local immune response in patients with active cavitary tuberculosis or with nonprogressive tuberculoma. J Infect Dis **192:**89-97.

195. **Park IN, Ryu JS, Shim TS.** 2008. Evaluation of therapeutic response of tuberculoma using F-18 FDG positron emission tomography. Clin Nucl Med **33:**1-3.

196. **Ford CB, Lin PL, Chase MR, Shah RR, Iartchouk O, Galagan J, Mohaideen N, Ioerger TR, Sacchettini JC, Lipsitch M, Flynn JL, Fortune SM.** 2011. Use of whole genome sequencing to estimate the mutation rate of *Mycobacterium tuberculosis* during latent infection. Nat Genet **43:**482-486.

197. **Kim AI, Ghosh P, Aaron MA, Bibb LA, Jain S, Hatfull GF.** 2003. Mycobacteriophage Bxb1 integrates into the *Mycobacterium smegmatis* groEL1 gene. Mol Microbiol **50:**463-473.

198. **Siegrist MS, Rubin EJ.** 2009. Phage transposon mutagenesis. Methods Mol Biol **465:**311-323.

199. **Lewis JA, Hatfull GF.** 2000. Identification and characterization of mycobacteriophage L5 excisionase. Mol Microbiol **35:**350-360.

200. **Sarkis GJ, Hatfull GF.** 1998. Mycobacteriophages. Methods Mol Biol **101:**145-173.

201. **Griffin JE, Gawronski JD, DeJesus MA, Ioerger TR, Akerley BJ, Sassetti CM.** 2011. High-Resolution Phenotypic Profiling Defines Genes Essential for Mycobacterial Growth and Cholesterol Catabolism. PLOS Pathogens **7:**e1002251.

202. **DeJesus MA, Ambadipudi C, Baker R, Sassetti C, Ioerger TR.** 2015. TRANSIT - A Software Tool for Himar1 TnSeq Analysis. PLOS Computational Biology **11:**e1004401.

203. **Li H, Durbin R.** 2009. Fast and accurate short read alignment with Burrows-Wheeler transform. Bioinformatics **25:**1754-1760.

204. **Sohaskey CD, Voskuil MI.** 2015. *In vitro* models that utilize hypoxia to induce non-replicating persistence in Mycobacteria. Methods Mol Biol **1285:**201-213.

205. **McClure R, Balasubramanian D, Sun Y, Bobrovskyy M, Sumby P, Genco CA, Vanderpool CK, Tjaden B.** 2013. Computational analysis of bacterial RNA-Seq data. Nucleic Acids Res **41:**e140.

206. **Tsugawa H, Cajka T, Kind T, Ma Y, Higgins B, Ikeda K, Kanazawa M, VanderGheynst J, Fiehn O, Arita M.** 2015. MS-DIAL: data-independent MS/MS deconvolution for comprehensive metabolome analysis. Nat Methods **12:**523-526.

207. **Martin A, Daniel J.** 2018. The ABC transporter Rv1272c of *Mycobacterium tuberculosis* enhances the import of long-chain fatty acids in *Escherichia coli*. Biochem Biophys Res Commun **496:**667-672.

208. **Kardan Yamchi J, Haeili M, Gizaw Feyisa S, Kazemian H, Hashemi Shahraki A, Zahednamazi F, Imani Fooladi AA, Feizabadi MM.** 2015. Evaluation of efflux pump gene expression among drug susceptible and drug resistant strains of *Mycobacterium tuberculosis* from Iran. Infect Genet Evol **36:**23-26.

209. **Rengarajan J, Bloom BR, Rubin EJ.** 2005. Genome-wide requirements for *Mycobacterium tuberculosis* adaptation and survival in macrophages. Proc Natl Acad Sci U S A **102:**8327-8332.

210. **Sassetti CM, Rubin EJ.** 2003. Genetic requirements for mycobacterial survival during infection. Proc Natl Acad Sci U S A **100:**12989-12994.

211. **Rengarajan J, Murphy E, Park A, Krone CL, Hett EC, Bloom BR, Glimcher LH, Rubin EJ.** 2008. *Mycobacterium tuberculosis* Rv2224c modulates innate immune responses. Proc Natl Acad Sci U S A **105:**264-269.

212. **Kieser KJ, Baranowski C, Chao MC, Long JE, Sassetti CM, Waldor MK, Sacchettini JC, Ioerger TR, Rubin EJ.** 2015. Peptidoglycan synthesis in *Mycobacterium tuberculosis* is organized into networks with varying drug susceptibility. Proc Natl Acad Sci U S A **112:**13087-13092.

213. **Vandal OH, Roberts JA, Odaira T, Schnappinger D, Nathan CF, Ehrt S.** 2009. Acid-susceptible mutants of *Mycobacterium tuberculosis* share hypersusceptibility to cell wall and oxidative stress and to the host environment. J Bacteriol **191:**625-631.

214. **Namugenyi SB, Aagesen AM, Elliott SR, Tischler AD.** 2017. *Mycobacterium tuberculosis* PhoY Proteins Promote Persister Formation by Mediating Pst/SenX3-RegX3 Phosphate Sensing. MBio **8**.

215. **Tischler AD, Leistikow RL, Ramakrishnan P, Voskuil MI, McKinney JD.** 2016. *Mycobacterium tuberculosis* Phosphate Uptake System Component PstA2 Is Not Required for Gene Regulation or Virulence. PLoS One **11:**e0161467.

216. **Tischler AD, Leistikow RL, Kirksey MA, Voskuil MI, McKinney JD.** 2013. *Mycobacterium tuberculosis* requires phosphate-responsive gene regulation to resist host immunity. Infect Immun **81:**317-328.

217. **Hsieh YJ, Wanner BL.** 2010. Global regulation by the seven-component Pi signaling system. Curr Opin Microbiol **13:**198-203.

218. **Saier MH, Jr., Reddy VS, Tsu BV, Ahmed MS, Li C, Moreno-Hagelsieb G.** 2016. The Transporter Classification Database (TCDB): recent advances. Nucleic Acids Res **44:**D372-379.

219. **Gardner SG, Johns KD, Tanner R, McCleary WR.** 2014. The PhoU protein from *Escherichia coli* interacts with PhoR, PstB, and metals to form a phosphate-signaling complex at the membrane. J Bacteriol **196:**1741-1752.

220. **Vuppada RK, Hansen CR, Strickland KAP, Kelly KM, McCleary WR.** 2018. Phosphate signaling through alternate conformations of the PstSCAB phosphate transporter. BMC microbiology **18:**8-8.

221. **Rifat D, Bishai WR, Karakousis PC.** 2009. Phosphate depletion: a novel trigger for *Mycobacterium tuberculosis* persistence. J Infect Dis **200:**1126-1135.

222. **Glover RT, Kriakov J, Garforth SJ, Baughn AD, Jacobs WR.** 2007. The Two-Component Regulatory System *senX3-regX3* Regulates Phosphate-Dependent Gene Expression in *Mycobacterium smegmatis*. Journal of Bacteriology **189:**5495.

223. **Parish T, Smith DA, Roberts G, Betts J, Stoker NG.** 2003. The senX3-regX3 two-component regulatory system of *Mycobacterium tuberculosis* is required for virulence. Microbiology **149:**1423-1435.

224. **Harris NC, Sato M, Herman NA, Twigg F, Cai W, Liu J, Zhu X, Downey J, Khalaf R, Martin J, Koshino H, Zhang W.** 2017. Biosynthesis of isonitrile lipopeptides by conserved nonribosomal peptide synthetase gene clusters in Actinobacteria. Proc Natl Acad Sci U S A **114:**7025-7030.

225. **Harris NC, Born DA, Cai W, Huang Y, Martin J, Khalaf R, Drennan CL, Zhang W.** 2018. Isonitrile Formation by a Non-Heme Iron(II)-Dependent Oxidase/Decarboxylase. Angew Chem Int Ed Engl **57:**9707-9710.

226. **Dhar N, McKinney JD.** 2010. *Mycobacterium tuberculosis* persistence mutants identified by screening in isoniazid-treated mice. Proceedings of the National Academy of Sciences **107:**12275.

227. **Hotter GS, Wards BJ, Mouat P, Besra GS, Gomes J, Singh M, Bassett S, Kawakami P, Wheeler PR, de Lisle GW, Collins DM.** 2005. Transposon mutagenesis of Mb0100 at the ppe1-nrp locus in *Mycobacterium bovis* disrupts phthiocerol dimycocerosate (PDIM) and glycosylphenol-PDIM biosynthesis, producing an avirulent strain with vaccine properties at least equal to those of M. bovis BCG. J Bacteriol **187:**2267-2277.

228. **Giovannini D, Cappelli G, Jiang L, Castilletti C, Colone A, Serafino A, Wannenes F, Giacò L, Quintiliani G, Fraziano M, Nepravishta R, Colizzi V, Mariani F.** 2012. A new *Mycobacterium tuberculosis* smooth colony reduces growth inside human macrophages and represses PDIM Operon gene expression. Does an heterogeneous population exist in intracellular mycobacteria? Microbial Pathogenesis **53:**135-146.

229. **Wang L, Zhu M, Zhang Q, Zhang X, Yang P, Liu Z, Deng Y, Zhu Y, Huang X, Han L, Li S, He J.** 2017. Diisonitrile Natural Product SF2768 Functions As a Chalkophore That Mediates Copper Acquisition in *Streptomyces thioluteus*. ACS Chemical Biology **12:**3067-3075.

230. **Minch KJ, Rustad TR, Peterson EJ, Winkler J, Reiss DJ, Ma S, Hickey M, Brabant W, Morrison B, Turkarslan S, Mawhinney C, Galagan JE, Price ND, Baliga NS, Sherman DR.** 2015. The DNA-binding network of *Mycobacterium tuberculosis*. Nat Commun **6:**5829.

231. **Rustad TR, Minch KJ, Ma S, Winkler JK, Hobbs S, Hickey M, Brabant W, Turkarslan S, Price ND, Baliga NS, Sherman DR.** 2014. Mapping and manipulating the *Mycobacterium tuberculosis* transcriptome using a transcription factor overexpression-derived regulatory network. Genome Biol **15:**502.

232. **Raman S, Puyang X, Cheng T-Y, Young DC, Moody DB, Husson RN.** 2006. *Mycobacterium tuberculosis* SigM Positively Regulates Esx Secreted Protein and Nonribosomal Peptide Synthetase Genes and Down Regulates Virulence-Associated Surface Lipid Synthesis. Journal of Bacteriology **188:**8460.

233. **Greendyke R, Byrd TF.** 2008. Differential Antibiotic Susceptibility of *Mycobacterium abscessus* Variants in Biofilms and Macrophages Compared to That of Planktonic Bacteria. Antimicrobial Agents and Chemotherapy **52:**2019.

234. **Dubnau E, Chan J, Raynaud C, Mohan VP, Laneelle MA, Yu K, Quemard A, Smith I, Daffe M.** 2000. Oxygenated mycolic acids are necessary for virulence of *Mycobacterium tuberculosis* in mice. Mol Microbiol **36:**630-637.

235. **Bhatt K, Machado H, Osorio NS, Sousa J, Cardoso F, Magalhaes C, Chen B, Chen M, Kim J, Singh A, Ferreira CM, Castro AG, Torrado E, Jacobs WR, Jr., Bhatt A, Saraiva M.** 2018. A Nonribosomal Peptide Synthase Gene Driving Virulence in *Mycobacterium tuberculosis*. mSphere **3**.

236. **Keren I, Kaldalu N, Spoering A, Wang Y, Lewis K.** 2004. Persister cells and tolerance to antimicrobials. FEMS Microbiology Letters **230:**13-18.